EFFECT OF EXTRUSION ON PHYSICO-CHEMICAL PROPERTIES OF QUINOA-CASSAVA EXTRUDATES FORTIFIED WITH CRANBERRY CONCENTRATE

by

SOUNDHARYA CHANDRAN

A thesis submitted to the

Graduate School-New Brunswick

Rutgers, The State University of New Jersey

in partial fulfillment of the requirements

for the degree of

Master of Science

Graduate Program in Food Science

written under the direction of

Dr. Mukund V. Karwe

and approved by

_____

_____

_____

_____

New Brunswick, New Jersey

January, 2015

ABSTRACT OF THESIS

Effect of extrusion on physico-chemical properties of quinoa-cassava extrudates fortified with cranberry concentrate

SOUNDHARYA CHANDRAN

Thesis Director: Mukund V. Karwe, Ph.D.

Extrusion is one among the major technologies used in food manufacturing. When extrusion is used to make puffed products such as breakfast cereals, it is a high temperature short time process, in which high shear and heat are applied on low moisture feed. During extrusion of cereal based food materials, several molecular transformations such as starch gelatinization and protein denaturation occur, leading to changes in the physico-chemical properties of the extrudates.

The major objectives of this study were to make extruded ready-to-eat (RTE) breakfast cereal from quinoa, fortified with cranberry concentrate and to study the effect of extrusion on the physico-chemical properties of the extrudates. Cassava flour was used as an extrusion aid for puffing. The base feed consisted of 50-50 blend of quinoa and cassava. Phenolic rich cranberry concentrate had anthocyanins which acted as natural colorants for the extrudates.

A single screw extruder equipped with a 4:1 compression ratio screw, set at 130 RPM, was used with a 4.5 mm diameter die hole. A 3^3 Box- Behnken Design was used to design the experiments for three independent variables: barrel temperature (120 ˚C, 140 ˚C, 160 ˚C), cranberry solids (3 %, 4 %, 5 % (d. b.)), and feed moisture (16 %, 18 %, 20 % (w.b.)). Physical properties such as Radial Expansion Index (REI), Bulk Density (BD), Breaking Strength (BS), Hue, Chroma, Water Absorption Index (WAI), and Water Solubility Index (WSI) along with chemical properties such as Total Phenolic Content (TPC) and anthocyanin content were evaluated.

Extrudates collected at barrel temperature of 160 ˚C, 16 % feed moisture and 4 % cranberry solids showed lowest Bulk Density of 0.281 g/mL and Breaking Strength of 0.46 N/mm^2. From the response surface analysis, it was found that barrel temperature and feed moisture were the two most important variables that affected the physical properties. The TPC of extrudates collected at higher barrel temperatures were found to contain higher phenolic values (~ 80 mg GAE/100 g d.m.), probably due to the formation of Maillard products. Extrudates collected under 140 ˚C barrel temperature, 16 % feed moisture and 5 % cranberry solids showed maximum anthocyanin content of 9.63 mg / kg d.m.

This study will open new avenues to develop gluten free extruded products that can be naturally colored with antioxidant loaded fruit concentrates.

ACKNOWLEDGEMENTS

First and foremost, I am sincerely thankful to my advisor, Dr. Mukund V. Karwe whose support, guidance and encouragement helped me in completing my thesis with a great deal of understanding the science and art of extrusion. I thank him for providing me the appropriate grounds to develop my soft skills and to have given me the opportunity to teach and train high school students during my time at the lab. I started developing interest in hiking trips after being on a couple of them with him.

I would like to specially thank Dr. Kit L. Yam and Dr. William C. Franke for serving my thesis committee and I would like to further extend my thanks to Dr. Yam for helping me during my Rutgers admission process and to Dr. Franke to have guided me during my internship time at Food Innovation Center. I would also like to thank Dr. Deepti Salvi for her encouragement to finish my work and for serving as an external thesis committee member.

I also wish to thank Dr. Soumya Roy from Ocean Spray Cranberries, Inc. (Lakeville-Middleboro, Massachusetts) for offering us cranberry concentrate and for sharing his knowledge. My thanks to Dr. Antelmo Santos from Ocean Spray Cranberries for performing anthocyanin analysis. My thanks to Mel Festjo from American Key Food Products (Closter, New Jersey) to have donated cassava flour.

Bill and Dave have always been there for all extrusion related help and troubleshooting and I extend my thanks to them.

Special mention to my friend J.S. Karthikeyan for being there always by my side and supporting me throughout my time at Rutgers. To Saikiran C for being my well-wisher for all these years. Thanks to Rajay to have taught me to use the extruder.

I extend my thanks to Noopur for her dedication and help. My seniors Swetha, Meenakshi and Jose were great inspiration to me. Special regards to my high school Math teacher Chandra and Chemistry teacher Kalyani.

I owe my thesis to Amma, Appa, and to all my family members, Prakash mama, Uma chithi, Karthi chithi, chithappa's and my cousin brothers Abishek and Aravindhan for their love and sacrifice has made me the person who I am. Ammaji and thatha's (my grandparents) blessings and prayers have led me to achieve many things in life. I cannot thank them enough. Last but definitely not the least, a special mention to my sweet little cousin sisters Neradhi and Prithivi.

TABLE OF CONTENTS

LIST OF TABLES

LIST OF FIGURES

1. INTRODUCTION

1.1 Background:

Recent awareness and interest in health and wellness has shifted focus on healthy eating and lifestyle changes in the U.S. population. Consumption of Ready to Eat (RTE) breakfast cereals has been on the rise since its inception due to its convenience and quick source of energy and nutrition. Alongside, numerous consumer and scientific studies suggest that consuming antioxidants that are naturally present in whole grains and fruits helps reduce incidences of chronic diseases such as cancer and cardiovascular disorders.

In 2011, Mintel market research survey concluded that 93 % of respondents consumed RTE cereals. In the RTE breakfast cereal brands category Kellogg's represents 33 %, General Mills represents 29 % and other private label brands occupy 31 % of the U.S. market share (2010-2011). Current consumer demands have influenced these companies to reformulate their cereals to have lower sodium and low sugar content. From 2005 to 2011, sodium content in the cereals has been reduced by 14 % and the added sugar has been reduced by 12 % (Thomas et al., 2013). The third most influential selection attribute of breakfast cereals was the presence of whole grains. In 2010, 2/3rd of RTE breakfast cereal had "whole grain" in them. Whole grain not only contributes to the fiber content but provides additional nutrition such as proteins, vitamins, minerals and antioxidants. Recent efforts (2012) by the American Bakers Association, National Pasta Association, Grain Foods Foundation, USA Rice and Wheat Foods Council along with corporate members like General Mills and Kellogg Company campaigned with the message "make at least half your grains whole" to strengthen the Dietary Guidelines Advisory (2010) message for young adult women and children to consume more grains

(USDA, 2012). However whole grains such as wheat and barley contain gluten, a protein which is not tolerated by those who have celiac disease. Approximately 1 % of the U.S. population is intolerant to gluten (Mintel, 2013). Grains such as wheat, rye, barley and triticale have relatively high gluten content, whereas corn, rice, amaranth, quinoa, millet and sorghum do not contain this protein.

Extensive extrusion studies have been conducted on corn and rice based RTE breakfast products. However, extrusion of non-conventional grains/flours like amaranth, quinoa, and millet is still limited. Hence this study focused on one such non-conventional grain/flour that is quinoa. Some shortcomings of quinoa are that, it is expensive and can have a strong influence on taste and flavor even at low substitution levels. Our preliminary studies suggested that quinoa extrudates had undesirable physical properties when made using a single screw extruder. Hence, cassava flour which is bland, was used as an extrusion aid. Since cassava flour has almost 85 % starch content, it should help in achieving desirable physical properties such as expansion, airiness, crispness, etc.

Phenolics and antioxidants present in fruits have long been associated with health benefits. Factors such as season changes, high price and perishability affect the consumption of fresh fruits (Rekhy and McConchie, 2014). Therefore, it becomes necessary to incorporate beneficial fruit compounds into the diet using other forms of food such as breakfast cereal. Besides, by-products from fruit processing industry are loaded with health beneficial compounds. One such by-product, cranberry concentrate, generated during the manufacturing of Craisins® has the potential of improving the antioxidant status of the extrudates. Apart from that, it also acts as a natural colorant due the presence of

anthocyanins. Therefore, keeping in mind the high demand for functional foods that are gluten free, the following raw materials were chosen for our study.

1.2. Quinoa:

Quinoa (*Chenopodium quinoa Willd.*) belongs to a class of grains known as pseudocereals (Vega-Galvez et al., 2010). The use of this crop traces back to pre-Columbian culture dating back to more than 5000 years. Quinoa is considered sacred and is called as the "mother grain" by the Incas of the Andes. It is an annual crop of the Andean region and grows at high altitudes to around 4000 m above the sea level (Abugoch, 2009). There are almost 250 species of quinoa worldwide (Ahamed et al., 1998). The adaptability of quinoa to very different climates makes it tolerable to extreme climates. Growing at a relative humidity of 40 % to 88 %, quinoa can grow at temperatures between -4 °C to 38 °C. It withstands dry dessert climate to regions with 100 mm to 200 mm of rainfall. Quinoa is also resistant to saline conditions (FAO, 2011). Quinoa was praised by NASA because of its future possibility to be grown on spacecraft for long-term space missions (Schlick and Bubenheim, 1993).

1.2.1. Morphology:

Figure 1.1 shows the internal structure of the Quinoa seeds. Quinoa is dicotyledonous plant with flat-oval shaped seeds. Seeds are shaped similar to a flattened sphere and their size varies from 1.4 mm to 1.6 mm (Varrianoo-Marston and DeFrancisco, 1984). The large central perisperm is the major storage region and is rich in starch. The embryo has rich reserves of lipids and some protein. The endosperm surrounds the embryo

in one or two layers and contains globoid crystals of protein in the matrix (Prego et al., 1998). The pericarp in quinoa seed contains saponins (Beatriz and Suzana, 2012). Saponins are the bitter anti-nutritional compounds that are believed to act like tannins in sorghum, protecting the seed from fungal infection and bird predation. The amount of saponins depends on the variety of quinoa.

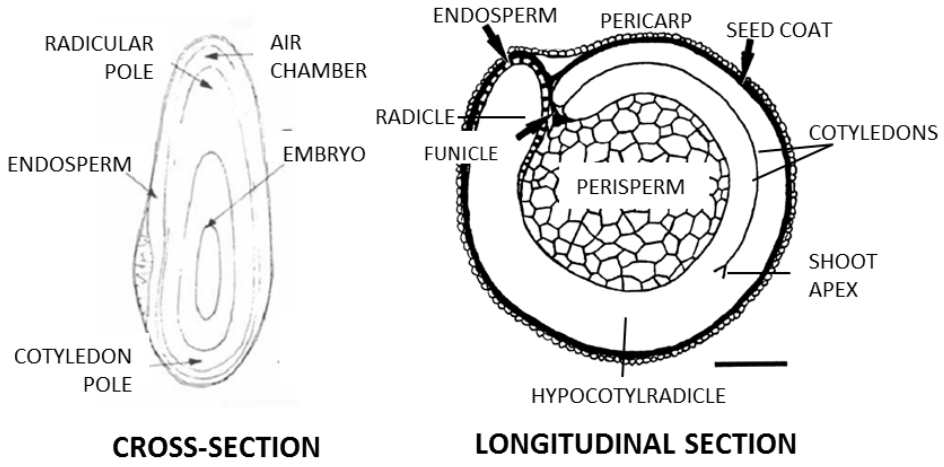

Figure 1.1: Internal structure of quinoa
(Image Source: Beatriz and Suzana, 2012)

Quinoa comes in a variety of colors from white, yellow, pink to black. The darker varieties have higher amounts of anthocyanins and betalains. Betalains are colored pigments that possess antioxidant properties like anthocyanins (Jacobsen et al., 2003) and are exclusively present only in Angiosperms and Caryophyllales. Betalains have broad pH stability whereas anthocyanins are widespread and exhibit narrow pH stability (Stintzing and Carle, 2004). The botanical classification of quinoa is shown in Table 1.1 and Fig. 1.2 shows images of the quinoa plant.

(a)

(b)

(c)

(d)

Figure 1.2: Images of quinoa grains and the plant

(a) Dark variety quinoa, (b) Quinoa Grains, (c) Quinoa seeds in the plant

(d) White Quinoa

Image Sources (Accessed on October 1, 2014):
http://www.wildflower.org/plants/result.php?id_plant=VAMA
http://gewoonlekkergroen.nl/wp-content/uploads/2011/09/quinoa.jpg
http://www.fao.org/docrep/019/ar895e/ar895e.pdf
http://plantfinder.sunset.com/plant-details.jsp?id=3359

Table 1.1: Quinoa botanical classification, (USDA)

RANK	SCIENTIFIC NAME AND COMMON NAME
Kingdom	**Plantae** – Plants
Subkingdom	**Tracheobionta** – Vascular plants
Superdivison	**Spermatophyta** – Seed plants
Division	**Magnoliophyta** – Flowering plants
Class	**Magnoliopsida** – Dicotyledons
Subclass	**Caryophyllidae**
Order	**Caryophyllales**
Family	**Chenopodiaceae** – Goosefoot family
Genus	***Chenopodium* L.** – Goosefoot
Species	***Chenopodium quinoa* Willd.** – Quinoa

1.2.2. Nutritional content:

Protein:

The protein rich seed contains 14.6 % (fresh weight) protein with a balanced amino acid spectrum and a rich availability of lysine and methionine. All ten essential amino acids namely, lysine, tyrosine, valine, isoleucine, phenylalanine, leucine, threonine, histidine, tryptophan and methionine are present in quinoa (Vega-Galvez et al., 2010). Non-essential amino acid histidine is also in abundance (FAO, 2011). The protein source of quinoa is in the form of storage proteins, albumins and globulins (Koziol, 1992). The major group is the 11s globulin called the chenopodin. It has two subunits A (22 kDa - 23 kDa) and B (32 kDa - 39 kDa). The protein quality of quinoa is equivalent to casein in terms of their Nitrogen Efficiency for Growth (NEG) value (Coulter and Lorentz, 1990). Quinoa is free of gluten and hence a useful source of protein for celiac patients. A comparison of the protein content of quinoa with other common cereals is shown in Table 1.2.

Table 1.2. Amino acid profile of quinoa compared with other common cereals (Ahamed et al., 1998)

Seed	Amino acid (g/100 g protein)							
	Trp	**Met**	**Thr**	**Ile**	**Val**	**Lys**	**Phe/Tyr**	**Cys**
Quinoa	1.1	2.6	4.4	4.2	4.8	6.3	8.9	1.4
Wheat	0.9	4.3	3.1	3.5	4.7	3.1	8.0	2.2
Oats	1.3	4.7	3.5	4.0	5.5	4.0	8.9	1.4
Soya bean	0.7	3.0	4.5	4.0	4.4	6.4	8.4	1.6
Corn	0.6	3.2	4.0	4.6	5.1	1.9	10.6	1.6
Rice	1.0	3.0	3.7	4.5	6.7	3.8	3.1	1.6

Starch:

Starch content of quinoa varies from 52.2 % to 69.2 % (USDA, 2005; Mundigler, 1998). The starch molecules are polygonal in shape and their size ranges from 0.7 µm to 3.2 µm (Qian and Kuhn, 1999). The Amylose content of starch is low (11 %) compared to other cereal grains and has an average chain length of 27 residues of de-branched starch molecule (Koziol, 1992). The gelatinization temperature of the starch is in the range 57 °C to 64 °C (Atwell, 1982). The other carbohydrates present are in the form of sugars and fiber. About 3 % of quinoa is in the form of simple sugars (Ranhotra et al., 1993). Some of the individual sugars present are maltose, D-ribose, fructose and glucose (Oshodi et al., 1999). Another 8 % of the quinoa grain is dietary fiber, which helps in eliminating toxins and in achieving satiety (Mundigler, 1998). Quinoa starch shows exceptional freeze thaw stability and resistance to retrogradation but shows low viscosity and solubility (Ahamed et al., 1996).

Lipids:

Quinoa is also popularly known as pseudo-oilseed crop because of the exceptional balance between oil and protein. On dry weight basis, quinoa contains about 9 % fat. Almost 58 % of this fat is polyunsaturated with over 90 % of it being linoleic acid. The PS ratio, defined as the ratio of polyunsaturated to saturated, is 4.9 in quinoa oil, which is comparable to that of corn oil (4.65) and higher than olive oil (3.92). Despite its high unsaturation, oxidative rancidity is prevented because of the presence of α-tocopherol. Oleic acid, at 24 %, dominates the monounsaturated category of quinoa lipids. Also, the free fatty acids content in quinoa (18.9 %) is higher than in wheat (11 %). This plays an important role in reducing incidence of arteriosclerosis, inflammation and thrombosis (Cusack, 1984; Ahamed, 1998; Przybylski et al., 1994; Youdim et al., 2000). A comparison of quinoa fatty acids composition with other common cereals is shown in Table 1.3.

Table 1.3: Oil quality of quinoa and common cereals grains (USDA, 2005)

	Quinoa	**Wheat**	**Barley**	**Rice**	**Corn**
Predominant acid	18:2	18:2	18:2	18:1	18:2
Saturated	13 %	23 %	26 %	32 %	16 %
Monounsaturated	34 %	22 %	16 %	37 %	31 %
Polyunsaturated	53 %	55 %	58 %	31 %	53 %

Sterols and minerals:

According to Ryan et al. (2007) quinoa contains considerable amount of squalene (33.9 mg/100 g - 58.4 mg/100 g), a sterol that helps in maintaining a healthy cardiovascular system (Nesaretnam, 2008). Phytosterols are also important dietary component as it helps in anti-inflammatory and anti-carcinogenic activities (Moreau et al., 2002). Reported

values of other sterols in quinoa are β-sitosterol at 63.7 mg/100 g, stigmasterols at 3.2 mg/100 g and 15.6 mg/100 g of campesterol. Lipid oxidation in quinoa occurs at lower rates due to the presence of Vitamin E (2.6 mg/100 g). Quinoa is also rich in mineral content, containing three times more iron and calcium content and two times more potassium than wheat. Apart from that, quinoa flour is also rich in iron, zinc, manganese and copper (Abugoch, 2009).

Saponin and phytic acid:

The seed coat or epicarp of quinoa contains saponins which are bitter in nature thus reducing the acceptability of this grain. Saponins are comprised of either monosaccharide or oligosaccharide moieties linked to steroidal aglycones or triterpenoid. When consumed in high amounts it can exhibit toxic anti-nutrient properties. Quinoa seeds contain around 1 % - 1.2 % saponins (Abugoch, 2009). Saponins can be removed by washing with water and polishing the seeds (FAO, 2011) before processing or consumption. Phytic acid (1 % d.m.) is another anti-nutrient present in endosperm and outer layer of quinoa. It makes minerals unavailable for metabolism by binding with them (Vega-Galvez et al., 2010). Koziol (1992), reported 10.5-13.5 mg/g phytic acid in five different varieties of quinoa. Ruales and Nair (1993) found that scrubbing and washing the seeds reduces phytic acid levels by 30 %.

Antioxidant and phenolics:

Laus et al. (2012) found that quinoa flour has a high ratio of free antioxidants to bound antioxidant, thus making them readily accessible during consumption. Most of the

phenolics present were in the conjugated form. Twenty three phenolics acids were found with predominating amounts of vanillic acid (63.45 mg/kg) and ferulic acid (37.52 mg/kg) derivatives. Among the flavonoids, quercetin-3-rutinoside (57.10 mg/kg) and kaempferol 3-galactoside (24.01 mg/kg) were the main constituents (Tang et al., 2014).

Table 1.4 gives an overall picture of quinoa nutrients compared with other common cereal grains.

Table 1.4: Proximate composition of quinoa seeds compared with that of other grains (Ahamad et al., 1998; Mundigler, 1998)

Seed	Moisture (%)	Ash (%)	Protein (%)	Fat (%)	Carbohydrate (%)	Crude Fiber (%)
Quinoa	12	3	14.5	7.5	68	8
Wheat	13	2	14	2	69	1
Oats	8	2	14	8	68	1
Rice	15	1	8	1	78	2
Maize	15	2	13	4	66	3
Sorghum	12	2	12	2	73	2
Soya bean	8	5	47	21	14	4
Barley	13	2-3	12	1	70	4

1.2.3. Global perspectives and economics:

The United Nations General Assembly paid tribute to quinoa by declaring the year 2013 as the “International Year of Quinoa” owing to its natural abundance of nutritional properties along with its adaptability to extreme climate. The governments of Andean region in South America prioritized development of quinoa sector by announcing investment programs and strategic plans. Bolivia and Peru are the major producers of

quinoa and Peru has increased its production by almost ten times since the mid-1990s (Fig. 1.3).

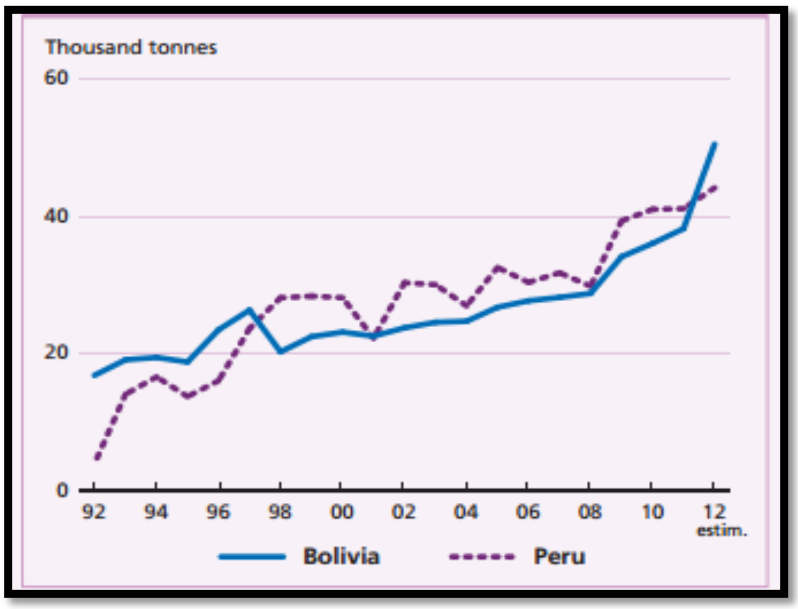

Figure 1.3: Quinoa production in Peru and Bolivia, FAO, 2013

Bolivia's export saw a steady growth from 2007 (10585 tones) to 2012 (25899 tones), meanwhile Canada, European Union and United states tripled their import during the same period. Quinoa export value increased six folds from USD 13.1 million in 2007 to USD 78.9 million in 2012. However, this dynamic growth in global market had led to the decline in per-capita consumption in Bolivia from (2.4 kg to 1 kg) since the mid-2000s and the because of the inequality in producer and consumer prices (Fig. 1.4). This shift of quinoa going from a traditional crop to a cash crop has led to emerging issues in the Andean countries. Some of them being, (i) whether the small scale traditional quinoa producers will be the direct beneficiary and (ii) the level of price increase consequently leading to a compromise in the nutritional benefits to the indigenous population (FAO, 2013).

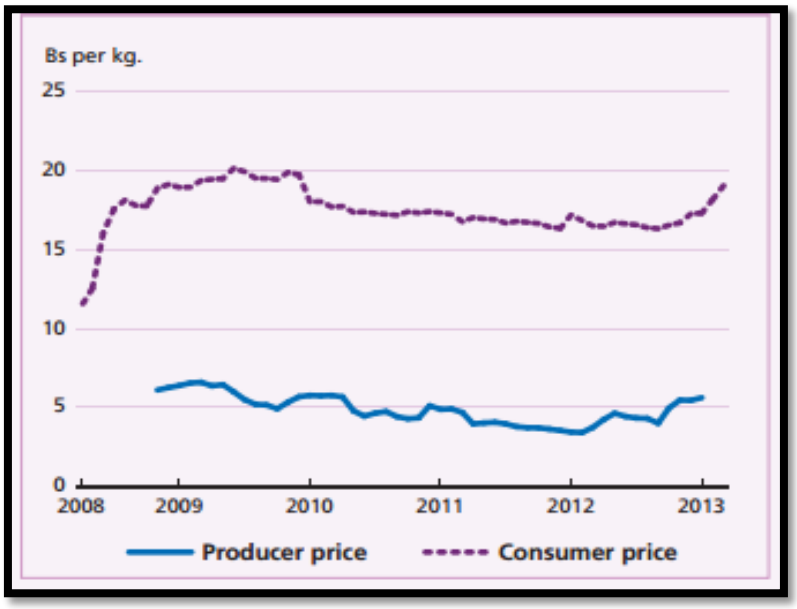

Figure 1.4: Consumer and producer price of quinoa in Bolivia (FAO, 2013)

1.3. Cassava:

The tropical crop Cassava (*Manihot esculenta* Crantz) is a woody perennial shrub and is native to the Amazon region and Central America. Cassava is commonly called by different names around the world. Some of them include tapioca, mandioca, yuca and manioc. Cassava flour obtained from cassava roots, is free of gluten and hence can be suitable for gluten-free diet for the population suffering from celiac disease. There are almost 100 species, but only *Manihot esculenta* Crantz is commercially cultivated.

1.3.1. Morphology:

Cassava is characterized by a bulky storage root (Brimer, 2014) and grows up to heights of 1 m to 4 m. About 88 % of production is used for human consumption worldwide and it is increasingly becoming the major cash crop of Africa (Tivana et al., 2010). The main storage region is the root which is a true root meaning that it cannot be used for

propagation. The number of roots per plant varies anywhere between 3-14 tubers with diameters ranging from 3 cm to 15 cm. More than 60 % of cassava root is made up of water. A mature cassava root can be distinguished into three regions. Bark (periderm) is made of few layers of cells and constitutes to 3 % of the total weight. The peel or the cortex forms 11 % - 20 % of weight containing the phloem, cortical parenchyma and sclerenchyma. The rest 85 % of the root weight is the parenchyma which is the edible portion that contains a matrix of starch cells (Wheatley and Chuzel, 1993). Table 1.5 shows the botanical classification of cassava.

Table 1.5: Cassava botanical classification, (USDA)

RANK	SCIENTIFIC NAME AND COMMON NAME
Kingdom	**Plantae** – Plants
Subkingdom	**Tracheobionta** – Vascular plants
Superdivison	**Spermatophyta** – Seed plants
Division	**Magnoliophyta** – Flowering plants
Class	**Magnoliopsida** – Dicotyledons
Subclass	**Rosidae**
Order	**Euphorbiales**
Family	**Euphorbiaceae** – Spurge family
Genus	***Manihot* Mill.** – cassava
Species	***Manihot esculenta* Crantz** – cassava

(a)

(b)

(c)

Figure 1.5: Images of cassava and the plant
(a) Cassava plant with roots, (b) Pictorial representation of cassava, (c) Cassava roots.
Image Sources (Accessed on October 1, 2014):
http://medicmagic.net/cassava-food-that-is-full-of-benefits.html
http://www.fao.org/ag/save-and-grow/cassava/en/1/index.html
http://theworldsmostunlikelyvegetarian.blogspot.com/2012/01/rachels-cassava-cookies.html

Figure 1.5 shows images of the cassava plant. Cassava starch is typically round in shape and has an average granule size of 15.6 µm. The Amylose/Amylopectin ratio is 20:80 (Tivana, 2010). Mejia-Aguero et al. (2012) reported the starch content of 25 cassava varieties to vary between 742 g/kg and 814 g/kg (dry basis) which is similar to potato starches (530–800) g/kg. Except seeds, all parts of the cassava plant contain cyanogenic glucoside, which is a toxin that causes death or paralysis when consumed in large amounts. The sweet varieties have less than 100 mg/kg fresh weight cyanogen and the bitter varieties can have up to 500 mg/kg fresh weight. The tubers carry the maximum concentration of around (1-40) mg/100 g fresh weight (Alves and Cunha, 2002). Cassava cyanides are classified according to how they are found in nature. There are three types, namely, bound glucosides, cyanohydrins and free glucoside. According to the type and proportion of these types of cyanides, cassava roots are processed differently to remove the cyanides. The data from Montagnac et al. (2009) given in Fig. 1.6 shows the different types of processing and their effect on cyanide removal.

Process	Retention %	Cyanogen glucoside mg HCN/kg
Fresh root	100	140
Boiling	55.5	77.6
Baking	87.1	122
Steaming	86.5	121
Frying	89.3	125
Changing size boiling (30 min)		
Fresh root	100	160
2-g pieces	25.6	41
5-g pieces	50	80
50-g pieces	75	120
Changing water ratio boiling (30 min)[b]		
Fresh root	100	165
Root:water (1:1)	69.6	115
Root:water (1:2)	36.7	60.5
Root:water (1:5)	24.2	40.1
Root:water (1:10)	22.3	36.8

Figure 1.6: Cyanide retention % after processing cassava roots (Image source: Montagnac et al., 2009)

Cassava roots are thus energy dense and rich in calories but their nutritional value is lower than that found in root tubers, cereals and legumes. It has low protein content and low fat content. However, mineral content of cassava flour is comparable to many legumes (except soybeans) and has relatively high amount of calcium (15 mg to 35 mg per 100 g edible portion) and vitamin C content (15 mg to 45 mg per 100 g edible portions) in the roots (Montagnac et al., 2009).

The cassava starch used in this study has 31.85 % pregelatinized starch. Gelatinization is defined as the process in which starch molecules swells and absorbs water under heat. Gelatinization of starch molecules alter the properties and functionally of the starch at various levels.

1.3.2. Pre-gelatinization:

Gelatinization is a process where semi crystalline structures of the starch molecules (amylose and amylopectin chains) break down due to heat and water resulting in starch polymer dispersion in solution. Native cassava starch has gelatinization onset temperature of 58.54 °C and a conclusion temperature of 68.14 °C (Rocha et al., 2010). By means of chemical, physical or enzymatic gelatinization, the properties of native starch can be modified to suit specific applications. Native cassava starch shows high cohesiveness, poor flow properties and high sensitivity to shear. Whereas, pre-gelatinized starch exhibits cold swell properties, better flow-ability, gel forming ability and also have good compaction. Also, Pre-gelatinized starch granules allow penetration of water at 30 °C, whereas in native form, the crystalline structure does not allow water to penetrate below 60 °C (Zhang et al., 2013).

The cassava flour used in this study had 31.85 % pre-gelatinized starch. The rest of the flour was in its native state. Therefore this combination of native and pre-gelatinized flour can be termed as partially pre-gelatinized cassava starch (PPCS). This kind of flour has demonstrated better process ability and thermal/shear stability. It also required lower heat for cooking and gelatinization. For example, in pharmaceutical formulations, PPCS as a result of partial cold water solubility character, showed both binding and disintegrating properties (Zhang et al., 2013).

1.3.3. Global perspectives and economics:

Cassava, the 21st century crop, has grown from being a food for the poor to a multipurpose crop by contributing to the economy and use in the developing countries. The world's annual cassava production has increased since the 2000s and an estimated 100 million tons of cassava has been produced owing to its demand, driven by Asia for dried cassava and starch for use in industrial applications and livestock feed in tandem with Africa's demand for more cassava food products to ensure food security. Nigeria and Brazil are the leading producers of cassava (UK AID, 2012). Although Nigeria is the world's leader in production (25575 tons annually), Thailand is the major exporter with almost 6000 tons/ year. Global production in 2013 is forecasted as 1 % increase from 2012, but it has been in the rise for the fifteenth consecutive year. Some virulent plant disease such as the brown steak disease has been rising alongside due to the intense yield/production expansion. This calls for more genetic modifications to improve robustness of the crop (FAO, 2013).

In 2011 high maize prices was the driving force to replace maize with cassava (UK AID, 2012). Figure 1.7 shows the recent developments in maize price reduction which contributed to an increased competitiveness for cassava starch in 2013 (FAO, 2013).

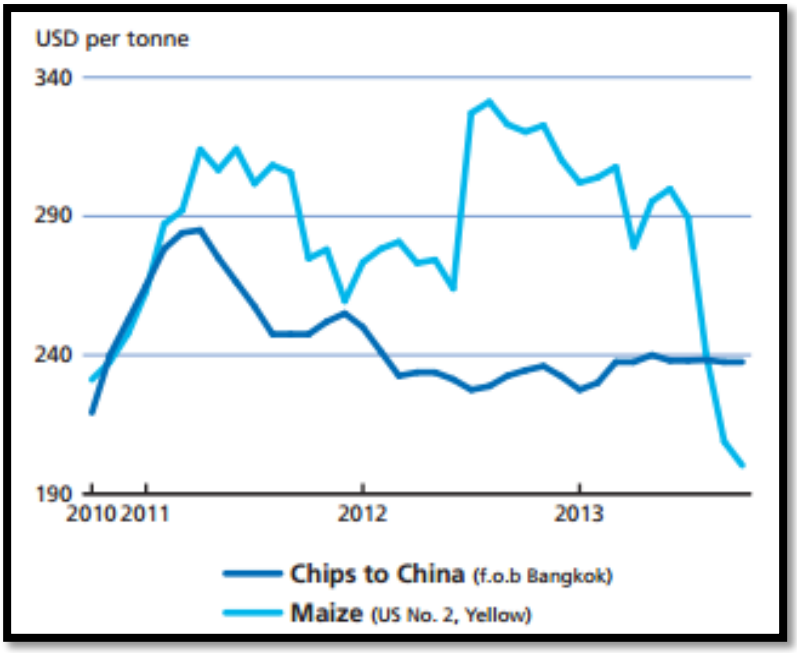

Figure 1.7: Maize and cassava chip prices (FAO, 2013)

1.3.4. Cassava in extrusion:

Cassava starch has many favorable properties for extrusion such as low gelatinization temperature (71 ^{o}C), clarity, low tendency to retrograde, bland taste, high viscosity, non-cereal flavor, high water binding capacity, and high degree of expansion (Nabeshima and Grossmann, 2001; Sriburi and Hill, 2000, Jyothi et al., 2005). Extruded products from cassava starch show a closed structure, light color, smooth surface, and have neutral flavor (Chang et al., 1998). Very few studies have been done on extrusion using only cassava flour. Mostly cassava flour has been used in combination with other flours

like pigeon pea flour (Rampersad et al., 2003), jatobá flour (Chang et al., 1998), cassava bran (Hashimoto and Grossmann, 2003). It has been combined with soybean flour, soybean oil and wheat bran (Badrie and Mellowes, 1991) to increase the protein and other nutrient content of cassava flour whereas the cassava flour improves the extrudability of the proteinacious materials. In a study by Badrie and Mellowes (1991) the effects of various extrusion variables including feed moisture content, temperature, screw speed, feed particle size, and feed rate on the physical properties (expansion, color, bulk density, water solubility and water absorption) of the extrudates were evaluated. Optimum expansion ratio (2.82) was found at 11 % feed moisture, (120–125) °C barrel temperature, 520 RPM screw speed, and 250 g/min feed rate. Chang and El-Dash (2003) found that addition of sulfuric acid (0.06 N) in cassava starch during extrusion resulted in softer and crispier extruded products. Leonel et al. (2009) found high moisture, low screw speed, and intermediate temperature provided lower starch degradation during extrusion for cassava starch.

Extrusion processing involves conversion of starch which can be measured in terms of the degree of gelatinization. In studies, where the extents of gelatinization of starch (wheat and corn) in extruded products and their structural attributes were measured (Case et al., 1992), it was found that maximum bulk density occurred between 55 % -75 % gelatinization of the extruded product.

1.4. Cranberry:

American Cranberry *(Vaccinium macrocarpon Aiton)* is one among three commercially available fruits in North America, only next to blueberry and concord grape (McKay and Blumberg, 2007). It is a perennial shrub and grows up to 1 ft - 3 ft in height.

Cranberry grows low, prostrate and has leathery, small and glossy leaves. Pine Barrens in New Jersey and Cape Cod in Massachusetts are the places that grow cranberry extensively. It requires wet and acidic (pH < 6.8) soil conditions and grows well in part shade (Wildflower center, 2013). About 95 % of cranberries in the USA are consumed as processed products. Some examples are sweetened dried cranberries, canned sauces and juice drinks. The remaining 5 % are sold as fresh cranberries (NAAS 2010). The botanical classification of American Cranberry is shown in Table 1.6.

Table 1.6: Cranberry botanical classification, (USDA)

RANK	SCIENTIFIC NAME AND COMMON NAME
Kingdom	**Plantae** – Plants
Subkingdom	**Tracheobionta** – Vascular plants
Superdivison	**Spermatophyta** – Seed plants
Division	**Magnoliophyta** – Flowering plants
Class	**Magnoliopsida** – Dicotyledons
Subclass	**Dilleniidae**
Order	**Ericales**
Family	**Ericaceae** – Heath family
Genus	***Vaccinium* L.** – Blueberry
Species	***Vaccinium macrocarpon* Aiton** – Cranberry

Cranberries contain naturally low amounts of fat and sodium and hence they are low in calories. Cranberry is said to have a broad spectrum of bioactive compounds and a majority of them are in the form of phenols and phytochemicals. Table 1.7 shows some of their other active substances (Viskelis et al., 2009; Uwieczkowska et al., 2004). Figure 1.8 shows the structure of anthocyanin aglycone. Glycosylation of the anthocyanidin aglycone

at position 3 gives rise to the formation of cranberry anthocyanins. (Cunningham et al., 2001).

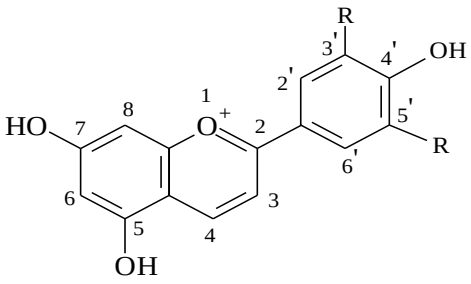

Figure 1.8: Chemical structure of anthocyanin
(Image Source: Cunningham et al., 2001)

Table 1.7: Active compounds in cranberry

Active compound	Amount
Ascorbic acid	13.7 to 28.5 mg/100g
Phenolic compounds	192.3 to 676.4 mg/100 g
Titratable acids	2.2 % to 2.3 %
Sugars	3.66 % to 4.90 %

Concentrates and pomace are by products of the cranberry processing industry. White et al. (2011) showed that cranberry skins had more anthocyanins (1705.2 mg/100 g based on dry wt), than peeled fresh fruits (101.5 g/100 g) while cranberry pomace retained about 15 % of cranberry anthocyanins during juice extraction. This shows the importance of cranberry industry by-products, and calls for research focus on using such products. Figure 1.9 illustrates the cranberry plant, physiology and the fruits.

(a)

(b)

(c)

Figure 1.9: Cranberry plant and fruits
(a) Image of cranberry shrub, (b) Fruits of cranberry, (c) Illustration of cranberry plant
Image Sources (Accessed on October 1, 2014):
http://commons.wikimedia.org/wiki/File%3AVaccinium_macrocarpon_%E2%80%94_Flora_Batava_%E2%80%94_Volume_v14.jpg
http://en.wikipedia.org/wiki/Cranberry#mediaviewer/File:Cranberries20101210.jpg
http://www.easybloom.com/plantlibrary/plant/american-cranberry

The major classes of phytochemicals identified in cranberries include phenolic acids such as benzoic acid and hyroxycinnamic acid, stilbenes such as reservatrol and flavonoids such as flavonols, flavan-3-ols and anthocyanin's (McKay and Blumberg, 2007). Of these, the predominant ones are the flavonoids that include the anthocyanins and the flavan-3-ol, particularly proanthocyanidins. Proanthocyanidin belong to a class of condensed tannins which acts as free radical scavengers and anthocyanins are phenols that are water soluble pigments which can act as natural food colorant. HPLC analysis revealed the presence of 6 anthocyanins namely, cyanidin-3-galactoside (20.5 %), cyanidin-3-arabinoside (19 %), cyanidin-3-glucoside (2.3%) peonidin-3-galactoside (32.7 %), peonidin-3-arabinoside (6.7 %) and peonidin-3-glucoside (3.5 %). Cyanidin-3-galactoside's antioxidant activity is higher than monoglycosides of quercetin and myricetin in cranberries. Quinic acid is exclusively present only in cranberry juice and is often used as an indicator to detect the amount of cranberry juice in a product (Cunningham et al., 2001).

Radical scavenging activity of ethanol extracts from cranberries ranged from 64.3 % to 81.4 %. Among various common fruits cranberry contained the highest amount of phenolics, has the highest antioxidant activity and antiproliferative effect on cancer cells. Apart from this, cranberry and their juice extracts shows antimicrobial properties and has been historically used for treating Urinary Tract Infection (UTI). This unique ability of cranberry to act against UTI is due to the ability of its proanthocyanidins to exhibit anti-adhesion properties for *E. coli* in the uroepithelial cell wall lining. The unusual A-type double linkages found in its structure is the cause for this effect. Food sources like chocolate, grape green tea and apple have proanthocyanidin with B-type linkages that does

not show preventive activity against bacterial cell wall adhesion (Prior et al., 2009). Other micro-organisms such as *Bacillus cereus* and *Micrococcus luteus* have shown sensitivity to cranberry extract (Viskelis et al., 2009).

Cranberry juice concentrate "essence returned" used in this study was donated by Ocean Spray Cranberries Inc. (Lakeville-Middleboro, MA). The term essence returned means that the volatile flavors that were trapped by condensation during the extraction process have been returned to the concentrate to achieve a product that has flavor closer to cranberries. The typical process by which the concentrate was obtained is as follows. A patented (Mantius and Peterson (), 1995) counter-current extraction process where the skin of cranberries is penetrated to expose the fruit to a counter current extraction liquid is used. The extraction liquid is pure water (with no added enzymes). The apparatus is a continuous moving helical screw conveyer which advances the fruit along a path while flowing extraction liquid uniformly and counter-currently. Berries are tumbled during the process and 75 °F process temperature is maintained. Such low process temperature ensures that high quality juice is obtained. Grace et al. (2012) found that cranberry anthocyanins were less stable and more sensitive to heat during juice processing than proanthocyanidins. A 2 °Brix juice obtained from this stage is de-pectinized using enzymes and then ultra-filtered using (0.1-0.5) micron pore size filters. The 2 °Brix juice is then passed through a reverse osmosis stage wherein the juice is concentrated further by passing it under pressure through a membrane system. This results in an 18 °Brix product. At this stage the product has low amounts of tannins (1900 mg/L) and has no off flavors. This also corresponded to 96 % fruit soluble solids recovery. Finally this product is concentrated through evaporation at higher degrees of heat (~ 165 °F) to 50 °Brix.

1.5. Extruder:

Extrusion can be defined as a process in which food material is forced out through an orifice or die. The final product takes shape depending upon the shape and geometry of the die. Extrusion process can be historically traced back to Archimedes time where he used a single screw inside a cylindrical open channel to convey water uphill. Later in the 1870s sausage manufacturing was done using extruders. In the early 1930s pasta was manufactured by mixing semolina and water using a single screw. High shear products like corn puffs came into commercial production in the 1940s (Karwe, 2003). Since then extrusion processing has been used extensively in the food processing industry.

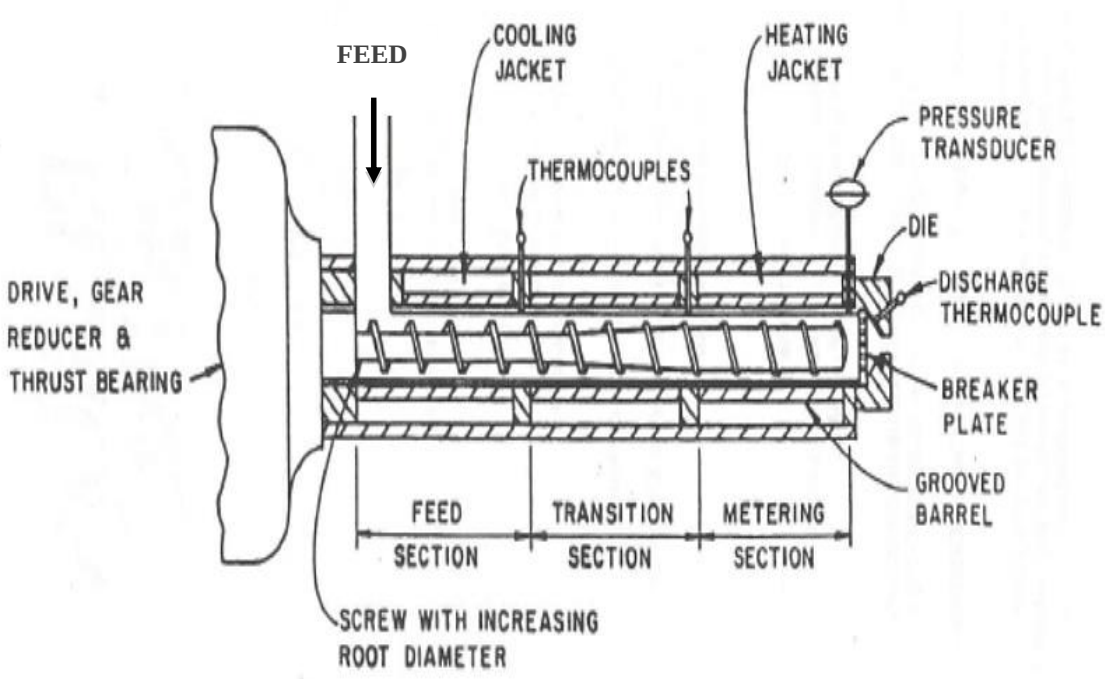

Figure 1.10: Schematic of a single screw extruder

A typical extruder in today's commercial use can be broadly classified into two major categories, namely, single-screw and twin- screw extruders. As the names suggest, a single screw has one screw that rotates inside the barrel and a twin screw has two screws

that rotates together in either co-rotating or counter-rotating manner. In our study we used a single screw extruder. Figure 1.10 shows some major components in a single screw extruder.

The extruder consists of three zones namely feed section, transition section and metering section. The feed material is fed through a hopper in the feed section and the temperature of this section ranges from 30 °C to 70 °C. The transition section is where the feed gets compacted and experiences high shear due to the increase in the screw root diameter. The conveyed feed then goes to the metering section where it gets cooked at high barrel temperatures ranging from 110 °C to 200 °C. Most single screw extruders have groves, helical or longitudinal, on the inner wall of the barrel to promote adhesion and friction forces. The screw in a single screw extruder is characterized by L/D (Length to Diameter) ratio and C.R. (Compression Ratio). The geometrical parameters of a single screw are shown in Fig. 1.11.

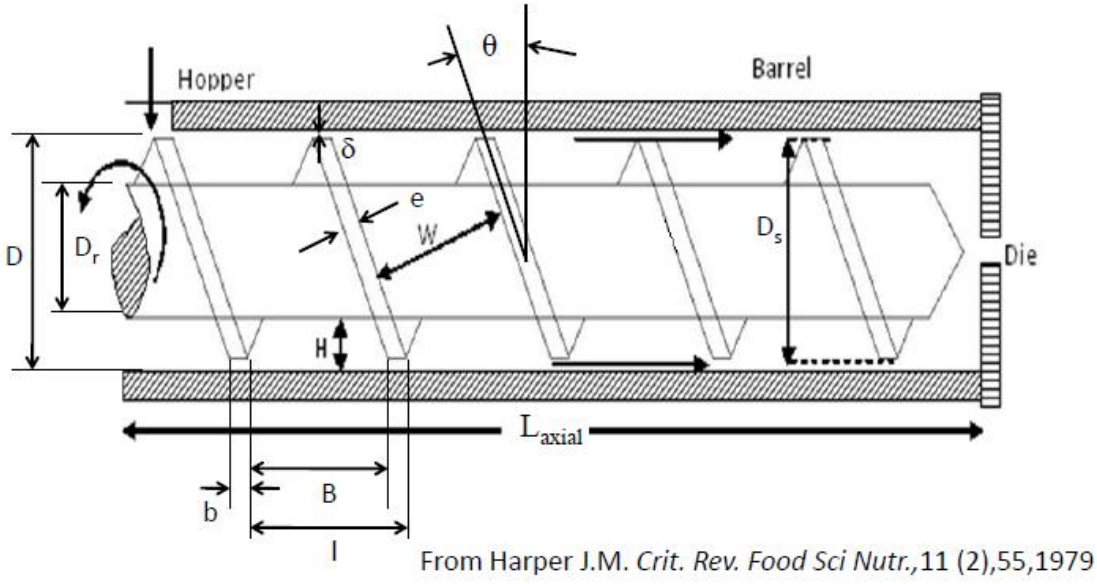

Figure 1.11: Screw configuration

where,

D = bore diameter

D_s = screw tip diameter

D_r = screw root diameter

H = gap between screw root and barrel

W = channel width perpendicular to flights

δ = radial clearance between the barrel and the screw tip

θ = helix angle

L (lead) = distance between consecutive flights, measured on the same side of the face of flights at D_s

B = axial channel width

b = axial flight width

e = flight width measured perpendicular to screw flights

L axial = axial length of the screw

p (pitch) = distance (axial) covered in one revolution

L/D = the distance from the internal rear edge to the discharge end of the barrel, divided by the bore diameter. Food extruders L/D ranges from 1:1 to 25:1.

C.R. = Compression ratio refers to the increase in screw root diameter which in turn ties to the volume fill near the feeding section and the die section. Typically C.R. ranges from 1:1 to 5:1.

The flow profile inside an extruder channel is majorly due to two counteracting flows namely the drag flow and pressure flow. Drag flow conveys the feed forward towards the die and is enhanced by friction and adhesion forces between the feed and the barrel.

The pressure flow pushes the feedback from the die because of the die pressure and causes the feed to mix well. The resultant net flow pushes the feed outside through the die.

Single screw extruders are majorly classified according to their screw configuration. Shear profiles inside the extruder are created by the screw configuration and barrel dimensions. Table 1.8 shows major classifications of single screw extruder according to their screw geometry and shear profiles.

Table 1.8: Single screw classification (Riaz, 2000)

	Low shear	Medium shear	High shear
Shear rate (1/s)	5-10	20-100	100-180
Diameter to channel height ratio	3-5.3	5-8.5	8-18
Compression ratio of screw	1:1	2-3:1	3-5:1
Length to diameter ratio	5-8	10-20	4-12
Screw Speed (RPM)	Less than 100	Greater than 100	Greater than 100
Parallel flow channels (n)	1	2	2 or 3
Feed Moisture (% w.b.)	25-35	20-30	12-20
Maximum Barrel Temperature (°C)	20-65	55-145	110-180
Energy conversion (kW/kg)	0.01-0.04	0.02-0.08	0.10-0.16
Product Examples	Pasta and Meat products	Semi-moist pet food and textured soy	Breakfast cereals and RTE snacks

Extrusion is a thus a High Temperature Short Time process (HTST) where temperatures go up to 200 °C for 1 s to 10 s (Riaz, 2000). Coupled with the mechanical

energy input, the heat and shear causes feed material to melt inside the extruder resulting in a high viscous fluid. This thermo-mechanical process helps in intensifying phenomena such as mass, heat and momentum transfer inside the screw-barrel assembly of an extruder. As a result, a number of unit operations and functions such as laminar mixing, grinding, shearing, conveying, agglomeration, degassing, dehydration, sterilization, homogenization, texturization and shaping along with chemical reactions and physical transformation like gelatinization, protein denaturation, flavor degradation, caramelization and lipid oxidation happens simultaneously. All these factors put together makes the end products to have very different characteristics in terms of both physical and chemical profile.

The versatility of extruders to produce a myriad of products makes extrusion a lucrative food processing technology. They are low cost - energy efficient and it is a high throughput process. Most importantly extrusion is environmental friendly process as it produces very little or no waste streams. Process scale up is much easier when compared to other food processing technologies such as retorting (Riaz, 2000). The low moisture cooking process in extruders considerably reduces downstream drying costs.

1.6. Breakfast cereals:

Directly expanded snack products such as RTE snacks and breakfast cereals are products that experience high shear stress in the extruder (Table 1.8). At low moisture contents (15 % - 22 % (w.b.)) and at high temperature (120 °C – 200 °C), food biopolymers like starch and protein convert into melt inside the extruder. Starch gelatinizes and dextrinizes while protein denatures. Gelatinization and uptake of water by the starch

component contributes substantially to the viscosity and the protein constituents play a role in impacting the elasticity and gas holding properties of the melt. As temperature and pressure build up inside the extruder, the superheated steam causes vapor pressure build up in the melt. When exiting the die the drop in pressure to external atmospheric pressure causes the moisture to rapidly flash into steam thereby inflating the melt. A proper elastic melt will turn into a porous friable texture, characteristic of breakfast cereal, as it sets. Mechanisms such as velocity distribution within die, viscous dissipation and elasticity affect the product characteristics (Frame, 1994). These mechanisms are in turn dictated by the factors such as feed composition, moisture content, mechanical shear and the barrel temperature. Every feed material is unique in its own way, as it alters and contributes to the characteristics of the final product by forming distinct macro and microstructures. Hence, in order to obtain an optimum process condition, it is important to understand and study these various factors that affect the physico-chemical properties of the extrudates.

1.7. Major physico-chemical changes during extrusion:

The amount or extent to which the complex carbohydrates such as starch and proteins modify depends on the extruder parameters. The physical and chemical functionality of the final product change according to the process conditions. In general the amount and type of biopolymer along with the moisture content affect the final product property in extrusion cooking (Hashimoto et al., 2002). The opening up of the tertiary and quaternary structures of the proteins results in breakdown and rearrangement of hydrogen and disulfide bonds. This in turn aids in plasticization and texture formation.

The transformation phenomenon affects product properties due to starch-lipid-protein interactions and the involvement of other small compounds such as salt and sugar. Most of these transformations are irreversible unlike those that happen at low temperatures and pressures. It is suggested that the limiting factor in such transformations during extrusion at temperatures below 110 °C is reaction rate and water diffusion rate above 110 °C (Linko et al., 1985).

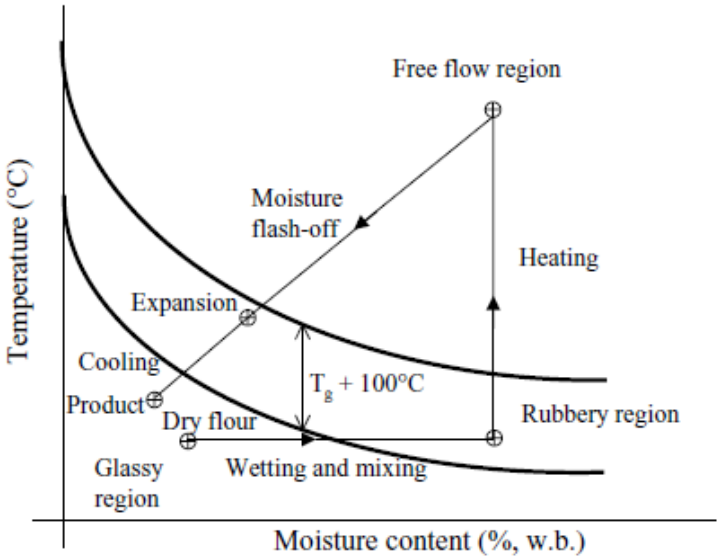

Figure 1.12: Typical phase transition during extrusion (Image source: Kokini et al., 1994)

The typical path of the extrusion process is shown in Fig. 1.12 which shows the effect of biopolymer transformation such starch degradation and protein denaturation. As starch cooks and undergoes denaturation and, the molecular weight changes due to random chain scissions. An important parameter affected due to this, is the glass transition temperature (T_g). It is a well-known fact that the molecular weight affects T_g. It is a highly important determinant of food texture as well as processing operations. Hydration of flour causes the glassy state of flour to go through to the rubbery amorphous state near the glass

transition temperature. Depending on the extrusion condition, after extrusion, the cooling off region might fall either into the rubbery region or the glassy region. Glassy product is crunchy whereas rubbery product is chewy (Karwe, 2003).

1.8. Effects of extrusion of physico-chemical properties:

Starch:

Starch is a polysaccharide and forms a melt as it undergoes gelatinization and fragmentation. The amylose: amylopectin ratio is an important determinant in how the starch transforms inside the extruder. Amylopectin is the branched structure and is more prone to fragmentation than amylose. An increase in specific mechanical energy input results in more breakdown of starch. As starch undergoes transformation, the T_g of the material is affected. Also the screw configuration influences the amount of starch breakdown. Under high shear conditions, starch can breakdown into glucose and dextrins, the process often known as dextrinization. In common terms, the overall disruption of granular structure, swelling and solubilization causes gelatinization and is influenced by the presence of lipids, salt, sugar and protein content. Non-ionic species like sugars increase the temperature needed for gelatinization by depressing the enthalpy of gelatinization. Starch digestion is made easier after extrusion as it makes it more readily available for amylolytic enzymes (Brennan et al., 2013).

Protein:

The other major biopolymer that determines the final product properties is the type and amount of proteins. Protein denatures during extrusion which subsequently improves

its digestibility. In general protein transformation mechanisms involve denaturation, association such as crosslinking, formation or disruption of covalent bonds. It is proven that vegetable protein nutrition is improved upon extrusion because of new sites opening up for enzyme attack. Solubility of proteins in water or salt solutions is observed to decrease after extrusion (Della Valle et al., 1994). Moisture content, screw speed and barrel temperatures affect the available lysine content. Lysine degradation is an indicator of protein degradation. A general suggestion to minimize lysine degradation is not to go higher than 180 °C barrel temperature and not below 15 % feed moisture (Singh et al., 2007). The reducing sugars react with the terminal amines of free amino acids and produce complex products, including Maillard reaction products. Fibrous texture to mimic meat products, formation of gels and emulsions, novel textures such as and cheese analogs are some examples of how protein modifications can be made using extruders.

Lipids:

Lipids are the class of non-polar heterogeneous chemical compounds including triglycerides, phospholipids, sterols, and waxes. Lipid content over 6 % generally reduces extruder performance by reducing the torque. Product expansion is compromised because of insufficient pressure development due to reduced slip between screw and barrel walls. Lipids in extrudates are reported to reduce after extrusion possibly due to loss of free oil at the die or because of the formation of lipids complexes between proteins or amylose. Extrusion denatures hydrolytic enzymes, which minimizes free-fatty acid release and subsequent oxidation of products. Some other factors like formation of Maillard reaction intermediates and complex compound formation also reduces oxidation. However

presence of lipids causes rancidity in extruded products (Singh et al., 2007; Brennan et al., 2012).

Vitamins:

Owing to the variety in their structure and composition, degradation of vitamins during extrusion cannot be generalized. In general higher extrusion temperatures cause loss in vitamin content. Over 50 % of trans β-carotene is reduced in wheat bran at 200 °C barrel temperature. Added Vitamin C was protected by the presence of 1 % blueberry concentrate and 50 % retention was observed when it was used as an aid in cassava starch (0.4 % - 1 %) conversion. Vitamin D, K (lipid soluble) and Niacin, riboflavin (water soluble) are fairly stable during extrusion. However, thiamine stability is highly variable (5 % - 100 %). About 63 % of vitamin E degraded during buckwheat extrusion. High screw speed and moisture content lead to riboflavin decrease (Singh et al., 2007; Riaz, 2000).

Minerals:

Solid crystalline chemical elements that cannot be synthesized or decomposed by ordinary chemical reactions are called minerals. They are present in small amounts but are increasingly important for nutrition and essential for certain enzyme related reactions. Changes in these small molecules are not affected by extrusion directly as extrusion generally affects the macromolecular structures. But the changes in macromolecules indirectly affect these mineral compounds. For example, it is reported that presence of dietary fiber interferes with mineral bioavailability by reorienting during extrusion. Also some polyphenols such as tannins acts as an inhibitor by hindering mineral absorption. On

the contrary iron bioaccessibility is increased in almost all extrusion process. Copper, phosphorous and calcium bioavailability also increases in extrudates because of the added water and leaching from extruder barrel walls. In peas, phytates hydrolysis occurred during extrusion causing mineral release. However, fortification with mineral compounds like calcium reduces expansion and added iron cause dark discoloration in extrudates (Singh et al., 2007).

Phenolic compounds:

Fruits and grains are naturally rich in phenolic compounds which exhibit antioxidant capacity and protect against diseases. Extrusion of pulses-cereal blend is reported to increase the phenol content, especially when using whole grain or colored grain. For instance, raw red-dark bean extrudate showed 14 % increase in phenolics as opposed to a 21 % decrease in cream colored beans, because of an 84 % increase in quercetin and 40 % increase of ferulic acid in the red-bean extrudate. Tannin-protein complex forms when protein is denatured and tannin can act as free radical scavenger when ingested. Significant increase in free/bound phenolic acids like coumaric acid syringic acids from buckwheat maybe caused due to the release of these compounds from the matrix during extrusion. Yet, free phenolic compounds such as chlorogenic acid, found in potatoes, is shown to significantly decrease after extrusion. In general high barrel temperatures seems to retain more phenolics possibly due to formation of insoluble compounds while low feed moisture caused loss of phenolics (Brennan et al., 2011).

1.9. Similar projects from literature:

- Potter et al. (2013) used fruit powders (apple, strawberry, banana and tangerine) at 11 % to find that children liked fruit flavored extrudates.
- Taverna et al. (2012) made acceptable extrudates from a single screw extruder using 10 % quinoa and 90 % sour cassava. Extrudates processed at 15% feed moisture, 250 rpm and 100 °C barrel temperature were found to have optimum physical properties.
- White et al. (2010) mixed cranberry pomace (30:70, 40:60, and 50:50 pomace/corn starch DW) and concluded that significant loses of anthocyanin and total antioxidants occurred during extrusion.
- Using a twin screw extruder Chaovanalikit et al. (2003) extruded corn breakfast cereals with blueberry concentrate and studied the effect of ascorbic acid addition on anthocyanin retention. They also found that addition of ascorbic acid accelerated anthocyanins degradation and also did not prevent browning reactions.

The uniqueness of this project lies in that fact that we used an industrial by-product (cranberry concentrate) to make value-added extrudates. Using this concentrate, in place of dried powder, is beneficial because it excludes the extra unit operation of drying. To our knowledge, this study is the first attempt to have such high substitution amounts of quinoa (50 %) in any given food product. Of utmost interest is the demonstrated cut-ability of this feed material that has sugars from concentrate that make it sticky at the die exit.

2. RATIONALE

A schematic representation of the rationale is depicted in Fig. 2.1. It explains that cassava will aid quinoa during extrusion and improve its physical properties. Quinoa will in turn provide the nutrition that is absent in cassava. By being a natural colorant, the cranberry concentrate will contribute to antioxidant and phenolic values.

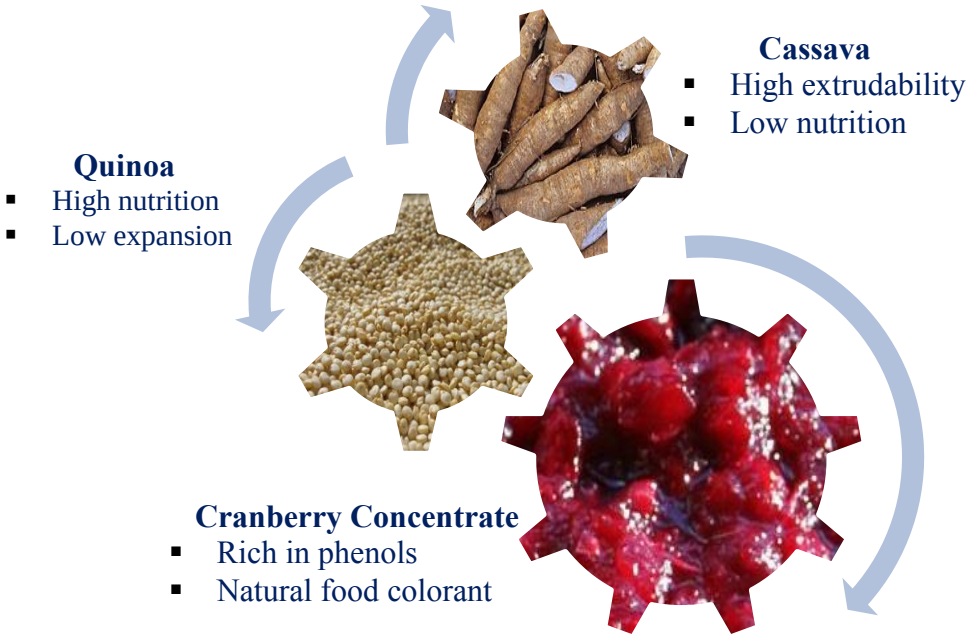

Figure 2.1: Schematic representation of rationale

- Quinoa (*Chenopodium quinoa* Wild) the pseudocereal contains a balanced amino-acid spectrum with high lysine and methionine content. It also provides good fiber and antioxidants such as squalene and tocotrienols.
- Cassava (*Manihot esculenta* Crantz), a major tropical food crop has many favorable properties for extrusion such as low gelatinization temperature, clarity, low

tendency to retrograde, non-cereal flavor, high viscosity, high water binding capacity, and high degree of expansion.

- Cranberry *(Vaccinium macrocarpon* Aiton) a major commercial crop in North America is rich in secondary plant metabolites such polyphenols, proanthocyanidins, anthocyanins, flavonols and phenolic acids.

2.1. Objectives:

- To extrude a RTE breakfast cereal with high nutrition raw materials like quinoa and cranberry concentrate, by using cassava as an extrusion aid, owing to its high starch content.
- To understand the effect of extrusion on Quinoa-Cassava-Cranberry concentrate extrudates, by evaluating and studying their physical and chemical properties at various process conditions.
- To use Response Surface Methodology to evaluate the independent and interaction effects of the input variables and process conditions on the physico-chemical properties of the extrudates.

3. DESIGN OF EXPERIMENTS

A 3^3 Box- Behnken Design (BBD) was used to design the experiments for the three independent variables or factors at three levels. The factors chosen were, barrel temperature (120 ˚C, 140 ˚C, 160 ˚C), feed moisture (16 %, 18 %, 20 % (w.b.)) and cranberry solids (3 %, 4 %, 5 % (d.b.)). As opposed to performing 81 runs for a 3^3 full factorial design, BBD allows to obtain Response Surface Models (RSM) with 15 experimental runs (12 + 3 center points). The number of runs is determined by the equation $N = 2p\ (p-1) + C_p$ where p are number of factors and C_p is number of central points (Swamy et al., 2014).

Box- Behnken Design (BBD) belongs to a class of second order rotatable designs and the experimental points are chosen from the center points of the cube edges as depicted in Fig. 3.1. According to Ferreira et al. (2007) BBD is more efficient than Central Composite and Full Factorial design. Another advantage of this design is that it avoids the combination of extreme levels (cube edges) and is also economical.

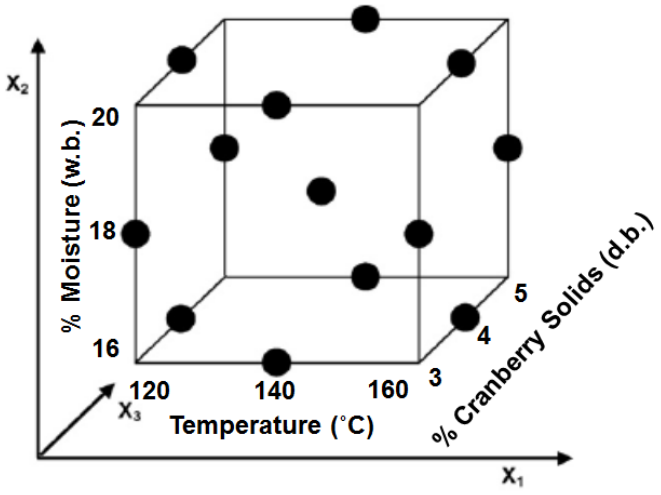

Figure 3.1: Graphical representation of Box Behnken Design (Adapted from Ferreira et al., 2007)

With the help of BBD, a RSM is used to study, optimize and evaluate the interaction effects (ex. Barrel temperature * Feed Moisture), quadratic effects (ex. Feed moisture^2) and main effects (ex. cranberry solids). RSM is a statistical and mathematical technique that helps in improving, quantifying and determining the functional relationship between a response and control or input variable in a given process. When changing the thermo-mechanical history of the product inside the extruder, RSM gives information and explains how a process parameter would affect product transformation.

The measured response y for a nonlinear quadratic Response Surface Model is given by the following model equation, Eq. (3.1).

$$y = \beta_0 + \beta_1 x_1 + \beta_2 x_2 + \beta_3 x_3 + \beta_{11} x_1^2 + \beta_{22} x_2^2 + \beta_{33} x_3^2 + \beta_{12} x_1 x_2 + \beta_{13} x_1 x_3 + \beta_{23} x_2 x_3 \quad \text{(Eq. 3.1)}$$

where, $\beta_0$is the model constant, β_{11}, β_{22}, β_{33} are the quadratic coefficients and β_{12} β_{13} β_{23} are cross product coefficients (Aslan and Cebeci, 2007). The independent variables are: $x_1 = Barrel\ Temperature$, $x_2 = Feed\ Moisture$ and $x_3 = Cranberry\ Solids$.

Six responses namely Radial Expansion Index (REI), Bulk Density (BD), Breaking Strength (BS), Water Absorption Index (WAI), Water Solubility Index (WSI), Hue, Chroma, Total Phenol Content (TPC) and Anthocyanins were studied. Table 3.1 and Table 3.2 show coded and un-coded levels of BBD, respectively. SAS version (9.2) was used to perform the statistical analysis.

Table 3.1: Coded values of BBD

Code	-1	0	1
Barrel Temperature (°C)	120	140	160
Feed Moisture (% w.b.)	16	18	20
Cranberry Solids (% d.b.)	3	4	5

Table 3.2: Coded and Un-coded levels

Run Number	Coded			Un-coded		
	x_1	x_2	x_3	Barrel Temperature (°C)	Feed Moisture (%)	Cranberry Solids (%)
1	-1	-1	0	120	16	4
2	1	-1	0	160	16	4
3	-1	1	0	120	20	4
4	1	1	0	160	20	4
5	0	-1	1	140	16	5
6	0	-1	-1	140	16	3
7	1	0	1	160	18	5
8	-1	0	1	120	18	5
9	1	0	-1	160	18	3
10	0	1	1	140	20	5
11	-1	0	-1	120	18	3
12	0	1	-1	140	20	3
13	0	0	0	140	18	4
14	0	0	0	140	18	4
15	0	0	0	140	18	4

4. MATERIALS AND METHODS

4.1. Raw materials:

The following information is obtained from their respective manufacturers specification sheets.

- Organic whole grain Quinoa flour (Product No. 1448) was brought from Bob's Red mill (Milwaukie, Oregon). It was coarse flour which had a creamy tan color and possessed a mild grain-like aroma.
- Cassava flour (Premium) was supplied by American Key Food Product (Closter, New Jersey). It had a creamy white appearance and 31.85 % was pre-gelatinized starch.
- Ocean Spray Cranberries Inc. (Lakeville-Middleboro, Massachusetts), donated cranberry juice concentrate (essence returned). It had a typical dark (cranberry red) and typical tart fruit flavor with no off odors. The concentrate was depectinized and treated by Ocean Spray Cranberries to achieve a five log pathogen reduction.

All the materials were stored in airtight container and kept cool at 4 °C. Flours were kept dry.

4.2 Proximate values:

Proximate analysis for quinoa and cranberry was provided by Bob's Red mill, and Ocean Spray Cranberries, respectively. Cassava proximate was taken from Charles et al. (2005). Table 4.1 shows proximate values for the raw feed material.

Table 4.1: Proximate analysis of quinoa, cassava and cranberry concentrate

Proximate analysis (Per 100 g)			
	Cassava	**Quinoa**	**Cranberry**
Carbohydrates (g)	83.8	59.87	46
Protein (g)	1.5	13.17	< 0.7
Lipid (g)	0.2	5.67	< 0.7
Fiber (g)	2.5	6.67	0
Ash (g)	1.8	2.23	0
Moisture (g)	10.3	12.4	52.67

4.3. Flour blend:

Quinoa flour and Cassava flour were blended using a Hobart mixer in the ratio of 50:50. Preliminary experiments (Fig. 4.1) showed the impact of cassava flour addition at equal proportions to quinoa flour, in terms of extrudate expansion. Even higher proportion of cassava flour would have achieved much more expansion, but that would have compromised the nutrient contribution from quinoa. To this blend, cranberry concentrate was added according to the design of experiments.

Figure 4.1: Effect of cassava addition (Quinoa : Cassava)

4.4. Moisture analysis:

A Sartorius moisture analyzer MA-30 000V3 (Göttingen, Germany) was used to measure the moisture content of flour, extrudates and concentrate. Moisture analysis is important during extrusion as it is one of the major control variables that contribute to both process and product variability. In general, to prevent extruder overloading, the raw material needs a minimum of 16 % w.b. feed moisture.

Analysis was performed based on Eq. 4.1 after warming up the moisture analyzer for at least 30 minutes. Approximately 1 g – 1.5 g of sample was evenly spread in a tarred aluminum pan. Analysis was performed in the fully automated mode at 110 °C. The principle behind this analyzer is that it determines the weight loss of the sample simultaneously as it heat dries the sample using infrared dark radiator tubes.

$$Moisture\ \% = \frac{Initial\ weight - Final\ weight}{Initial\ weight} * 100 \qquad \text{(Eq. 4.1)}$$

Three replicate values of moisture were measured to achieve better accuracy. The moisture content of Quinoa: Cassava flour blend was in the range of 10.15 % - 10.25 % (w.b.) and the cranberry concentrate had 47 % - 48 % moisture (w.b.).

4.5. Extruder:

A C.W. Brabender (Hackensack, New Jersey) single screw extruder equipped with a PL-2100 motor drive (Type DR-2072) was used for conducting the experiments. A single tapered screw with 4:1 compression ratio was used in all experiments, based on the experience from the preliminary experiments. Compression ratio approximately denotes the ratio of the channel depth near feed section to the channel depth near metering section. In our case, this equated to the screw geometry which had a root diameter of 11.35 mm at

the feed section and 17.1 mm near the die. The screw has an L/D ratio of 20:1 and a uniform pitch with a helix angle of 18.29 °. Samples were collected from a cylindrical single hole die, 4.5 mm in diameter and 5 mm in length. A spring loaded twin blade cutter was used to cut the samples. The screw compression ratio and die geometry was selected after various preliminary experiments (data not shown).

4.6. Flour preparation:

In order to attain the final desired feed moisture, the inherent moisture contribution from the cranberry concentrate was taken into account. Distilled water was then added to achieve the desired final value. Flour, concentrate and distilled water were then blended and mixed in a planetary Hobart mixer (Model K5-A) for 5 minutes. Any large lumps formed were sieved through a US No.10 sieve (2 mm opening). The lumps were then broken down using a motor pestle and added back to the remaining flour. After mixing well, this conditioned flour was kept to hydrate and equilibrate at 4 °C for 24 h in a stainless steel container covered with Aluminium foil. After equilibration, the flour was brought back to room temperature on the day of extrusion. Moisture was measured to a precision of ±0.20%.

4.7. Extrusion:

The extruder was set at the desired barrel temperature and allowed to attain equilibrium for minimum of 30 min. A PID (proportional, integral and derivative) controller helped maintain extruder temperatures at preset limits. The feed section temperature was always kept constant at 60 °C for all experiments. The temperature of the

transition and metering section was set according to the design. For all experiments, the screw speed was set at 130 RPM and feed rate was kept constant at 70 RPM using a C.W. Brabender screw feed hopper. The experimental runs according to Table 3.2 were conducted in a random order and under steady state conditions. A steady state characterized by torque stability and constant mass flow rate was achieved for all experiments, except at 160 °C. After the system achieved steady state, samples were collected in cylindrical rods and spherical balls (using the cutter, set at 25 RPM). A Forma Scientific® 391 drying oven was used to dry the extrudates at 40 °C for 24 hours. Dried extrudates were stored in Aluminium covered glass bottles and flushed with nitrogen. The samples were kept at 4 °C until further analysis.

4.8. Sample preparation for analysis:

Extrudates were ground using a motor pestle and passed through US No. 35 sieve (500 µm opening). The powdered sample was used to measure extrudate moisture, TPC, WAI, WSI, Hue and Chroma.

4.9. Radial Expansion Index:

Radial Expansion Index (REI) is defined as the ratio of diameter of the extrudate to the diameter of the die (Eq. 4.2).

$$REI = \frac{D_e}{D_d} \quad \text{(Eq. 4.2)}$$

where D_e is the diameter of the extrudate and D_d is the diameter of the die. The diameter was measured using a Manostat, Switzerland (15-100-500) Vernier calipers. Cylindrical extrudate samples of about 60 mm in length were chosen and a minimum of 10 values of

extrudate diameter were recorded for each rod. At least 10 such rods were randomly chosen and a total of 100 diameter values were recorded per sample.

4.10. Bulk Density:

Bulk density (BD) is defined as the ratio of mass of the extrudate to the volume of the extrudate (Eq. 4.3) (Barret and Peleg, 1992). Since the uncut extrudates were very close to a cylindrical shape, the glass beads method was not used to measure the bulk density. Ten randomly chosen extrudate cylinders were weighed in a Metler Toledo AE 200 balance separately and their respective length and diameters were noted down. Using Eq. (4.3), the BD values were calculated and expressed in g/ml.

$$Bulk\ Density = \frac{Mass\ of\ extrudate\ cylinder}{Volume\ of\ extrudate\ cylinder} = \frac{4*m}{\pi* D_e^2* L_e} \quad \text{(Eq. 4.3)}$$

where m is the mass of the extrudate, D_e and L_e are the diameter and the length of the extrudate, respectively.

4.11. Breaking Strength:

A CT3 Brookfield Texture Analyzer (Middleboro, MA) shown in Fig. 4.2 equipped with a TA-VBJ Volodkevitch bite jaw probe-receptor was used to measure the Breaking Strength (BS) of the extrudates. This method can measure the perceived hardness when biting the extrudate between the molars. Breaking strength or peak stress is an expression of hardness and is defined as the maximum force per unit area of the extrudate that is required to break the sample into two pieces (Atre, 2011). Ten randomly chosen extrudate rods were placed in between the probe and receptor. A trigger force of

0.07 N was set. This is the amount of force the probe should sense before starting to measure the breaking strength. During measurement a compression test was used and the probe was lowered at 1 mm speed until the extrudate broke in two pieces.

Figure 4.2: CT3 Brookfield texture analyzer with TA-VBJ Volodkevitch bite jaw probe receptor

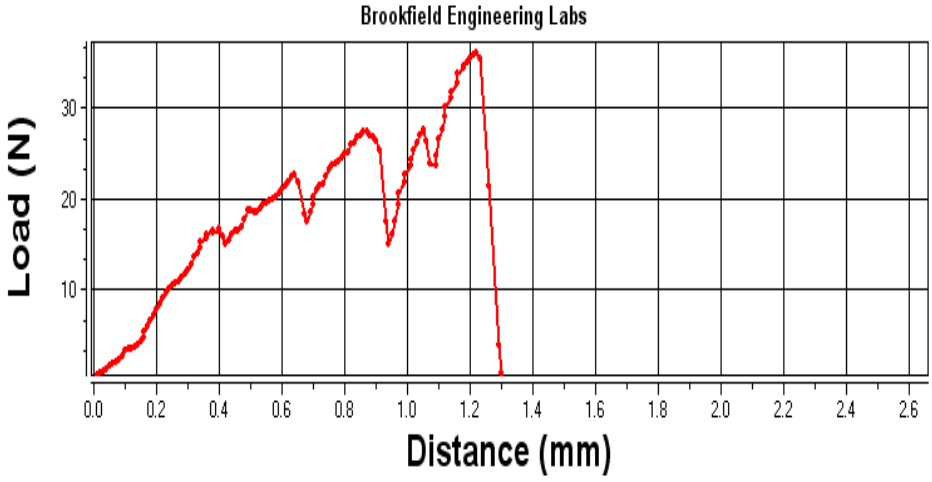

Figure 4.3: Typical texture graph on load vs distance

A typical force-distance curve is shown in Fig. 4.3. The peak stress was recorded using TexturePro CT software. Breaking strength is expressed in N/mm^2 as shown in Eq. (4.4).

$$Breaking\ Strength = \frac{Maximum\ load\ to\ break\ extrudate\ (N)}{Area\ of\ cross\ section\ of\ extrudate\ (mm^2)}$$

(Eq. 4.4)

4.12. Color:

Konica Minolta CR-410 colorimeter (Tokyo, Japan) was used to measure the color of extrudates. Following Berrios et al. (2004) method, ground extrudate samples were made to pass through US No. 35 sieve and placed in a white opaque base. Calibration was done with a white plate for D_{65} standards (Y = 94.7, x = 0.3156, and y = 0.33199). Munsell color system (Fig. 4.4) was used to measure the Hue and Chroma of extrudates. The standardized values of L*a*b* (CIE lab color space) were measured and converted to Munsell color system (Zhang et al., 1998). Each sample was measured three times and the mean values were noted. Human perception is more closely related to CIE lab scales as the eye perceives colors as pairs of opposites. L^* represents brightness and a larger number indicates it is lighter in color, a^* represents greenness (-value)/redness (+value) and $b*$ represents blue (-value)/yellow (+value). In the Munsell color system, VAULE or L^* is the y-axis which represents the lightness or darkness. Chroma is defined as the amount of saturation or purity of a particular color (Fig. 4.5) and Hue is the angular representation of color and is expressed in terms of degrees, starting from Red at 0° to Yellow at 90°, then Green at 180° to Blue at 270° as explained in Fig. 4.4. Therefore Chroma (Eq. 4.5) indicates how red (shade) the sample is (Wrolstad et al., 2005) and the hue degree (Eq. 4.6) indicates what color class (either red or yellow) the extrudates belong in.

$$Chroma = \sqrt{(a^{*2} + b^{*2})} \quad \text{(Eq. 4.5)}$$

$$Hue = h_{ab}^{\circ} = \tan^{-1}\frac{a^*}{b^*} \quad \text{(Eq. 4.6)}$$

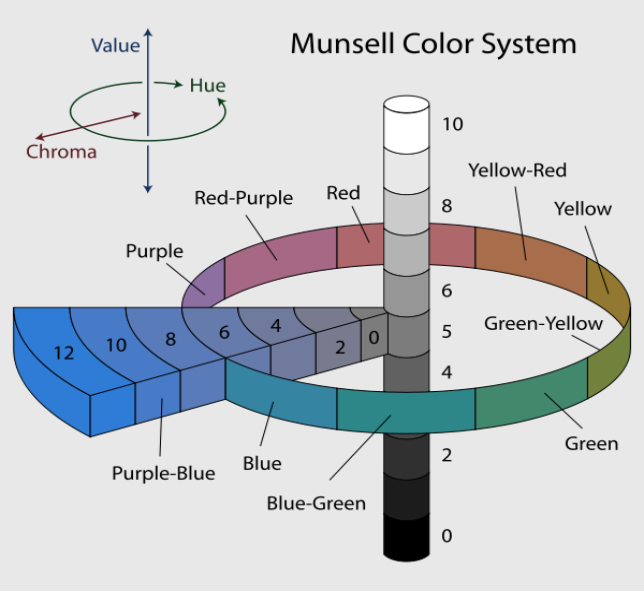

Figure 4.4: Munsell color system
(Image source: Cochrane, 2014)

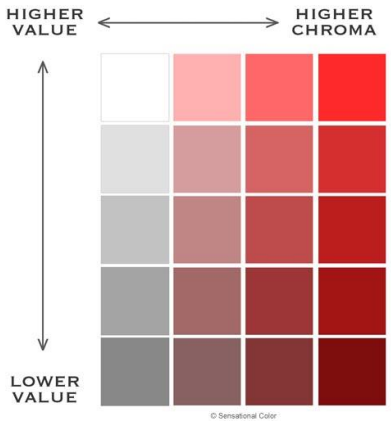

Figure 4.5: Representation of chroma values

Image source, Accessed on Oct 1, 2014:
http://www.sensationalcolor.com/understanding-color/color-theory/characteristics-of-color-5150#.U-1a9vldXUU

4.13. Water Absorption Index and Water Solubility Index:

Water Absorption Index (WAI) (Eq. 4.7) is commonly used as an indicative technique for measuring starch gelatinization and shows the swelling capacity of the starch (Ding et al., 2006) whereas starch degradation or dextrinization is measured in terms of Water Solubility Index (WSI) (Eq. 4.8) (Kirby et al., 1988). A slightly modified method of Anderson et al. (1969) was used to perform the analysis for WAI and WSI. Tarred 50 ml centrifuge tubes were filled with 2.5 g of ground sample (passed through US No 35 sieve). 25 ml of distilled water was used to suspend the ground sample. After vortexing for 15 sec, the centrifuge tubes were kept in the shaker for 30 min. The resultant slurry was centrifuged (using a Thermo Scientific Model, Sorvall Legend X1R) at 10,000 g for 10 min. The supernatant was separated and the dry solids were measured using a moisture analyzer. The remaining gel weights in the centrifuge tube were noted down.

$$WAI\ \left(\frac{g}{g}\right) = \frac{weight\ of\ sediment(gel)\ \ (g)}{dry\ solids\ in\ sample\ \ (g)} = \frac{(w_e + w_w - w_s) - (w_e + w_m + w_{ss})}{(w_e + w_m + w_{ss})} \qquad \text{(Eq. 4.7)}$$

$$WSI\ (\%) = \frac{water\ soluble\ matter\ (g)}{dry\ solids\ in\ sample\ (g)} * 100 = \left(\frac{w_{ss}}{w_e - w_m}\right) * 100 \qquad \text{(Eq. 4.8)}$$

where,

$w_e = Mass\ of\ ground\ extrudate\ (2.5\ g)$

$w_w = Mass\ of\ distilled\ water\ (25\ g)$

$w_s = Mass\ of\ supernatant\ (g)$

$w_m = Mass\ of\ moisture\ in\ flour\ (g)$

$w_{ss} = Mass\ of\ solids\ in\ supernatant\ (g)$

4.14. Total Phenolic Content:

An adapted and modified method of Singleton and Rossi (1965) was used to determine the Total Phenolic Content (TPC) of the extrudates, flour and the cranberry concentrate. Quantitative determination of phenolic compounds is done using the Folin-Ciocalteu (FC) test. The principle of this technique lies in the ability of phenol to reduce the Folin-Ciocalteu reagent in an alkaline medium. The yellow molybdotungstophosphoric heteropolyanion is reduced to a molybdotungstophophate blue (Nunzia Cicco et al., 2009). The blue pigment absorption spectra has a maximum at 765 nm. The absorption was measured using the Bio-tek spectrophotometer (Synergy HT) (Winooski, Vermont) (Fig. 4.6).

Figure 4.6: Spectrophotometer

Gallic acid was used as a standard and a curve for absorption at 765 nm was plotted for gallic acid concentration ranging from 0.05 mg/ml to 0.25 mg/ml. One gram of sample was suspended in 10 ml of 80 % methanol and was kept to rotate in a Nutating (Fisher Scientific ®, Pennsylvania) shaker for 60 min. This solution was then centrifuged at

10,000g for 10 min. The supernatant (extract) was removed and the volume was measured. 250 µl of extract/gallic acid solution was taken in a test tube to which 250 µl of freshly prepared Folin-Ciocalteu (diluted 1:1 with distilled water) was added. After five minutes, 500 µl of saturated sodium bicarbonate (20 % (w/v)) solution was pipetted into the test tubes. A final volume of 5 ml was reached by the adding 4 ml of distilled water. This was kept in dark and incubated at room temperature for 60 min. The blue solution sans any precipitate was pipetted into a 96 well plate (Fig. 4.7). Measurement was done in triplicates for each sample and values were expressed in mg GAE/100g dry weight.

Figure 4.7: 96-well plate with standards and extracts

4.15. Anthocyanins:

The test for anthocyanin content of the extrudates and raw material was performed by Ocean Spray Cranberries Inc. (Lakeville-Middleboro). An AOAC HPLC method as described by Brown and Shipley (2011) was used for quantification of the anthocyanins. The primary anthocyanins of Cranberries are cyanidin-3-*O*-galactoside (C3Ga), peonidin-3-*O*-galactoside (P3Ga), cyanidin-3-*O*-arabinoside (C3Ar), peonidin-3-*O*-arabinoside

(P3Ar), and smaller amounts of petunidin-3-*O*-galactoside and cyanidin-3-*O*-glucoside (C3Gl).

Equipment: A HPLC system, Agilent HP1100 (Santa Clara, California) Series liquid chromatograph equipped with a Cosmosil C18 (5C18-PAQ) Reverse Phase column (Waters Corp., Milford, MA), 5 mm particle size, 4.6 mm x 150 mm was used for this study. Attached with a 2D ChemStation Software (G2175AA), the HPLC had a quaternary pump and degasser (G1354A). A 10 mm, 13 mL, 120 bar (G1315-60012) flow-cell was used. The detection was done using a diode-array detector (G1315B).

Solutions: The extraction solvent was a methanol (40 %) - HCl (98%). The mobile phase A (MPA) used was water–phosphoric acid (99.5 + 0.5,); and the mobile phase B (MPB) was water–acetonitrile–glacial acetic acid–phosphoric acid (50.0 + 48.5 + 1.0 + 0.5). The ratios are in v/v basis.

Analysis: The auto-sampler temperature was maintained at 4 °C and the column was kept at 25 °C. The injection volume was 5 µL and the flow rate was kept at 0.9 mL/min. With a total run time of 35 min (5 min post time equilibration), the gradient elution was as follows: Time, min / % MPB: 1, 10; 28, 50; 32, 75; 32.1/10; 35/10. As shown in Fig. 4.8, the order of elution for the mixed standard was C3Ga (15.8–15.9 min), C3Gl (16.7–16.9 min), C3Ar (17.7–17.9 min), P3Ga (18.3–18.5 min), and P3Ar (20.2–20.4 min).

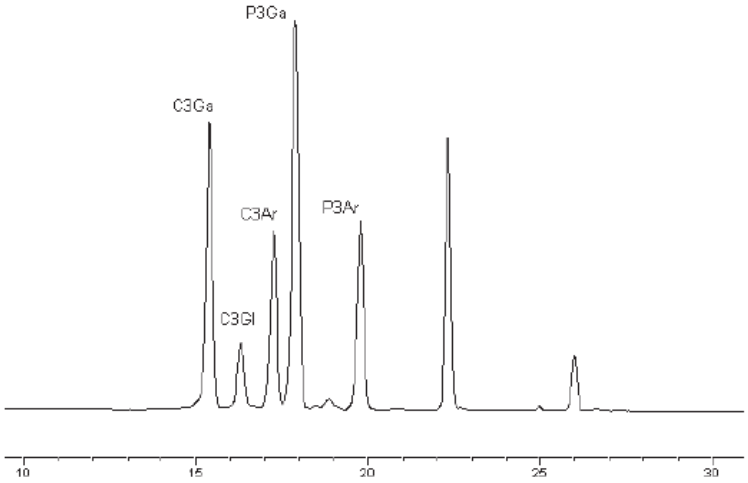

Figure 4.8: Typical cranberry anthocyanin chromatogram.
The order of anthocyanin elution in a mixed anthocyanin standard shown as absorbance units (y-axis) per min (x-axis).
(Image source: Brown and Shipley, 2011)

Sample preparation: Around 0.250 g of ground powder passed through the 60 mesh was weighed in a 50 mL conical tube. 20 mL extraction solvent was added to the ground powder and vortexed for 10 s. After centrifugation at 5000 rpm for 5 min, the supernatant was decanted into a 25 ml volumetric flask and brought to volume with extraction solvent. After mixing well, 1 mL of the solution was passed through a 0.45 mm Teflon filter into an amber HPLC vial.

Individual anthocyanins from the extrudate powder and cranberry concentrate were calculated using Eq. 4.9 and Eq. 4.10, respectively.

$$\frac{P_0 - b_0}{m_0} \times \frac{V}{W} \times \frac{D}{100} \qquad \text{(Eq. 4.9)}$$

$$\frac{P_0 - b_0}{m_0} \times D \qquad \text{(Eq. 4.10)}$$

where,

P_0 = peak area of target analyte in sample chromatogram,

b_0 = *y*-intercept of calibration curve for the target analyte

m_0 = slope of calibration curve for the target analyte

V = volume of test solution in mL

W = dry weight of sample in g,

D = dilution factor = 1.

4.16. Specific Mechanical Energy:

Specific Mechanical Energy (SME) is a characterization of the extrusion process. It is the amount of mechanical work input into the feed material from the drive motor. The mechanical energy is thus dissipated as heat energy inside the extruder (Guerrero et al., 2012). Melt rheology and shear conditions developing inside the extruder reflect on SME values (Akdogan, 1996). SME influences product properties such as Bulk Density, Breaking Strength, WSI and REI. The single screw extruder we used had a rated power of 6.21 kW. The mass flow rate (M_f) values were obtained by collecting the extrudates for 30 s and weighing the mass. The extrudate moisture, immediately after exiting the die was estimated from Fig. 4.9. SME was then calculated using Eq. (4.11).

$$SM = \frac{((Torque\ \% - Friction\ torque\ \%) * 6.21 * Experiment\ screw\ speed\ (130\ RPM)}{100 * Max\ screw\ speed(226\ RPM) * M_f}\ (kJ/kg)$$

(Eq. 4.11)

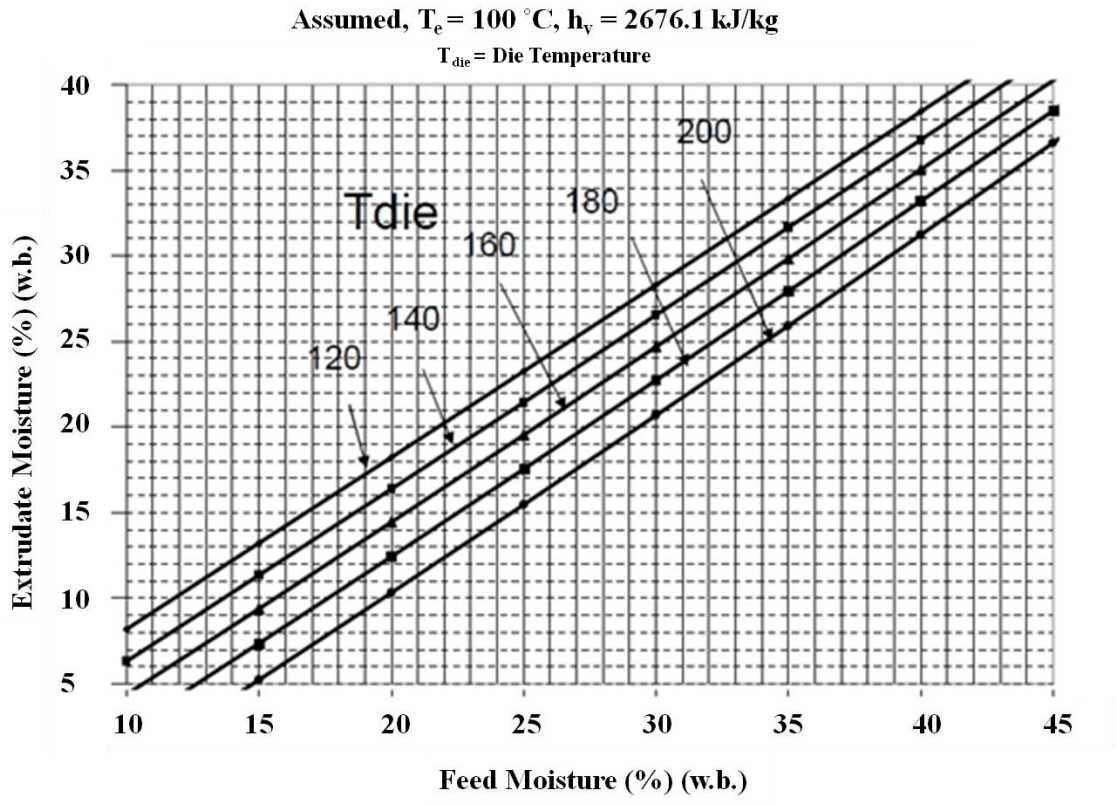

Figure 4.9: Extrudate moisture estimation graph (Karwe, 2014)

Figure 4.9 was obtained by applying heat and mass balance before and after the die. h_v stands for specific enthalpy of water for saturated vapor. T_e stands for boiling point of water at 0.1 MPa. T_{die} values are in °C (Karwe, 2014).

5. RESULTS AND DISCUSSION

5.1. Regression analysis:

Product responses, affected by the independent parameters are represented by means of regression analysis. The coefficients were calculated on the coded levels.

C: Model Constant

T: Barrel Temperature (°C)

M: Feed Moisture (% w.b.)

S: Percentage cranberry solids (% d.b.)

T*T: Quadratic effects of barrel temperature

M*M: Quadratic effects of feed moisture

S*S: Quadratic effects of cranberry solids

T*M: Interaction effects of barrel temperature and feed moisture

T*S: Interaction effects of barrel temperature and cranberry solids

M*S: Interaction effects of feed moisture and cranberry solids

In Response Surface Analysis, the linear, quadratic, and interaction effects of independent parameters on product parameters are expressed in two ways; master model equation and predictive model equation. Master model takes into account all the factors (linear, interaction, and quadratic) and thus has higher value of correlation coefficient whereas predictive model considers only the significant factors ($p < 0.05$) affecting the particular product response and thus has lower value of correlation coefficient. Table 5.1 shows the values for correlation coefficient for all the responses measured in this study. Since the design of experiments were done using BBD, Fig. 5.1 shows the BBD in cubic form with barrel temperature on the x-axis, % moisture on the y-axis and % cranberry solids on the z-axis. The run/experiment numbers are marked on each point. The

corresponding extrudates are marked in Fig. 5.2. Spherical extrudates could not be cut in run numbers 12-15 (processed at 160 °C) because of occasional extruder surging at such high barrel temperatures. Appendix has ANOVA and FIT statistics for all responses namely, REI, Bulk Density, Breaking Strength, WAI, WSI, Hue, Chroma, TPC and Anthocyanins.

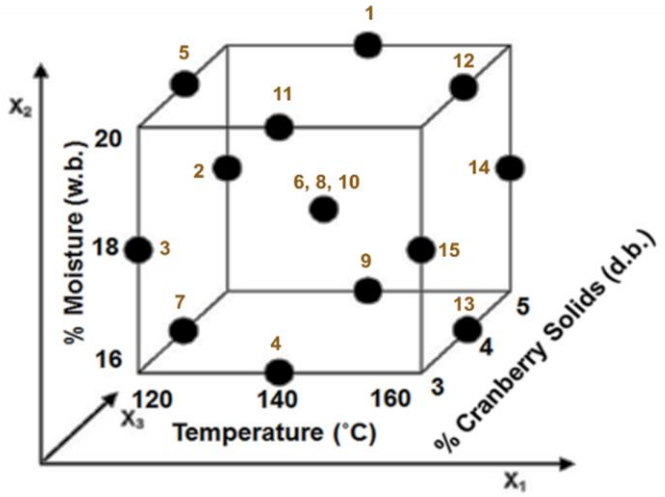

Figure 5.1: BBD with run numbers marked.

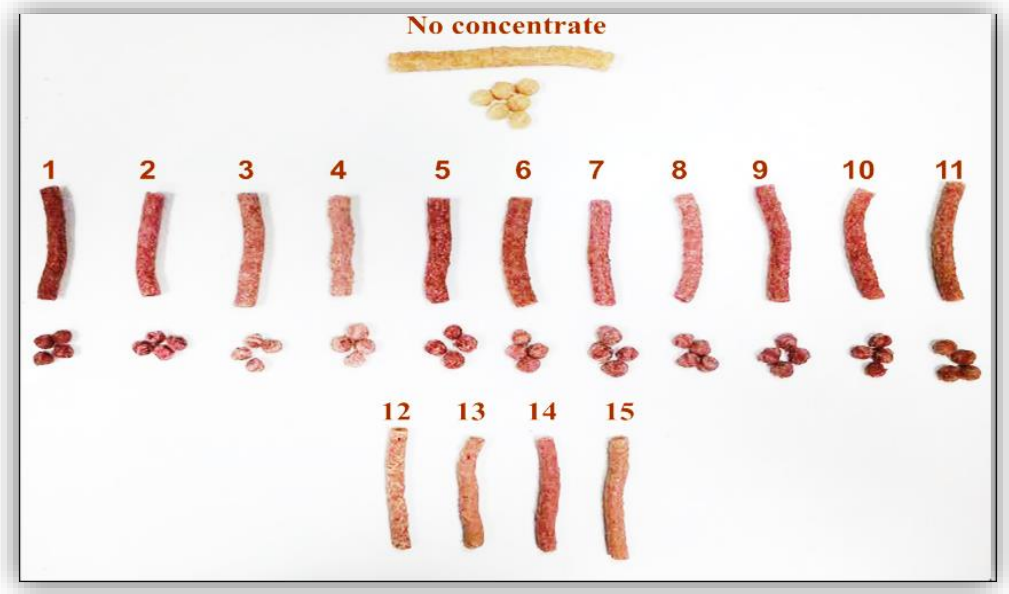

Figure 5.2: Extrudates with run numbers marked corresponding to BBD shown in Fig. 5.1

Table 5.1: Results of regression analysis

Levels	REI	Bulk Density (g/ml)	Breaking Strength (N/mm^2)	Hue (°)	Chroma	WAI (g water/ g d.s.)	WSI (%)	TPC in (mg GAE/100 d.s.)	Anthocyanins in (mg/100 d.s.)
T	**-0.114****	**-1.633****	-0.140	**6.873****	**0.939****	**-0.633****	**5.959****	**3.734****	**0.779***
M	**-0.101****	**0.054****	**0.159***	-0.204	0.220	0.150	**-1.516***	**-3.705****	-0.643
S	**-0.040***	0.024	0.074	**-8.729****	**1.071****	-0.015	0.133	**3.254****	**1.249****
T×T	0.016	**-0.087****	**-0.243***	**3.223****	0.080	**0.443***	0.929	**4.568****	0.108
T×M	**-0.098****	0.037	**0.263****	0.500	-0.200	0.070	0.620	**1.928****	**1.253****
T×S	-0.020	0.015	-0.033	0.330	-0.558	0.235	-0.233	**-2.320****	0.295
M×M	0.051	-0.031	-0.145	**1.460***	-0.268	-0.167	0.374	1.340	0.060
M×S	-0.005	0.023	-0.050	-0.768	-0.115	0.260	**-2.088***	**2.238****	-0.648
S×S	-0.016	0.0005	0.015	0.585	0.195	0.078	0.317	**2.193****	-0.573
R^2	***0.950***	***0.971***	***0.826***	***0.992***	***0.911***	***0.857***	***0.945***	***0.982***	***0.878***

**** = p<0.01; * = p<0.05**

5.2. Radial Expansion Index:

REI represents diametric expansion and hence higher values are desirable. The measured values for radial expansion index (REI) ranged from 1.28 to 1.78.

The master model equation for REI is given by Eq. 5.1 and the predictive model is given by Eq. 5.2. From the Eq. 5.2, linear effects of barrel temperature, feed moisture and interaction effects of barrel temperature and feed moisture were found to be the significant factors that affected the REI. The negative correlation between feed moisture content and expansion is due to the fact that the viscosity of the plasticized starch is reduced at higher moisture content and thus the extrudate shrank or collapsed after expansion.

Master model equation:

$$\mathbf{REI = 1.58 - 0.12*T - 0.10*M - 0.04*S + 0.02*T*T - 0.10*T*M - 0.02*T*S + 0.05*M*M - 0.01*M*S - 0.02*S*S} \ \boldsymbol{(R^2 = 95.01\ \%)} \quad \text{(Eq. 5.1)}$$

Predictive model equation:

$$\mathbf{REI = 1.587333 - 0.11375*T - 0.10125*M - 0.0975*T*M} \ \boldsymbol{(R^2 = 0.849)} \quad \text{(Eq. 5.2)}$$

As seen from the contours (Fig. 5.3), extrudates produced at higher barrel temperatures showed lower REI. This might be because of degradation of starch and protein, subsequently leading to a loss in its capacity to retain the die swell after exiting the die, to atmospheric pressure. Another possible reason is that, at high barrel temperatures, longitudinal expansion is much pronounced than the radial expansion.

At low feed moistures, the viscosity of the melt is increased. In low moisture content feed/melt, starch undergoes more mechanical shear which aids in gelatinization process, leading to an increase in the elastic properties of the melt (Launay and Lisch, 1983). The elastic property exhibits capacity to hold structure after exiting the die,

subsequently leading to higher REI. Also, unlike the extrudates from high barrel temperature, there is no rapid release of steam from the built up vapor pressure. At high barrel temperature, because of reduced viscosity, the expansion in radial direction is reduced, instead, the melt/product expands in the longitudinal direction. This is termed as Longitudinal Expansion Index (LEI). LEI is a ratio of velocity of the extrudate after expansion to the velocity at the die orifice. In this study, we could not measure the LEI because of limitations in measuring melt density inside extruder. The contour plot also shows that, as feed moisture increased, the effect of barrel temperature was much pronounced. Also, the interaction effect of high temperature and high moisture resulted in very low expansion.

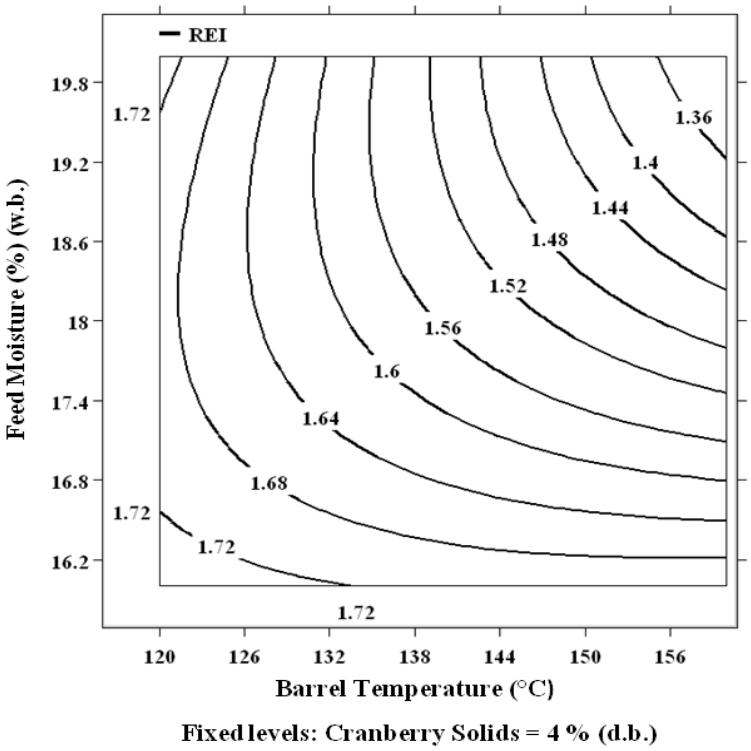

Figure 5.3: Contour plot for REI at 4 % Cranberry Solids

The effect of cranberry solids (4 %) addition at 140 °C barrel temperature and 18 % feed moisture led to a decrease in the REI from 1.92 to 1.5. The decrease in expansion maybe attributed to the presence of sugars and acids in the concentrate.

Maximum REI: 120 °C Barrel Temperature, 16 % Feed Moisture, 4 % Cranberry Solids

Minimum REI: 160 °C Barrel Temperature, 20 % Feed Moisture, 4 % Cranberry Solids

5.3. Bulk Density:

Bulk density (BD) values for extrudates ranged from 0.281 g/ml to 0.721 g/ml. A low density product is generally desirable for RTE type products. From the predictive model equation (Eq. 5.4), it is suggested that the liner effect of barrel temperature and feed moisture and quadratic effect of barrel temperature are the significant factors that influence bulk density.

Master model equation:

$$\mathbf{BD = 0.61 - 0.16*T + 0.05*M + 0.02*S - 0.09*T*T + 0.04*T*M + 0.02*T*S - 0.03*M*M + 0.02*M*S + 0.001*S*S} \ \boldsymbol{(R^2 = 97.10\ \%)} \quad \text{(Eq. 5.3)}$$

Predictive model equation:

$$\mathbf{BD = 0.61 - 0.16*T + 0.05*M - 0.08*T*T} \ \boldsymbol{(R^2 = 91.32\ \%)} \quad \text{(Eq.5.4)}$$

From the contours (Fig. 5.4) it is seen that at any given temperature, feed moisture had negligible effect on bulk density. But, as the barrel temperature increased, the BD decreased, at given feed moisture. This is because of higher moisture loss and starch degradation at high barrel temperatures. Also, it is evident that at low barrel temperature, higher BD values were obtained.

For extrudates collected at 140 °C barrel temperature and 18 % feed moisture, the effect of cranberry solids (4 %) addition increased BD from 0.416 g/ml to 0.626 g/ml. The increase in BD due to addition of cranberry concentrate is because it had 12.5 % (as citric, w/w) titratable acids. Citric acid addition (0.5%) on extrudates made from fruit concentrates (cranberry, pineapple, orange and grape) using a single screw extruder made extrudates that were dense and had less expansion than the ones without acid addition (Maga and Kim, 1989). Cereal bulk density for common breakfast varies from 0.13 g/ml for Cheerios® to 0.26 g/ml for Raisin Bran® (FAO/INFOODS Density Database version 2). The Bulk Density of Noodles/pasta is about 0.8 g/ml.

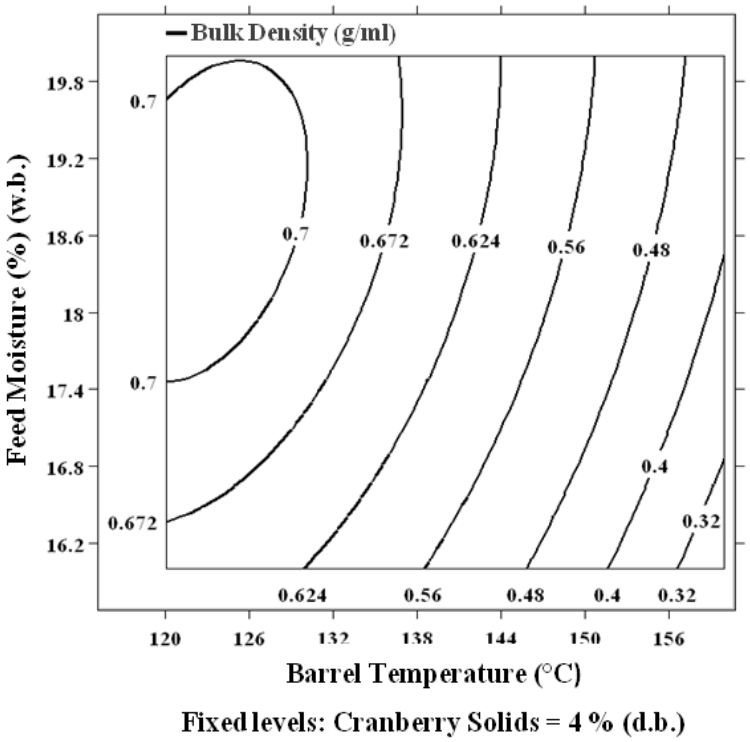

Figure 5.4: Contour plot for Bulk Density at 4 % Cranberry Solids

Maximum BD: 140 °C Barrel Temperature, 20 % Feed Moisture, 5 % Cranberry Solids

Minimum BD: 160 °C Barrel Temperature, 16 % Feed Moisture, 4 % Cranberry Solids

5.4. Breaking Strength:

The values for Breaking Strength (BS) ranged from 0.46 N/mm^2 to 1.44 N/mm^2. Since Breaking Strength is a measure of the hardness of extrudates, higher values are not desirable. The breaking strength of extrudate without cranberry concentrate was 0.65 N/mm^2 while the one with cranberry concentrate was 1.25 N/mm^2, which is almost twice that of the former. This proves a strong influence of cranberry solids addition on texture of extrudates. A negative correlation between REI and breaking strength was also observed. Breaking strength of prickly pear-corn extrudates increased with increasing fruit solids and also correlated negatively with radial expansion (Sarkar et al., 2011). The presence of sugars and acid in the cranberry concentrate would have contributed and caused the increase in BS. Appendix has a graph that shows force vs. distance curves of ten different samples from the same run conditions indicating variation from sample to sample.

From the predictive model equation, (Eq. 5.6), it is observed that linear effects of barrel temperature and feed moisture along with interaction effect of them were the most significant factors that influenced breaking strength.

Master model equation:

$$\mathbf{BS = 1.02 - 0.14*T + 0.16*M + 0.07*S - 0.24*T*T + 0.26*T*M - 0.03*T*S - 0.15*M*M - 0.05*M*S + 0.02*S*S} \ \boldsymbol{(R^2 = 82.63\ \%)} \quad \text{(Eq. 5.5)}$$

Predictive model equation:

$$\mathbf{BS = 1.02 - 0.13*T + 0.15*M + 0.26*T*M} \ \boldsymbol{(R^2 = 53.73\%)} \quad \text{(Eq. 5.6)}$$

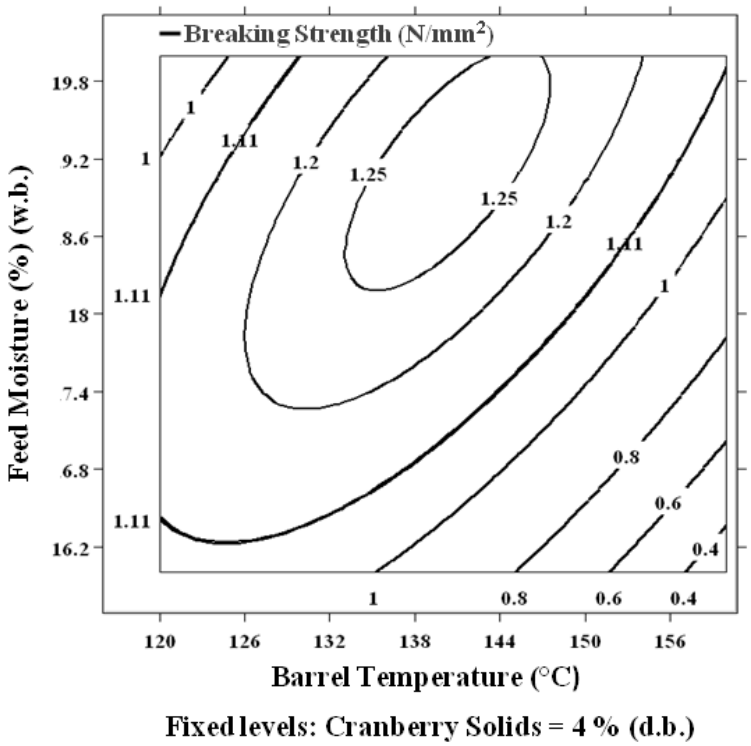

Figure 5.5: Contour plot for Breaking Strength at 4 % Cranberry Solids

From the contours (Fig. 5.5), it is observed that at lower feed moisture, as temperature increased, breaking strength decreased whereas when the feed moisture increased, the temperature had little effect on breaking strength. Also, at high moisture and low temperatures, breaking strength was maximum. Ilo et al. (1999) extruded rice starch and amaranth at different ratios and found that the breaking strength of the extrudates increased with increasing amounts of amaranth. Their breaking strength values (measured using a shear blade) ranged from 0.13 N/mm^2 to 0.59 N/mm^2. These values are comparable to quinoa: cassava extrudates without cranberry concentrate.

Maximum BS: 120 °C Barrel Temperature, 18 % Feed Moisture, 5 % Cranberry Solids

Minimum BS: 160 °C Barrel Temperature, 16 % Feed Moisture, 4 % Cranberry Solids

5.5. Water Absorption Index:

Depending on the time-temperature profile, the extrudates have different states of starch due to the temperature, shear gradients and velocity profiles inside the extruder. WAI and WSI are affected by these phenomena. The sequence of starch degradation is: $raw \rightarrow gelatinized \rightarrow dextrinized$ (Gomez and Aguilera, 1984).

WAI is an indicator of the relative amount of gelatinization in the extrudates. WAI values ranged from 5.95 g water / g dry solids to 8.11 g water / g dry solids. To put in perspective, the WAI values of gun puffed rice and gun puffed buckwheat are reported to be 6 g water / g dry solids and 6.5 g water/g dry solids respectively (Mariotti et al., 2006).

Predictive model equation (Eq. 5.8) suggests that the linear effect of barrel temperature had the most significant effect and had negative correlation with WAI. The addition of cranberry solids (4 %) to extrudates collected at 140 °C barrel temperature and 18 % feed moisture, had no effect on WAI when compared with the extrudates that had no concentrate. The one without concentrate had WAI value 6.42 g water / g dry solids and the one with concentrate had 6.37 g water / g dry solids. This shows that the addition of cranberry solids did not affect the gelatinization degree of the extrudates.

Master model equation:

WAI = 6.56 - 0.63*T + 0.15*M - 0.15*S + 0.44*T*T + 0.07*T*M + 0.23*T*S -

0.16*M*M + 0.26*M*S + 0.08*S*S *(R^2 = 85.72 %)* (Eq. 5.7)

Predictive model equation:

WAI = 6.56 - 0.63*T *(R^2 = 57.38 %)* (Eq. 5.8)

From the contours (Fig. 5.6), it is observed that at higher barrel temperatures WAI decreases and the effect of cranberry solids was prominent at higher barrel temperatures.

An increase in cranberry solids had no influence at lower barrel temperatures. Also, at higher barrel temperatures, WAI decreased.

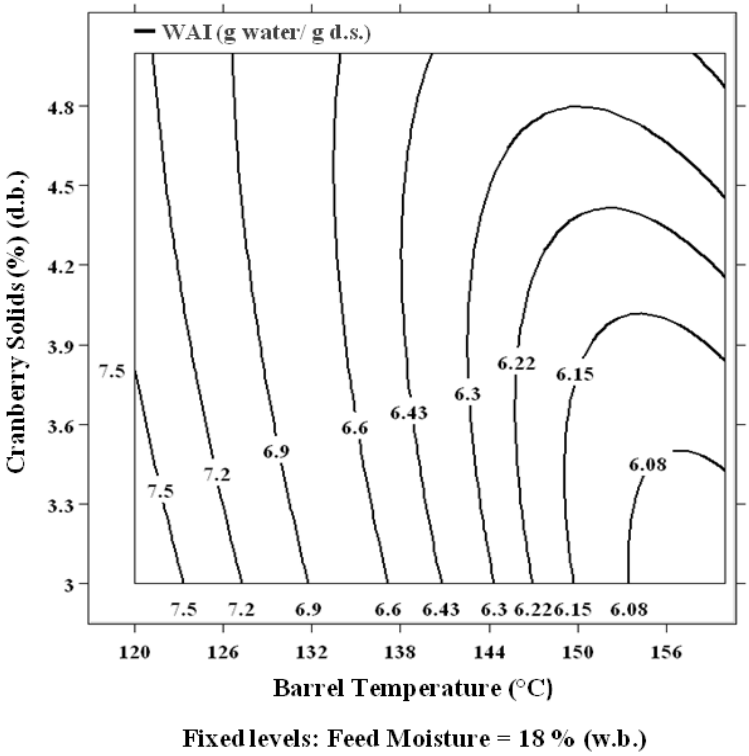

Figure 5.6: Contour plot for WAI at 18 % Feed Moisture

However, as opposed to this conclusion, Tacer-Caba et al. (2014) found that WAI of high amylose starch-grape extract blend extrudates increased with increasing extrusion temperature because of starch gelatinization at higher temperatures. A possible explanation of this is that, the cassava used in this study was partially pregelatinized. Hence, the final state of starch in the extrudate might have reached the dextrinized state much sooner than the grape extrudates.

Maximum WAI: 120 °C Barrel Temperature, 18 % Feed Moisture, 3 % Cranberry Solids

Minimum WAI: 160 °C Barrel Temperature, 16 % Feed Moisture, 4 % Cranberry Solids

5.6. Water Solubility Index:

WSI values indicate the amount of starch degradation or dextrinization, which ranged from 5.93 % to 21.3 %. The WSI of gun puffed rice is 7.5 % and gun puffed rye has WSI of 21.5 % (Mariotti et al., 2006).

From predictive model equation (Eq. 5.10), it is seen that linear effect of barrel temperature is the single most influential factor that determined the WSI values. Also, cranberry solids did not contribute to the WSI values. When 4 % cranberry solids were added and processed at 140 °C barrel temperature and 18 % feed moisture, WAI increased just around 2 % from the extrudates that had no concentrate.

Master model equation:

$$\mathbf{WSI = 13.47 + 5.96*T - 1.51*M + 0.13*S + 0.92*T*T + 0.62*T*M - 0.23*T*S + 0.37*M*M - 2.09*M*S + 0.32*S*S} \ \boldsymbol{(R^2 = 94.50\ \%)} \quad \text{(Eq.5.9)}$$

Predictive model equation:

$$\mathbf{WSI = 13.47067 + 5.96*T} \ \boldsymbol{(R^2 = 82.47\ \%)} \quad \text{(Eq.5.10)}$$

From the contours (Fig. 5.7), it can be seen that the feed moisture had negligible effect on WSI at higher barrel temperature because of starch breakdown and small molecule formation that easily leaches out into water. This finding is also consistent with those observed by Singh and Smith, (1997) for oat extrudates and barley-grape pomace extrudates (Altan et al., 2009). Melt viscosity and gelatinization is affected by available moisture because water acts as plasticizer. Therefore, the limited water content in the low moisture feed material might have led to competition for the water molecules between the fiber (non-starch polysaccaride) (Seth and Rajamanickam, 2012) in quinoa and the starch in cassava, thus promoting more degradation at higher barrel temperatures. At low barrel

temperature (120 °C) WSI decreased as moisture increased possibly due to water availability for gelatinization of cassava starch.

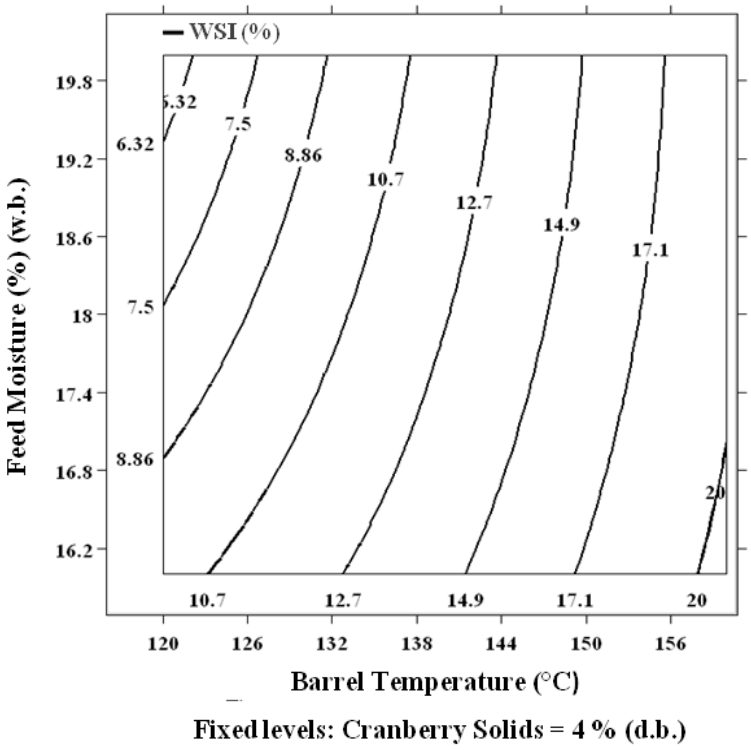

Figure 5.7: Contour plot for WSI at 4 % Cranberry Solids

Maximum WSI: 160 °C Barrel Temperature, 18 % Feed Moisture, 5 % Cranberry Solids

Minimum WSI: 120 °C Barrel Temperature, 18 % Feed Moisture, 3 % Cranberry Solids

5.7. Hue:

Hue values close to 0° (red) indicate more red extrudates than values nearing 90° (yellow). Hue values ranged from 33.58° to 65.07°. The hue value changed from 85.02 ° (yellow is at 90°) to 45.06° when cranberry solids (4 %) were added to extrudates and processed at 140 °C barrel temperature and 18 % feed moisture.

Master Model equation:

HUE = 47.01 + 6.87*T – 2.0*M - 8.73*S + 3.22*T*T + 0.5*T*M + 0.33*T*S + 1.46*M*M – 0.76*M*S + 0.59*S*S *(R^2 = 99.19 %)* *(Eq.5.11)*

Predictive model equation:

HUE = 47.01 + 6.87*T - 8.73*S + 3.08*T*T *(R^2 = 97.96 %)* *(Eq.5.12)*

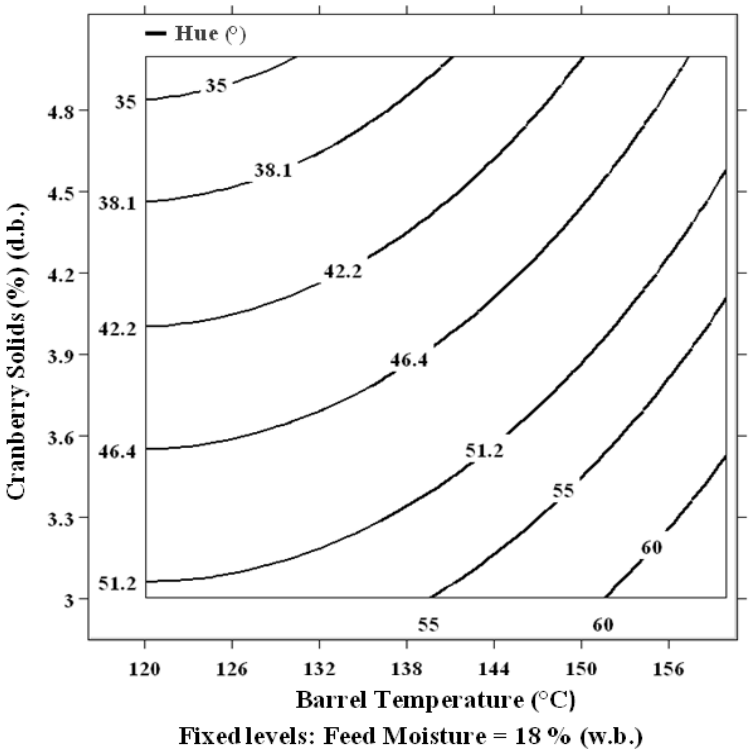

Figure 5.8: Contour plot for hue at 18 % Feed Moisture

Predictive model equation (Eq. 5.12) shows that linear effects of barrel temperature and cranberry solids and quadratic effects of barrel temperature were the most significant factors that influenced the hue degree.

From the contours (Fig. 5.8), plotted with the cranberry solid content on the y axis and the barrel temperature in the x-axis, it is seen that higher solid content produces more red colored extrudates, as expected. Maga and Kim (1989) also found that red color was

preserved in cranberry concentrate-rice extrudates due to their acid content. However, at higher barrel temperature, redness is lost as it moves to brownish color due to material breakdown, brown product formation and caramelization.

Maximum HUE: 160 °C Barrel Temperature, 18 % Feed Moisture, 3 % Cranberry Solids

Minimum HUE: 120 °C Barrel Temperature, 18 % Feed Moisture, 5 % Cranberry Solids

5.8. Chroma:

Purity or saturation of a given hue or color is represented by Chroma. In this study, a higher Chroma value means that the extrudates were redder. Chroma values ranged from 17.71 to 21.32 for the extrudates. For comparison purposes, the Chroma value of an 8 °Brix cranberry juice is 34.3 (Giacarini-Chiappe, 2008)

From the predictive model equation (Eq. 5.14), the linear effect of barrel temperature and cranberry solids were the most significant factors that influence the Chroma values.

Master model equation:

$$\textbf{CHROMA} = 19.72 + 0.93T + 0.22M + 1.07S + 0.08T^2 - 0.20TM - 0.55TS - 0.27M^2 - 0.12MS + 0.19S^2 \quad (R^2 = 91.14\ \%) \qquad \text{(Eq. 5.13)}$$

Predictive model equation:

$$\textbf{CHROMA} = 19.72 + 0.93T + 1.07S \quad (R^2 = 79.80\ \%) \qquad \text{(Eq. 5.14)}$$

From the contour plot (Fig. 5.9), it is evident that as cranberry solids content increased, the chroma value also increased, which is to be expected. Also, at a given cranberry solid percentage, the Chroma values increased as barrel temperature increased.

The intensity in red color at higher barrel temperature may be caused by the dark coloration imparted by brown products formed at high temperatures.

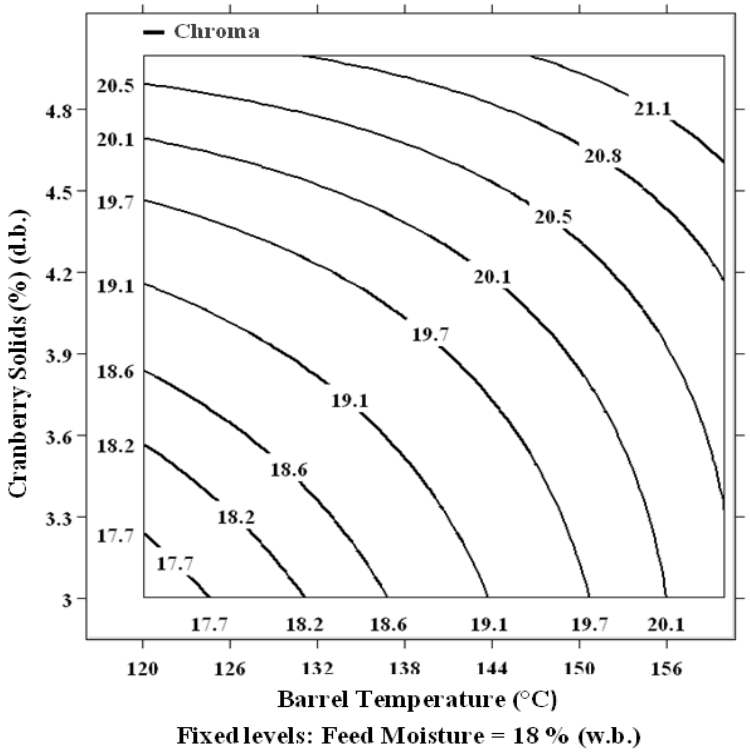

Figure 5.9: Contour plot for Chroma at 18 % Feed Moisture

Maximum Chroma: 140 °C Barrel Temperature, 20 % Feed Moisture, 5 % Cranberry Solids

Minimum Chroma: 120 °C Barrel Temperature, 18 % Feed Moisture, 3 % Cranberry Solids

5.9. Total Phenolic Content:

The effect of cranberry solids addition was expected to contribute significantly to the total phenolic content (TPC) of the extrudates. In a typical feed material that had 4 % cranberry solids, quinoa contributed 51 %, cassava contributed 13 % and cranberry concentrate contributed 36 % to the TPC. Values for TPC of the extrudates ranged from 67.43 mg GAE/ 100 g dry solids to 83.48 mg GAE/ 100 g dry solids.

Figure 5.10 shows the standard curve for Gallic acid which was used to calculate the amount of TPC in extrudates.

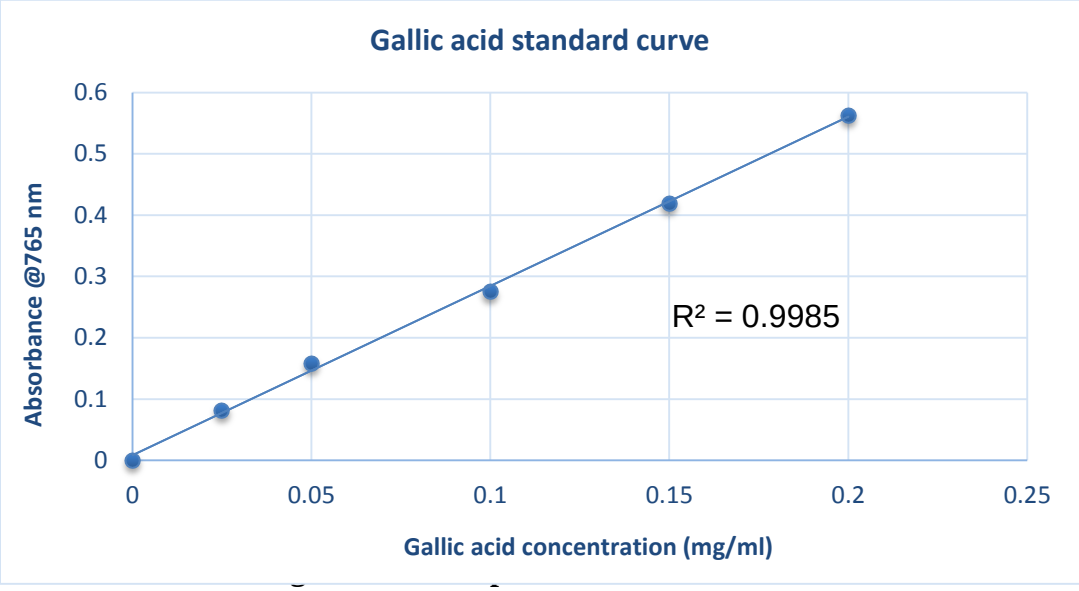

Figure 5.10: Gallic acid standard curve

In general, higher values for TPC were found at higher barrel temperatures. Some of this can be because of formation of Maillard reaction products and intermediates (Pokorny and Schmidt, 2006). The phenolic values of wheat flour extrudates substituted at various levels with dry cauliflower by-products increased after extrusion (Stojceska et al., 2008). Camire et al. (2007) reported similar range of values for TPC in cranberry powder corn extrudates.

The predictive model (Eq. 5.16) shows that a lot of factors are significantly influencing TPC. Except for the quadratic effect of feed moisture, all other linear, interaction and quadratic effects are significant in TPC.

Master Model equation:

TPC= 73.32 + 3.73*T - 3.71*M + 3.25*S + 4.56*T*T + 1.92*T*M - 2.32*T*S + 1.34*M*M + 2.24*M*S + 2.20*S*S *(R^2 = 98.23 %)* (Eq. 5.15)

Predictive model equation:

TPC= 73.32 + 3.73*T - 3.71*M + 3.25*S + 4.46*T*T + 1.92*T*M - 2.32*T*S + 2.24*M*S + 2.08*S*S *(R^2 = 96.80 %)* (Eq. 5.16)

From the contours (Fig. 5.11), plotted between barrel temperature and feed moisture, it is seen that at lower barrel temperatures, the effect of feed moisture is much pronounced since the TPC values decreased as feed moisture increased. At 120 °C barrel temperature, 16 % feed moisture had 80 mg GAE phenols but at 20 % feed moisture it reduced to less than 70 mg GAE phenols. However, as temperature increased the effect of feed moistures started to diminish.

Observed from the contours shown in Fig. 5.12 is that the higher barrel temperatures lead to higher TPC. At the same time, the contribution of phenols by cranberry solids started to diminish at higher barrel temperature. This also supports our theory that the higher TPC in extrudates processed at high barrel temperature might come from other Maillard reaction intermediates or products.

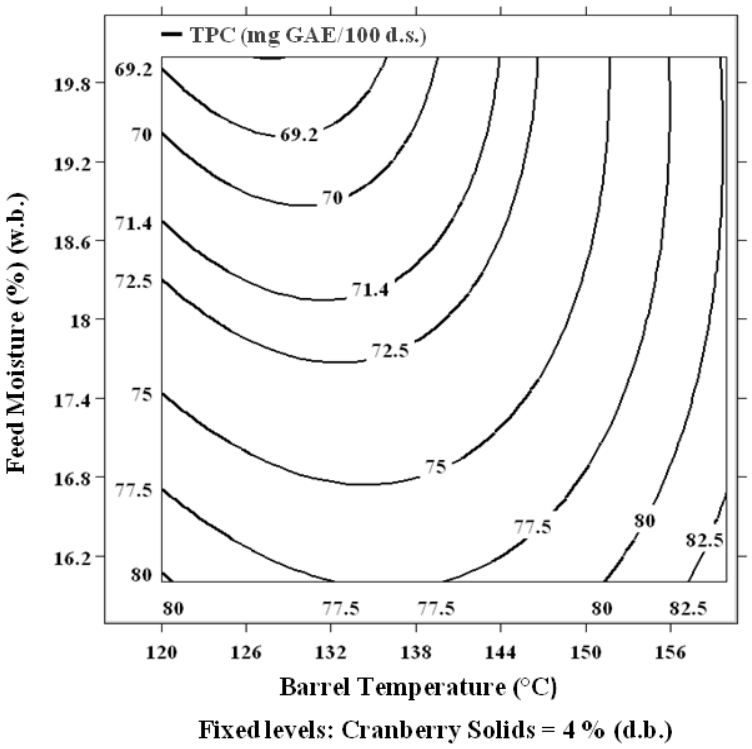

Figure 5.11: Contour plot for TPC at 4 % Cranberry Solids

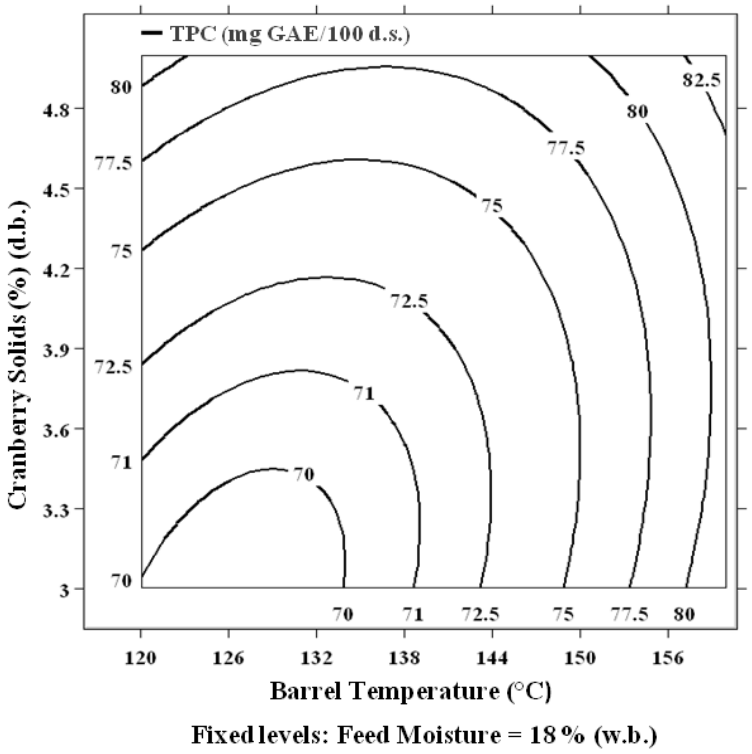

Figure 5.12: Contour plot for TPC at 18 % Feed Moisture

Figure 5.13 shows that, at a given cranberry solids percentage, TPC decreased as feed moisture increased. Sharma et al. (2012) also observed similar effect of moisture on barley extrudates. Increasing feed moisture from 15 % to 20 % led to a decrease in TPC values from 8 % to 29 %. One possible explanation for this phenomenon is that, the moisture protects the feed material from heat which is responsible for the formation of complex antioxidants and Maillard products. On the other hand, the moist heat from high moisture feed might have contributed to more damage of phenols (Sharma et al., 2012)

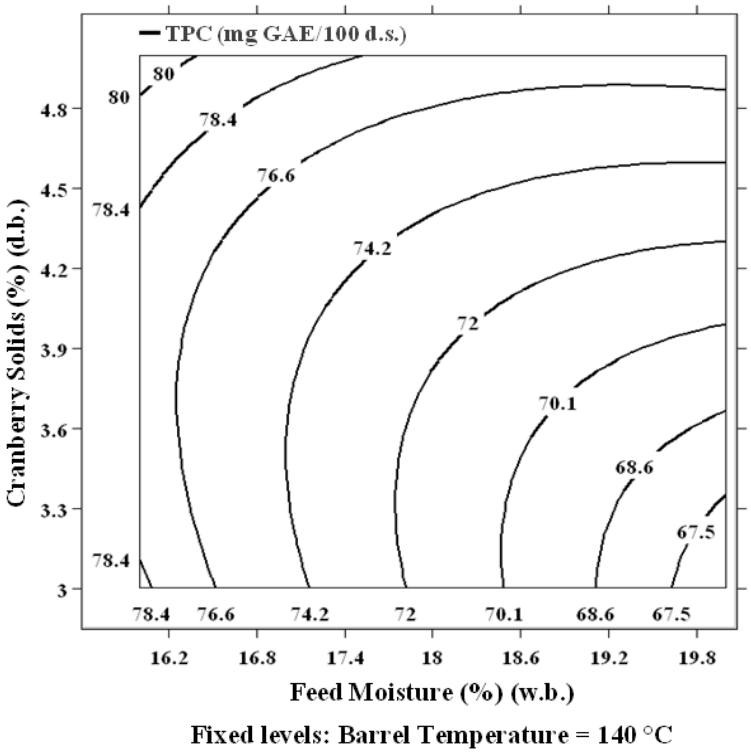

Figure 5.13: Contour plot for TPC at 140 °C Barrel Temperature

From the Fig. 5.14 the isolated effect of barrel temperature at a given percentage solids and feed moisture can be observed. At both 3 % and 5 % cranberry solids, lower percent loss is observed at 160 °C barrel temperature. However, the effect of temperature is much less pronounced at higher percentage cranberry solids.

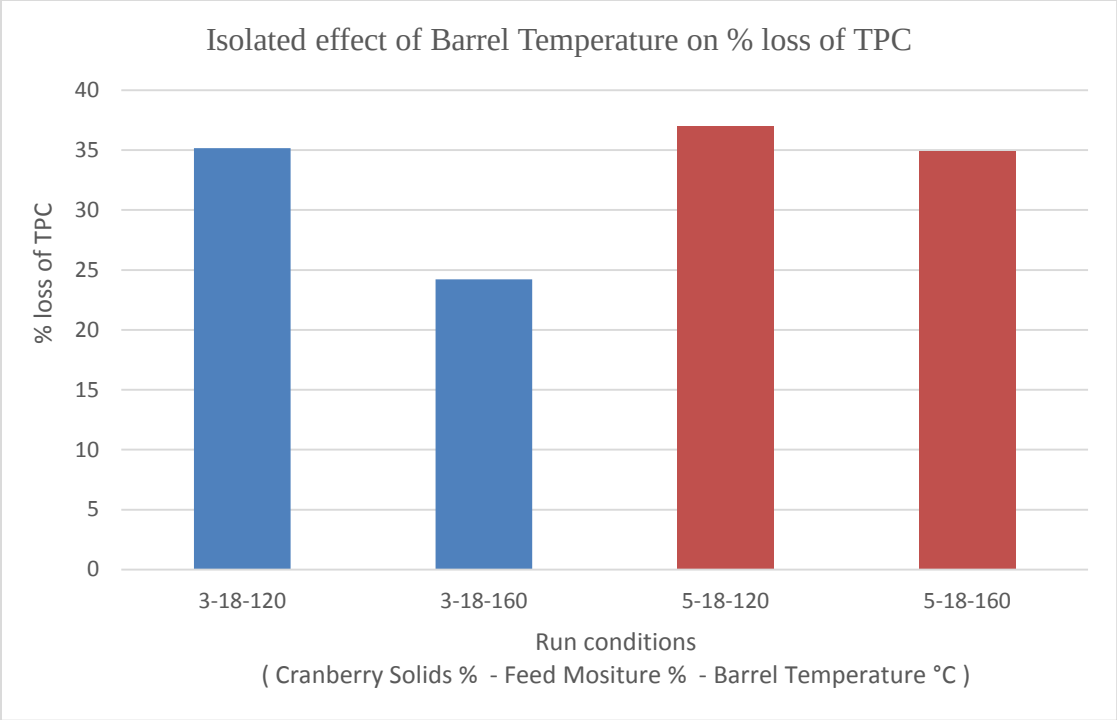

Figure 5.14: Isolated effect of Barrel Temperature on % loss of TPC

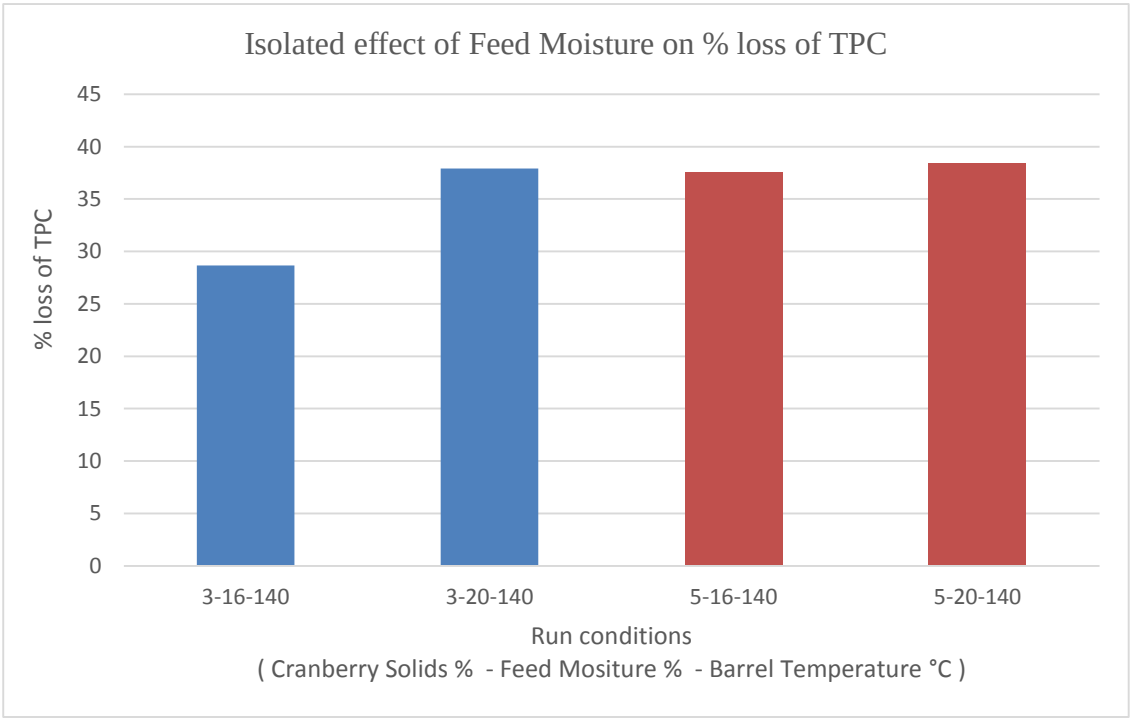

Figure 5.15: Isolated effect of Feed Moisture on % loss of TPC

From Fig. 5.15, the isolated effect of feed moisture at a given percentage solids and barrel temperature can be observed. At both 3 % and 5 % cranberry solids, lower percent loss is observed at 16 % feed moisture. However, the effect of feed moisture is much less pronounced at higher percentage cranberry solids. Therefore at 3 % cranberry solids addition, both effect of barrel temperature and feed moisture was more pronounced than at 5 %.

The addition of 4 % cranberry solids produced extrudates that had TPC of 73.7 mg GAE/100 g d.s., which is an 18 % increase from extrudates with no concentrate (both processed at 140 °C barrel temperature and 18 % feed moisture).

Maximum TPC: 160 °C Barrel Temperature, 18 % Feed Moisture, 5 % Cranberry Solids

Minimum TPC: 140 °C Barrel Temperature, 20 % Feed Moisture, 3 % Cranberry Solids

Table 5.2 shoes values for TPC in flour and extrudates and their corresponding % loss. Significant number of studies have shown that phenolic content decreases after extrusion. Owing to their unique chemical structure, different phenolic compounds are affected differently during extrusion. Altan et al. (2009) recorded about 60 % decrease in the TPC of barely flour-pomace blends. A 3-fold decrease in TPC was found in extrudates made from dehulled buckwheat seeds (Zielinski et al., 2006) possibly because of polymerization of phenols and decarboxylation or decomposition of some phenolic compounds (Dlamini et al., 2007). On the other hand, a 200 % increase in phenolic content was observed in four whole grain extrudates, (barely, wheat, oat, and rye), because of the breakdown on ester bonds and increase of free phenolics (Zielinski et al., 2001).

Table 5.2: TPC of flour and extrudates according to BBD, with % loss.

Run	Barrel Temperature (°C)	Feed Moisture (%)	Cranberry Solids (%)	TPC in flour (mg GAE/100 d.s.)	TPC in extrudates (mg GAE/100 d.s.)	TPC loss (%)
1	140	20	5	128.32	79.09	38.36
2	120	18	5	128.32	80.87	36.97
3	120	18	3	108.58	70.40	35.16
4	140	16	3	108.58	77.45	28.67
5	120	20	4	118.45	68.01	42.58
6	140	18	4	118.45	72.91	38.45
7	120	16	4	118.45	81.13	31.50
8	140	18	4	118.45	76.15	35.71
9	140	16	5	128.32	80.17	37.52
10	140	18	4	118.45	72.28	38.98
11	140	20	3	108.58	67.43	37.90
12	160	20	4	118.45	79.54	32.84
13	160	16	4	118.45	84.97	28.27
14	160	18	5	128.32	83.48	34.94
15	160	18	3	108.58	82.29	24.21

5.10. Anthocyanins:

Anthocyanins are pigments present in cranberry solids that are partly responsible for the phenolic content of the extrudates along with imparting red color to the extrudates. Anthocyanin values in the extrudates varied from 0.427 mg - 0.963 mg per gram of dry solids. Appendix also shows a typical chromatogram from the anthocyanin analysis and a typical datasheet generated by SAS 9.2.

From the predictive model equation (Eq. 5.18), all three linear effect of barrel temperature, feed moisture and cranberry solids were significant. The interaction effect of barrel temperature and feed moisture is also the most significant.

Master mode equation:

Anthocyanins = 6.61 + 0.78*T - 0.64*M + 1.24*S + 0.02*T*T + 1.25*T*M

+ 0.20*T*S + 0.06*M*M – 0.65*M*S - 0.57*S*S *(R^2 = 87.83 %)* (Eq.5.17)

Predictive model equation:

Anthocyanins = 6.61 + 0.78*T - 0.64*M + 1.24*S + 1.25*T*M *(R^2 = 78.10 %)*

(Eq. 5.18)

A saddle point in the contour plot (Fig. 5.16) denotes that there is an intersection between two contour lines. Since the critical point here is a saddle point, the interpretation is that, in the x direction (barrel temperature), the anthocyanin values increased as feed moisture decreased, until ~ 155 °C, after which the effect of feed moisture is positively correlated and becomes less pronounced.

Extruder barrel temperature and percent cranberry pomace was the most significant input factor that affected the anthocyanin content of corn-cranberry pomace extrudates. Anthocyanin losses were the least when low amounts of pomace were present (50 % loss)

and the greatest loss of anthocyanin was observed at high amounts of pomace (65 % loss) (White et al., 2010).

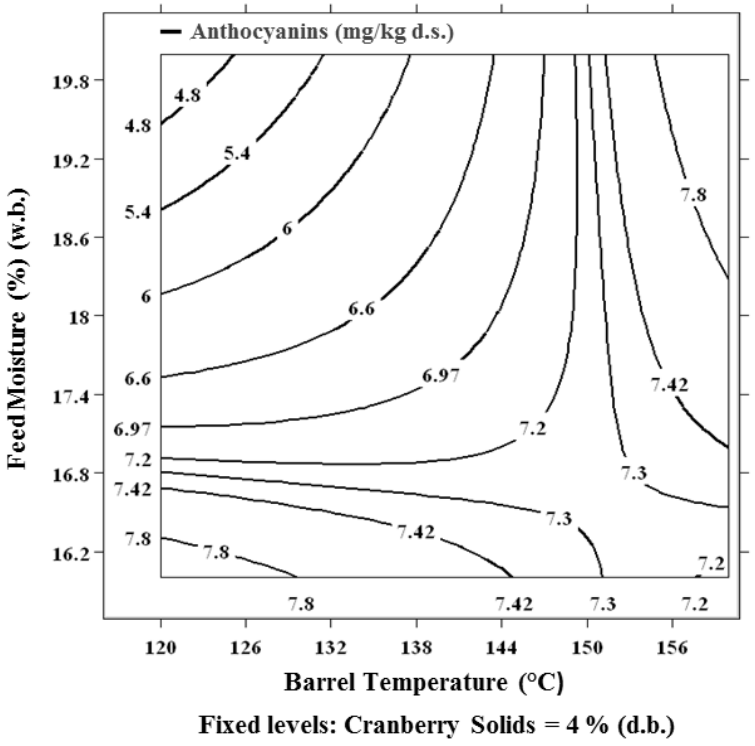

Figure 5.16: Contour plot for Anthocyanins at 4 % Cranberry Solids

Since cranberry solids are the contributors to the anthocyanin content, contours in Fig. 5.17 and Fig. 5.18 have been plotted to analyze the interaction effect of cranberry solids with barrel temperature and feed moisture, respectively.

From the contours of anthocyanin levels (Fig. 5.17) plotted against cranberry solids and barrel temperature, it can be seen that higher retention of anthocyanins were observed at higher barrel temperature. This might be due to the lower residence time of melt inside the extruder at higher temperatures (due to decreased melt viscosity).

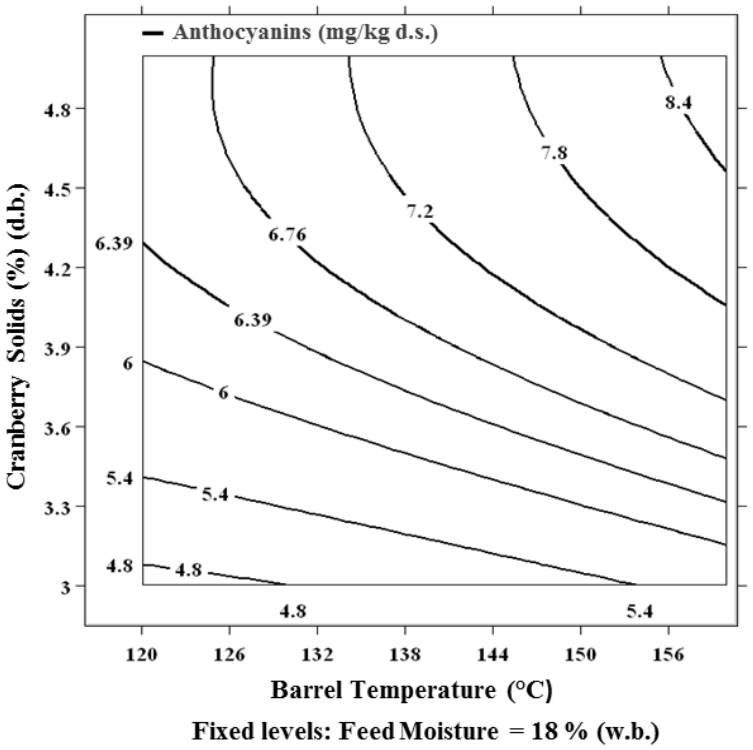

Figure 5.17: Contour plot for Anthocyanins at 18 % Feed Moisture

From the contours (Fig. 5.18) plotted as a function of cranberry solids and feed moisture, it was observed that at lower percentage solids, feed moisture had little or no effect on anthocyanin values. However, as cranberry percentage solids increased, lower feed moisture retained more anthocyanins. These results are contradicting from the findings of Hirth et al. (2014). Their maize - bilberry extract extrudates showed higher retention of anthocyanins at higher moisture content. Camire et al. (2002) found that blueberry anthocyanins decreased by 90 % and grape anthocyanins decreased by 74 % during extrusion of corn cereals.

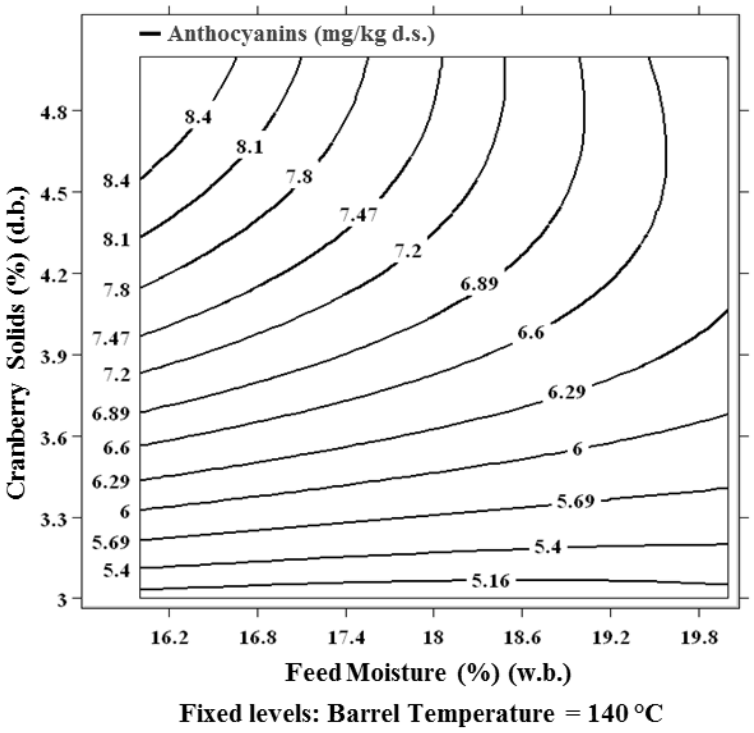

Figure 5.18: Contour plot for Anthocyanins at 140 °C Barrel Temperature

From Fig. 5.19, at a given percentage cranberry solids and feed moisture, the effect of barrel temperature alone could be observed. At 3 % solids, loss percentage is lower when compared to 5 % solids. However, at 5 % solids, higher barrel temperature resulted in lower loss of anthocyanins.

Figure 5.20 shows the effect of feed moisture content on anthocyanin loss percentage. At higher 5 % cranberry solids, 20 % feed moisture led to 75 % loss as opposed to 62 % loss in lower moisture feed. The degree of difference is also much pronounced in 5 % cranberry solids than at 3 % cranberry solids.

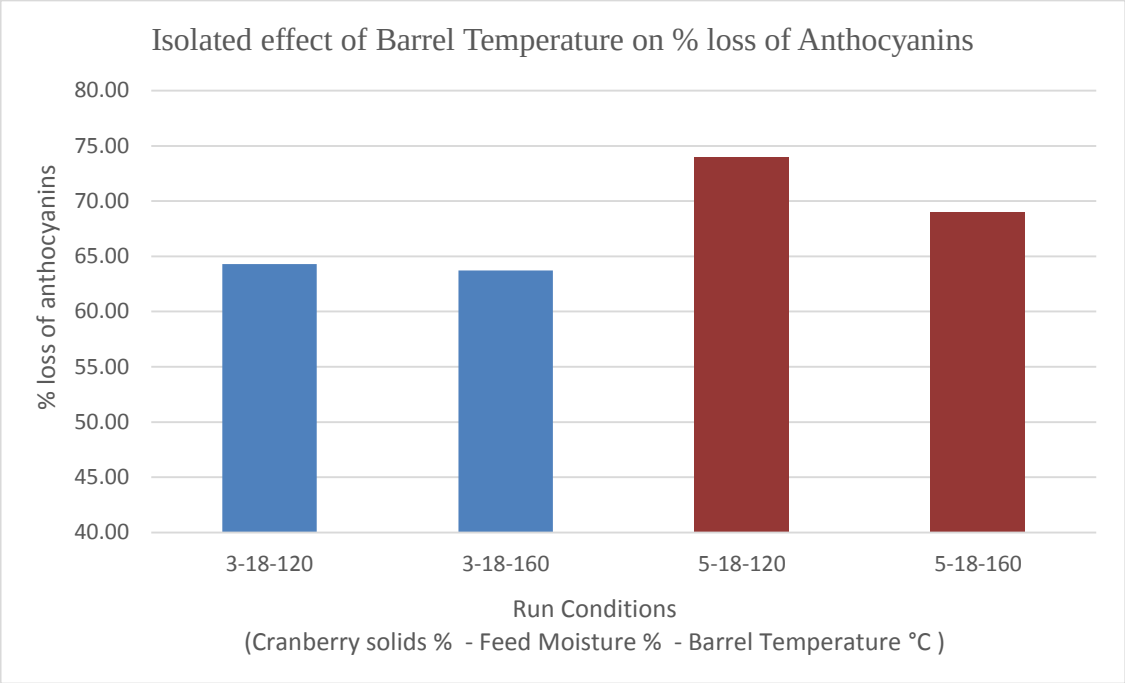

Figure 5.19: Isolated effect of Barrel Temperature on % loss of Anthocyanins

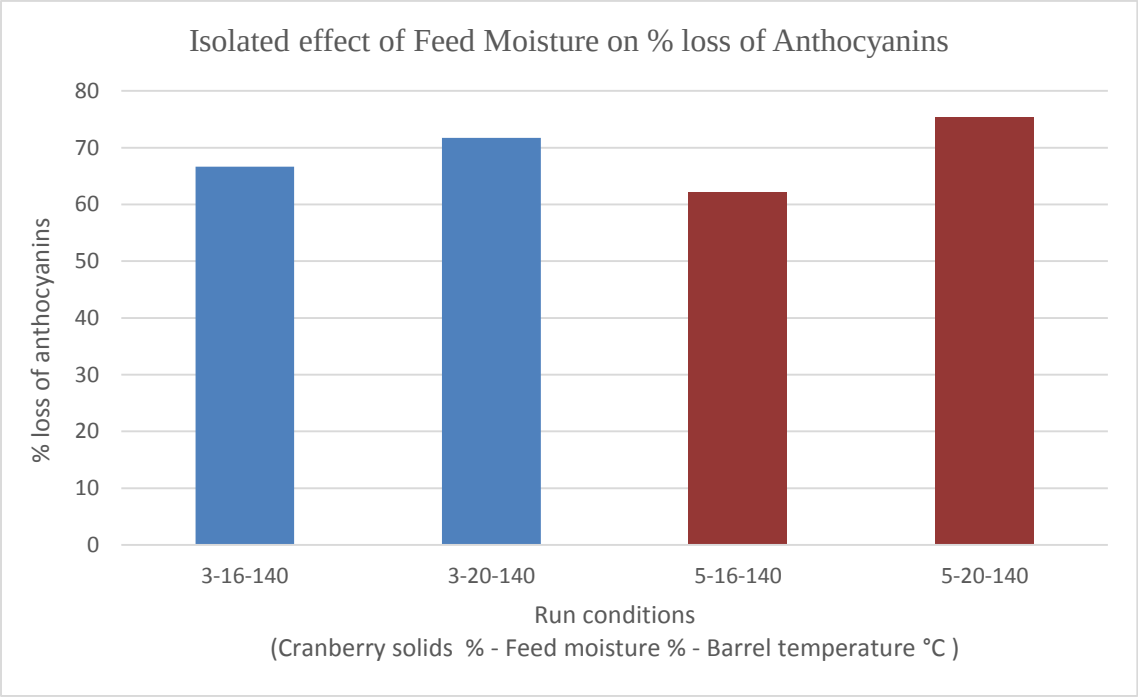

Figure 5.20: Isolated effect of Feed Moisture on % loss of Anthocyanins

Using a twin screw extruder Chaovanalikit et al. (2003) extruded corn breakfast cereals with blueberry concentrate and studied the effect of ascorbic acid addition on anthocyanin retention. They found that addition of ascorbic acid accelerated anthocyanins degradation and also did not prevent browning reactions. Since the cranberry concentrate used in our study, also had citric acid at 12.5 %, it is possible that it led to such low retentions of anthocyanins. A total of 6 anthocyanins were present in the concentrate: Cyanidin-3-Arabinoside (52.51 mg/kg), Cyanidin-3-Galactoside (74.32 mg/kg), Cyanidin-3-Glucoside (3.19 mg/kg), Peonidin-3-Arabinoside (36.6 mg/kg), Peonidin-3-Galactoside (78.92 mg/kg), Peonidin-3-Glucoside (4.15 mg/kg) but only four survived the extrusion process, namely Cyanidin-3-Arabinoside, Cyanidin-3-Galactoside, Peonidin-3-Arabinoside and Peonidin-3-Galactoside.Table 5.3 gives individual values of four anthocyanins and the total anthocyanins for each extrudate along with its percentage loss during processing.

Table 5.3: Anthocyanins in extrudates according to BBD, with % loss.

Run	Barrel Temperature (°C)	Feed Moisture (%) (w.b.)	Cranberry Solids (%) (d.b.)	Cyanidin-3-Arabinoside		Cyanidin-3-Galactoside		Peonidin-3-Arabinoside		Peonidin-3-Galactoside		Total Anthocyanins	
				Content (mg/ kg d.s.)	Loss (%)	Content (mg/ kg d.s.)	Loss (%)	Content (mg/ kg d.s.)	Loss (%)	Content (mg/ kg d.s.)	Loss (%)	Content (mg/ kg d.s.)	Loss (%)
1	140	20	5	1.26	75.99	1.74	76.62	0.99	73.08	2.00	74.63	0.626	75.39
2	120	18	5	1.25	76.22	1.99	73.20	1.00	72.65	2.11	73.27	0.662	73.98
3	120	18	3	1.13	64.17	1.59	64.31	0.91	58.39	1.83	61.40	0.545	64.29
4	140	16	3	1.03	67.44	1.57	64.77	0.77	64.96	1.72	63.66	0.509	66.67
5	120	20	4	0.85	79.71	1.32	77.78	0.78	73.44	1.72	72.83	0.427	79.01
6	140	18	4	1.30	69.08	1.85	68.94	1.28	56.38	2.08	67.02	0.724	64.40
7	120	16	4	1.42	66.21	2.11	64.45	1.38	52.98	2.37	62.47	0.729	64.18
8	140	18	4	1.23	70.63	2.32	61.02	0.98	66.66	2.40	61.94	0.675	66.83
9	140	16	5	1.71	67.42	2.94	60.39	1.39	61.97	3.06	61.23	0.963	62.16
10	140	18	4	1.41	66.31	1.97	66.93	1.18	59.79	2.19	65.27	0.650	68.06
11	140	20	3	0.89	71.64	1.26	71.75	0.73	66.66	1.42	69.99	0.432	71.72
12	160	20	4	1.68	59.97	2.73	54.06	1.27	56.47	2.72	56.91	0.922	54.69
13	160	16	4	1.43	66.05	2.12	64.28	1.18	59.79	2.53	59.92	0.732	64.49
14	160	18	5	1.42	72.90	2.28	69.33	1.16	68.43	2.56	67.60	0.787	69.05
15	160	18	3	0.92	70.89	1.92	56.92	0.92	58.24	1.78	62.40	0.554	63.74

5.11. Specific Mechanical Energy:

The isolated effect of barrel temperature on SME is shown in Fig 5.21. It is observed that in general, the SME decreases at lower barrel temperatures (120 °C) probably because of reduction in water diffusion rates leading to decreased potential for starch gelatinization (Lai and Kokini, 1991). Gelatinized starch contributes to more melt viscosity, thus resulting in higher SME at higher barrel temperatures. However the degree of difference is much pronounced when the feed material had 3 % cranberry solids maybe due to more available starch for gelatinization. Al-Rabadi et al. (2011) found that SME reduced at low barrel temperatures in sorghum and barely extrudates.

Figure 5.22 shows the isolated effect of feed moisture on SME. The general observation is that addition of 5 % cranberry solids in the feed, resulted in overall reduction of SME. The sugars in the concentrate would have altered the conformation of quinoa proteins by binding with them. Increase in sugar content led to decrease in SME of soy protein extrudates (Guerrero et al., 2012). Water acted as a lubricant and also reduced viscosity, leading to a decrease in SME when the feed moisture was higher (20 %). Waramboi et al. (2014) also found that decreasing feed moisture led to increase of SME in sweet potato flour.

Table 5.4 also shows the average values for all measured physical responses namely, REI, Bulk Density, Breaking Strength, WAI, WSI, Hue, Chroma and SME.

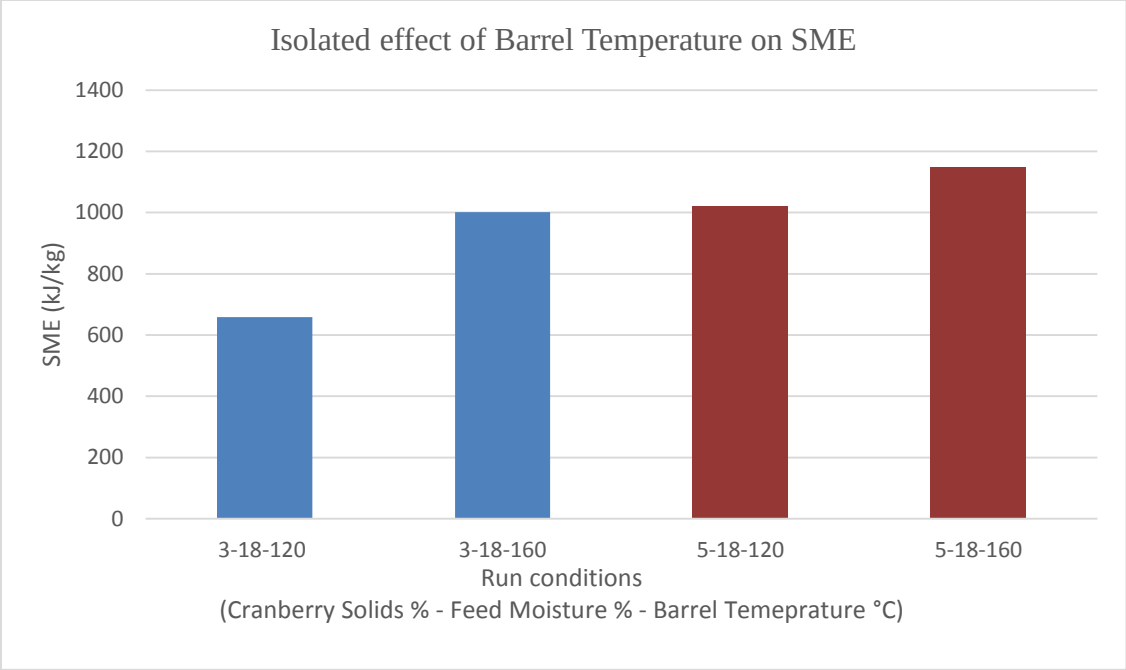

Figure 5.21: Isolated effect of Barrel Temperature on SME

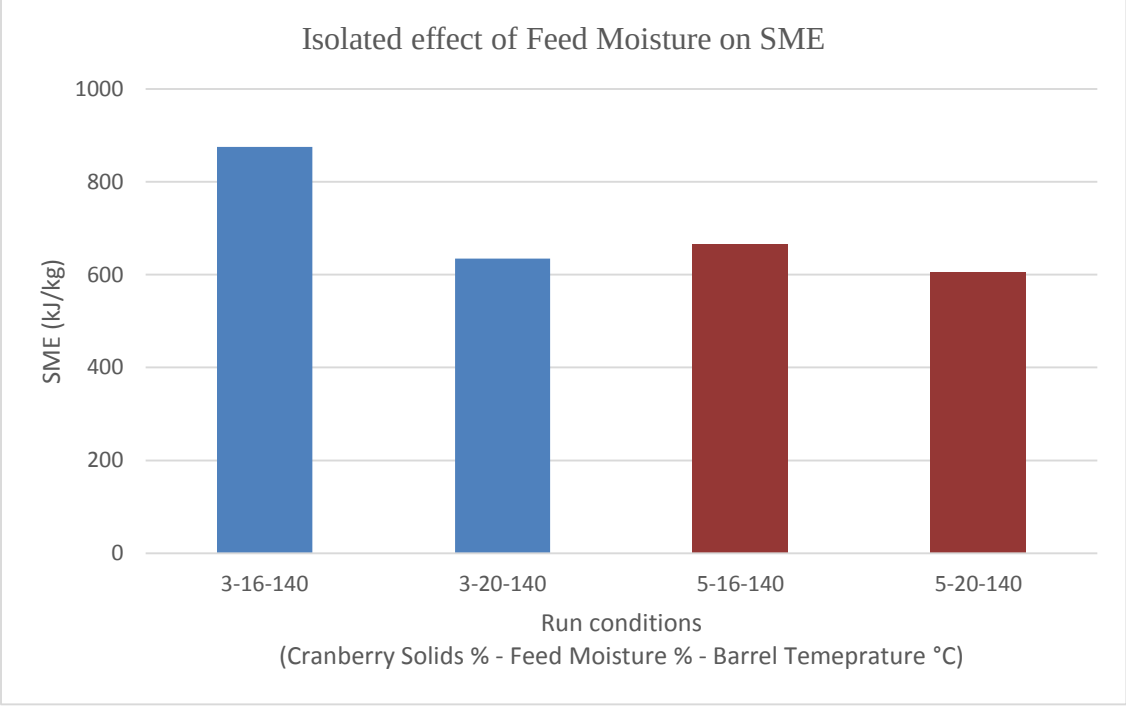

Figure 5.22: Isolated effect of Feed Moisture on SME

Table 5.4: Values for physical properties of extrudates according to BBD

Run	Barrel Temperature (^{o}C)	Feed Moisture (%) (w.b.)	Cranberry solids (%) (d.b.)	REI	Bulk Density (g/ml)	Breaking Strength (N/mm^2)	Hue (^{o})	Chroma	WAI (g water/ g d.s.)	WSI (%)	SME (kJ/kg)
1	140	20	5	1.45	0.721	1.26	37.22	21.32	7.01	8.06	606.20
2	120	18	5	1.61	0.718	1.44	33.58	20.32	7.1	8.4	1020.06
3	120	18	3	1.66	0.693	1.07	50.82	17.71	8.11	5.93	658.82
4	140	16	3	1.73	0.523	0.82	57.03	17.73	6.08	14.36	875.04
5	120	20	4	1.78	0.67	0.68	44.07	18.86	7.21	7.44	929.13
6	140	18	4	1.54	0.665	1.21	45.52	19.44	6.65	11.6	759.98
7	120	16	4	1.78	0.684	1.02	44.41	18.38	7.2	9.92	869.95
8	140	18	4	1.56	0.64	1.22	46.96	20.39	6.42	12.52	762.52
9	140	16	5	1.67	0.518	0.91	40.23	20.75	6.04	17.06	665.79
10	140	18	4	1.58	0.584	1.23	45.06	19.31	6.05	13.7	764.47
11	140	20	3	1.53	0.634	1.37	57.09	18.76	6.01	13.71	634.32
12	160	20	4	1.28	0.413	1.17	57.65	20.27	6.24	19.14	1089.89
13	160	16	4	1.67	0.281	0.46	55.99	20.59	5.95	19.14	1105.24
14	160	18	5	1.42	0.425	0.85	49.15	21.15	6.15	21.31	1147.75
15	160	18	3	1.55	0.339	0.61	65.07	20.77	6.22	19.77	1001.87

5.11. Cross-correlation between responses:

Figure 5.23 shows the relationship between WAI and WSI. As the WSI values decreased, the WAI values increased. One possible reason is that the degraded starch and other polymers would have interacted to form high molecular weight compounds thus decreasing the WSI and increasing WAI (Dogan and Karwe, 2003). In other words, more gelatinization leads to less soluble solids.

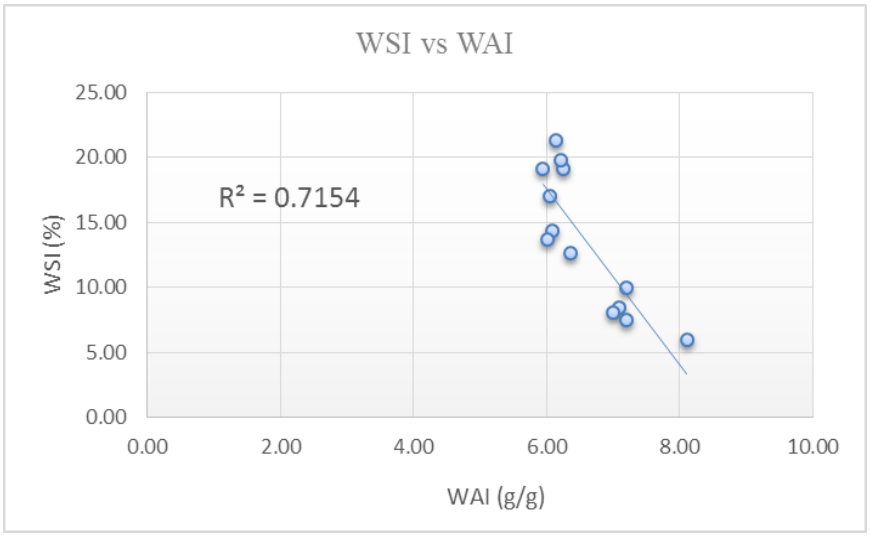

Figure 5.23: Correlation between WAI and WSI

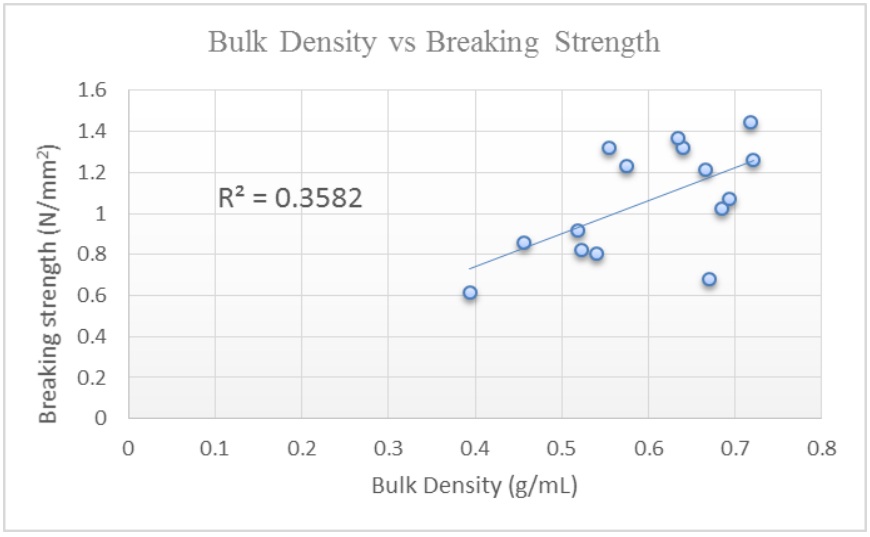

Figure 5.24: Correlation between Bulk Density and Breaking Strength

Figure 5.24 shows the relationship between the response Breaking Strength and Bulk Density. The increase in breaking strength as bulk density increases is due to the tight packing, less porous structure of the extrudates.

The correlation graph (Fig. 5.25) between REI and Breaking Strength shows negative correlation indicating that the breaking strength increased as the REI decreased. However as discussed earlier, low values for both breaking strength and REI of extrudates were observed at higher barrel temperature. Therefore porosity is not the reason for the negative correlation between REI and BS. It is due to extensive degradation of polymers in the feed material.

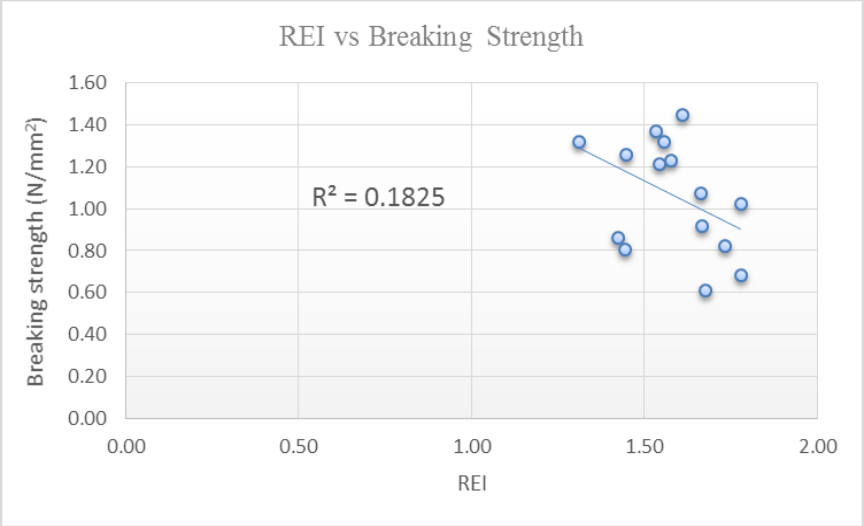

Figure 5.25: Correlation between REI and Breaking Strength

The positive correlation between Anthocyanins and TPC shown from the below correlation graph (Fig. 5.26) is suggestive that some amount of TPC comes from the anthocyanin content.

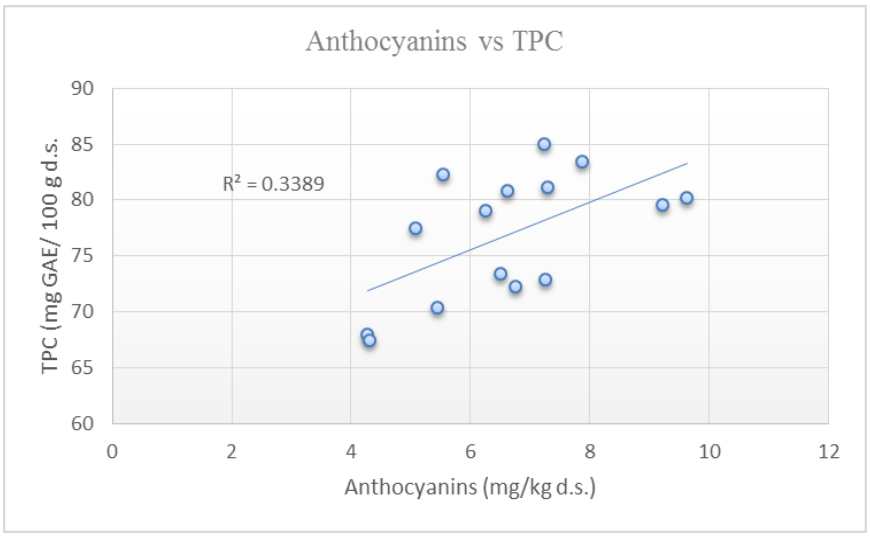

Figure 5.26: Correlation between Anthocyanins and TPC

Figure 5.27 shows a negative slope between Specific Mechanical Energy and Bulk Density which means that as the SME increases, the BD decreases. However, the correlation was very weak. The more mechanical energy input gives rise to more shear and pressure development leading to lower density extrudate.

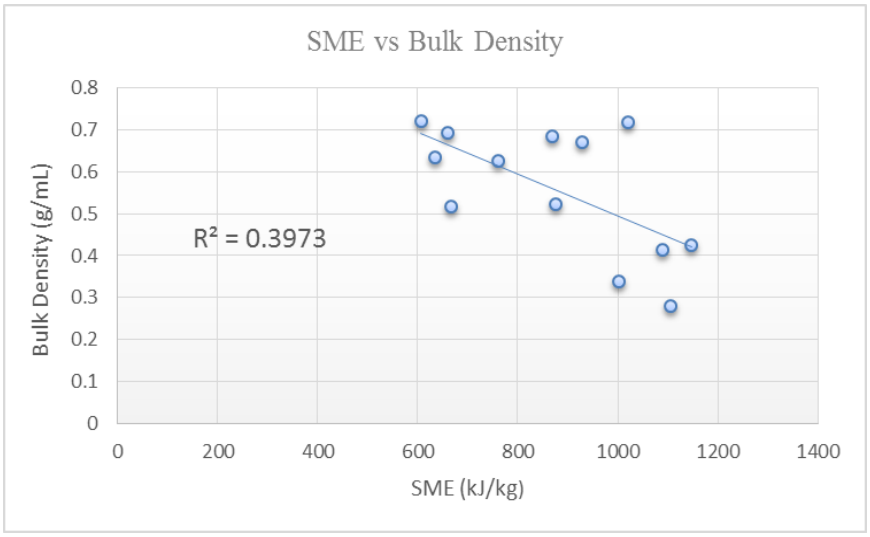

Figure 5.27: Correlation between SME and Bulk Density

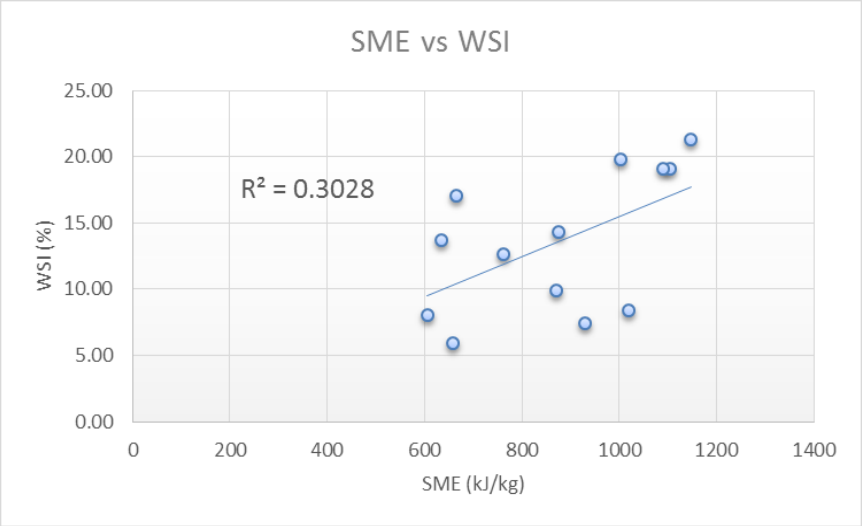

Figure 5.28: Correlation between SME and WSI

The correlation between SME and WSI is a positive relationship indicating that, more the mechanical energy input, more the degradation of feed material inside the extruder. Higher SME leads to higher shear causing more breakdown of raw material.

The R^2 values of the above correlations are low, indicating very weak correlation. This may be due to just 15 data points. But the graphs do indicate whether a given cross-correlation is in the positive or the negative direction. Even though the correlations are not statistically strong it helps us to gain some insights into possible trends.

Figure 5.29 shows an overall schematic representation of the major mechanisms that led to physico-chemical changes in the extrudates.

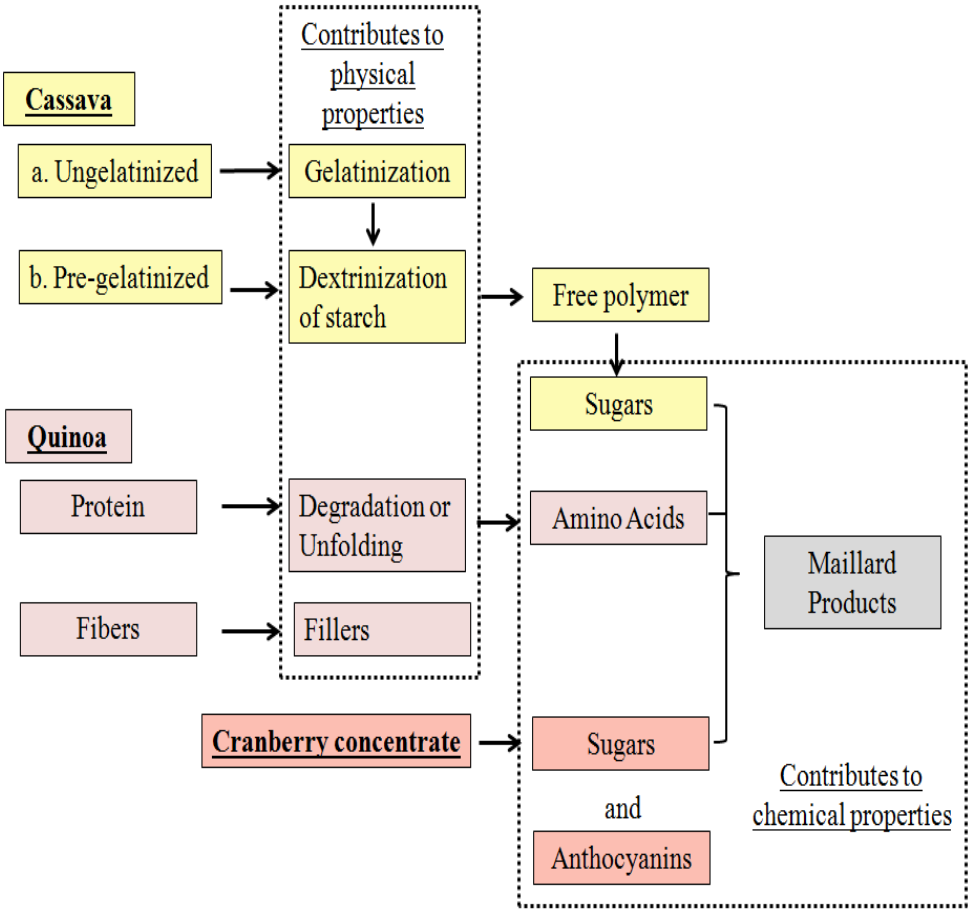

Figure 5.29: Schematic representation of changes during extrusion

5.12. Residual plots:

Residuals are plotted to find the adequacy of the model for the data and to detect if there are any unusual patterns. Residuals (ε_i) as shown in equation (Eq. 5.19) is calculated as mean experimental value – regressed/fitted value.

$$\varepsilon_i = y_{Experimental\ mean} - y_{Calculated} \quad \text{(Eq. 5.19)}$$

Under null hypothesis, a correct parametric model will show no visible pattern or trend when residuals are plotted against fitted/predicted values (Velilla, 1998). A goodness of fit is achieved when the residuals are randomly scattered in the plot. Therefore, apart from R^2 values, residuals were plotted for all the responses to make sure that the model fits the data and assumptions of the model are met by the predicted data. In general, if a non-random pattern (U shaped or inverted U shaped) is observed, transformations are required in order to achieve an adequate model (Teraiya, 2012). Figures 5.30-5.8 shows residual plots for REI, Bulk Density, Breaking Strength, WAI, WSI, Hue, Chroma, TPC and Anthocyanin content. None of them showed any trend or pattern, indicating that the model was a good fit for all the responses.

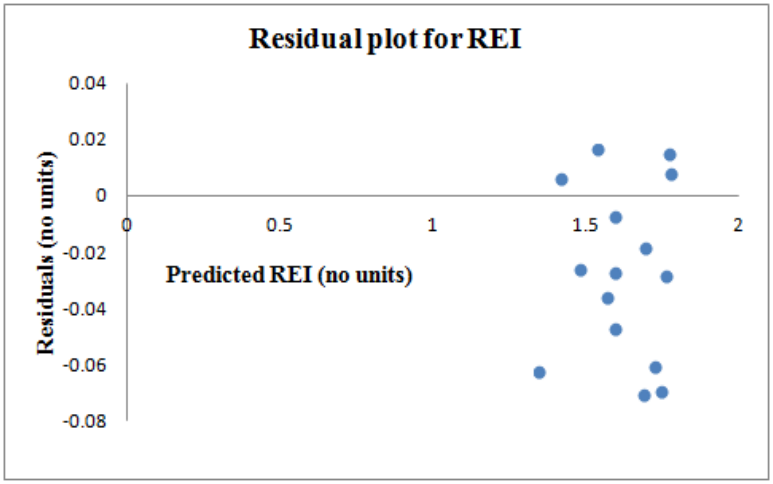

Figure 5.30: Residual plot for REI of extrudates

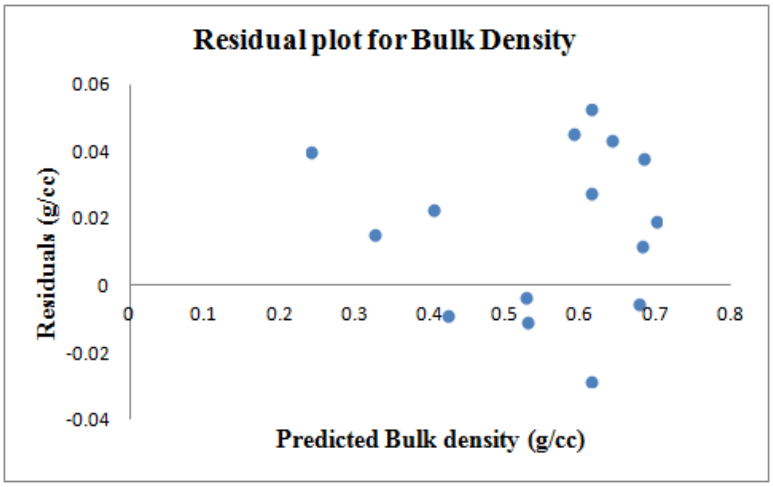

Figure 5.31: Residual plot for Bulk Density of extrudates

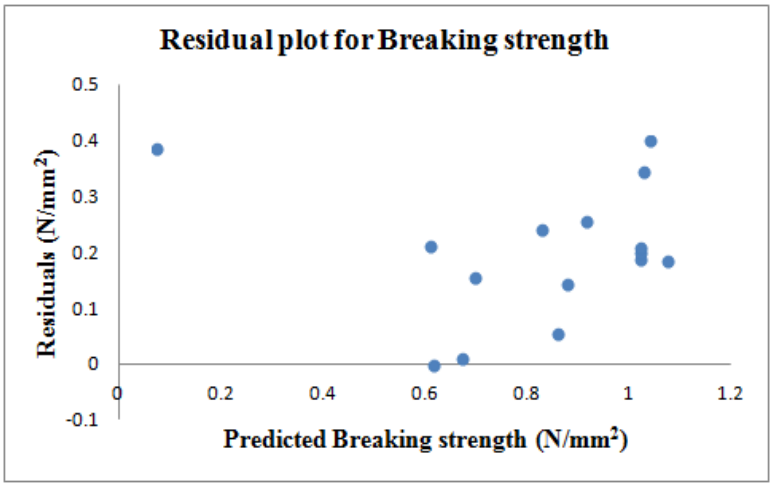

Figure 5.32: Residual plot for Breaking Strength of extrudates

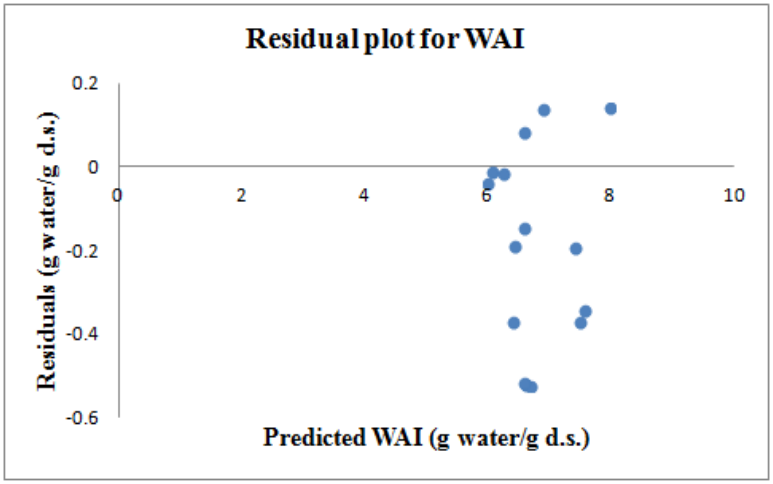

Figure 5.33: Residual plot for WAI of extrudates

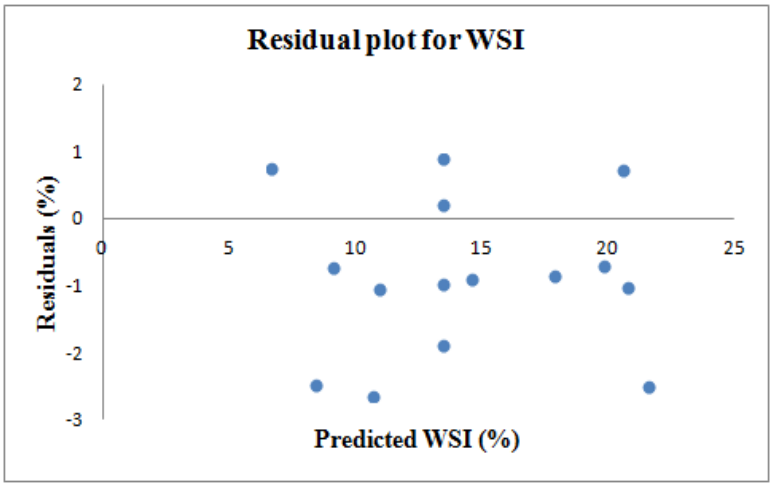

Figure 5.34: Residual plot for WSI of extrudates

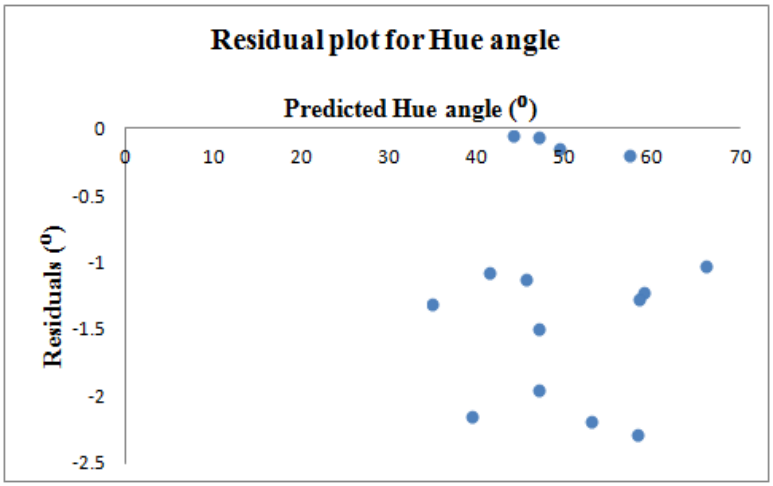

Figure 5.35: Residual plot for Hue of extrudates

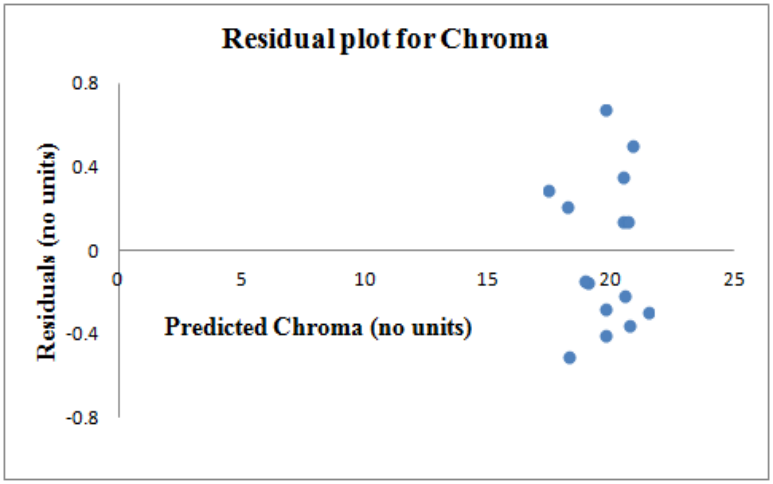

Figure 5.36: Residual plot for Chroma of extrudates

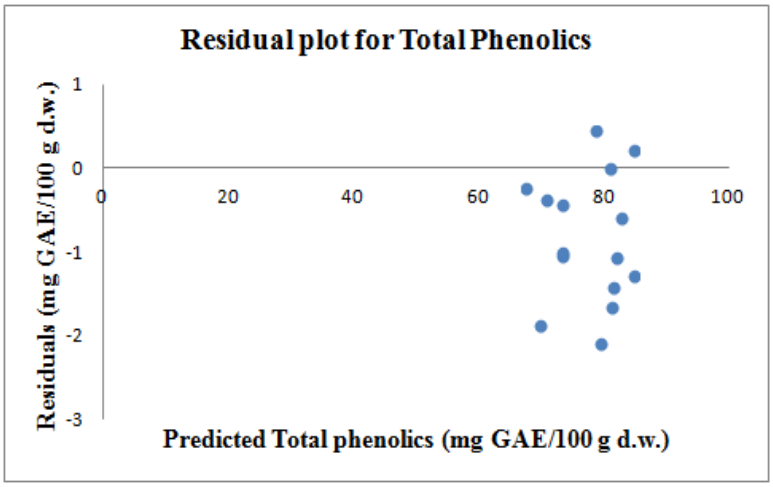

Figure 5.37: Residual plot for TPC of extrudates

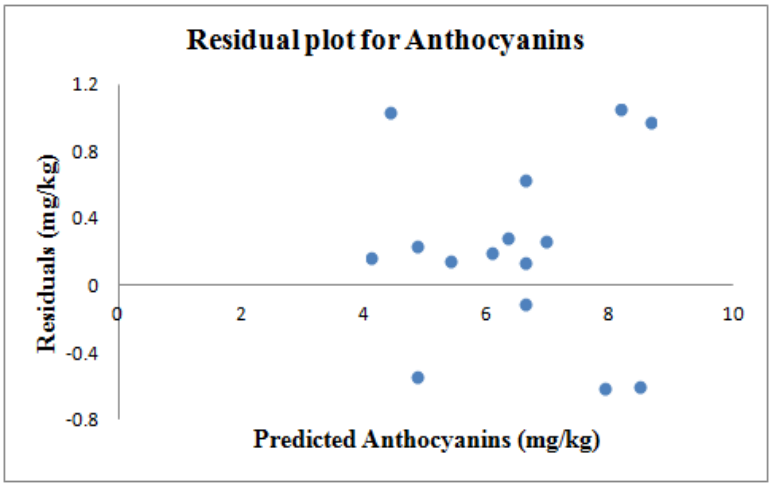

Figure 5.38: Residual plot for Anthocyanins of extrudates

6. CONCLUSIONS

1. The results show the proof-of-concept that extruded RTE breakfast cereals fortified with cranberry concentrate can be made using quinoa-cassava blends.
2. Cassava acted as an extrusion aid and helped in expansion of quinoa extrudates.
3. Cranberry solids provided extrudates with natural red color and contributed to the anthocyanin content of the extrudates.
4. On the other hand, the addition of cranberry concentrate caused textural changes and led to increase in the breaking strength of the extrudates.
5. Higher cranberry solids (5 % d.b.) produced extrudates that had appealing pink look. Extrudates that contained low percentage cranberry solids processed at higher barrel temperatures were brown in color.
6. Overall, barrel temperature and feed moisture were the two most important factors that affected physical characteristics of the extrudates.
7. Phenolic content and anthocyanin content of extrudates was majorly affected by barrel temperature and feed moisture.
8. Extrudates processed at high temperatures showed maximum values for both TPC and anthocyanin content.
9. Higher percentage losses (~ 73 %) due to both barrel temperature and/or feed moisture, were observed in extrudates that had 5 % cranberry solids.
10. Higher values for TPC at high barrel temperature was probably due to the formation of Maillard reaction products.

7. FUTURE WORK

1. The anthocyanin loss percentage varied from 54.69 % to 79.01 %. Such high losses can be possibly minimized by encapsulating the anthocyanins.
2. Since the cranberry concentrate had 50 °Brix, it affected some physical properties, especially the breaking strength of the extrudate. Hence, one can try using a lower °Brix concentrate or 7.5 °Brix fruit juice.
3. The lowest feed moisture used in this study was 16 % w.b. In future, the feed moisture can be reduced to 14 % w.b., if the extruder can handle it without jamming.
4. In order to not compromise on the nutrition benefits, we did not go higher in cassava ratio of the base feed in this study. But, to improve some physical properties, 60 % or 75 % of cassava can be used in the base blend, and studied.
5. Cassava flour used in this study was 31.85 % pre-gelatinized. A possible future direction could be to increase this pre-gelatinization % to improve some physical properties.
6. The extrusion study could be carried out on a twin screw extruder, for the feed material will undergo more shear and produce products that might have very different physical and chemical properties.
7. Use colored quinoa in place of the white quinoa in this study and compare the chemical profiles.

REFERENCES:

1. Abugoch, J. L. E. (2009). Quinoa (*Chenopodium quinoa* Willd.): Composition, chemistry nutritional and functional properties. *Advances in Food and Nutrition Research*. 58.

2. Ahamed, N. T., Rekha, S. S., Pushpa, R. K., and Mohinder, P. (1996). Physicochemical and functional properties of Chenopodium quinoa starch. *Carbohydrate polymers*. 31: 99-103.

3. Ahamed, N. T., Rekha, S. S., Pushpa, R. K., and Mohinder, P. (1998). A lesser-known grain, Chenopodium quinoa: Review of the chemical composition of its edible parts. *Food and Nutrition Bulletin*. 19: 61-68.

4. Al-Rabadi, G. J., Torley, P. J., Williams, B. A., Bryden, W. L., and Gidley, M. J. (2011). Particle size of milled barley and sorghum and physico-chemical properties of grain following extrusion. *Journal of Food Engineering*. 103: 464–472.

5. Altan, A., McCarthy, K. L., and Maskan, M. (2009). Effect of extrusion process on antioxidant activity, total phenolics and betaglucan content of extrudates developed from barley-fruit and vegetable by-products. *International Journal of Food Science and Technology*. 44: 1263–1271.

6. Akdogan, H. (1996). Pressure, torque, and energy responses of a twin screw extruder at high moisture contents. *Food Research International*. 29 (5–6): 423–429.

7. Alves, A. and Cunha, A. (2002). Cassava botany and physiology. CAB International Cassava. Biology production and Utilization. Chapter 5: 67-89.

8. Anderson, R. A., Conway, H. F., Pfeiffer, V. F., and Griffin, L. E. J. (1969). Gelatinization of corn grits by roll-and extrusion cooking. *Cereal Science Today*. 14: 4-12.

9. Atre, A. (2011). Master's thesis: Application of G*arcinia indica* as a colorant and antioxidant in rice extrudates. Food Science Department. Rutgers University.

10. Atwell, A., Patrick, B. N., Johnson, L. A., and Glass, R. W. (1982). Characterization of quinoa starch. *Cereal Chemistry*. 60: 9-11.

11. Aslan, N. and Cebeci, Y. (2007). Application of Box–Behnken design and response surface methodology for modeling of some Turkish coals. *Fuel*. 86: 90–97.

10. Badrie, N. and Mellowes, W. A. (1991). Effect of Extrusion Variables on Cassava Extrudates. *Journal of Food Science,* 56: 1334–1337.

11. Barret, A. M. and Peleg, M. (1992). Extrudate cell structure-texture relationship. *Journal of Food* Science. 53: 1464–1469.

12. Beatriz, V. Y. and Suzana, C. D. S. L. (2012). Applications of Quinoa (*Chenopodium Quinoa* Willd.) and Amaranth (Amaranthus Spp.) and Their Influence in the Nutritional Value of Cereal Based Foods. *Food and Public Health.* 2(6): 265-275.

13. Berrios, J. J., Wood, D. F., Whitehand, L., and Pan, J. (2004). Sodium bicarbonate and the microstructure, expansion and color of extruded black beans. *Journal of Food Processing and Preservation*. 28: 321-335.

14. Brennan, M. A., Derbyshire, E., Tiwari, B. K., and Brennan, C. S. (2013). Ready-to-eat snack products: the role of extrusion technology in developing consumer acceptable and nutritious snacks. *International Journal of Food Science & Technology*. 48: 893-902.

15. Brown, N. P. and Shipley, R. P. (2011). Determination of Anthocyanins in Cranberry Fruit and Cranberry Fruit Products by High-Performance Liquid Chromatography with Ultraviolet Detection: Single-Laboratory Validation. *Journal of AOAC International*.94, 2.

16. Brimer, L. (2014). Chapter 10 – Cassava Production and Processing and Impact on Biological Compounds. Processing and Impact on Active Components in Food, 81–87.

17. Camire, M. E., Chaovanalikit, A., Dougherty, M.P., and Briggs, J. (2002). Blueberry and grape anthocyanins as breakfast cereal colorants. *Journal of Food Science*. 7(1):438–41.

18. Camire, M. E., Dougherty, M. P., and Briggs, J. L. (2007). Functionality of fruit powders in extruded corn breakfast cereals. *Food Chemistry.* 101 (2): 765-770.

19. Chang, Y. K. and El-Dash, A. A. (2003). Effects of acid concentration and extrusion variables on some physical characteristics and energy requirements of cassava starch. *Brazilian Journal of Chemical Engineering*, 20(2), 129-137.

20. Chang, Y. K., Silva, M. R., Gutkoski, L. C., Sebio, L., and Da Silva, M. A. (1998). Development of extruded snacks using jatobá (Hymenaea stigonocarpaMart) flour and cassava starch blends. *Journal of the Science of Food and Agriculture*, *78*(1), 59-66.

21. Charles, A. L., Sriroth, K., and Tozou-chi, H. (2005). Proximate composition, mineral contents, hydrogen cyanide and phytic acid of 5 cassava genotypes. *Food Chemistry*. 92(4): 615-620.

22. Chaovanalikit, A., Dougherty M. P., Camire, M. E., and Briggs, J. (2003). Ascorbic acid fortification Reduces anthocyanins in Extruded blueberry-corn cereals. *Journal of Food Science.* 68(6): 2136-2104.

23. Cochrane, S. (2014). The Munsell Color System: A scientific compromise from the world of art. *Studies in History and Philosophy of Science.* 47: 26-41.

24. Coulter, L. A. and Lorenz, K. (1990). Quinoa-Composition, Nutritional value, food applications. *LWT- Food Science and Technology*. 23: 203-207.

25. Della Valle, G., Quillien, L., and Gueguen, J. (1994). Relationships between processing conditions and starch and protein modifications during extrusion-cooking of pea flour. *Journal of Agricultural and Food Chemistry*. 64: 509-517.

26. Ding, Q. B., Ainsworth, P., Plun-Kett, A., Tucker, G., and Marson, H. (2006). The effect of extrusion conditions on the functional and physical properties of wheat based expanded snacks. *Journal Food Engineering*. 73: 142-148.

27. Dlamini, N. R., Taylor, J. R. N., and Rooney, L. W. (2007). The effect of sorghum type and processing on the antioxidant properties of African sorghum-based foods. *Food Chemistry*. 105: 1412–1419.

28. Food and Agriculture Organization of the United Nations. (2011). Quinoa: An ancient crop to contribute to world food security. Brochure from Regional office for Latin America and the Caribbean.

29. Food and Agriculture Organization of the United Nations. (2013). Food Outlook. Biannual Report on Global Food Markets. (Quinoa : June 2013)

30. Food and Agriculture Organization of the United Nations. (2013). Food Outlook. Biannual Report on Global Food Markets. (Cassava : November 2013)

31. Ferreira, S. L. C., Bruns, R. E., Ferreira, H. S., Matos, G. D., David, J. M., Brandão, G.C., da Silva, E. G. P., Portugal, L. A., dos Reis, P. S., Souza, A. S., and dos Santos, W. N. L. (2007). Box-Behnken design: An alternative for the optimization of analytical methods. *Analytica Chimica Acta*. 597: 179-186.

32. Frame, N. D. (1994). The technology of extrusion cooking. First edition Chapman & HallSalisbury,Wiltshire; Blackie Academic & Professional.

33. Giacarini-Chiappe, G. (2008). Master's thesis. Effect of high hydrostatic pressure and thermal processing on cranberry juice. Rutgers University, New Brunswick, New Jersey.

34. Gomez, M. H. and Aguilera, J. M. (1984). Physicochemical model for extrusion of corn starch. *Journal of Food Science*. 9(1): 40-43.

35. Grace, H. M., Aaron, R. M., Flaubert, M., Gad, G. Y., and Mary, A. L. (2012). Comparison of Health-Relevant Flavonoids in Commonly Consumed Cranberry Products. *Journal of Food Science.* 77:176-183.

36. Guerrero, P., Beatty E., Kerry J. P., and Caba, K. de la. (2012). Extrusion of soy protein with gelatin and sugars at low moisture content. *Journal of Food Engineering*. 110: 53–59.

37. Hashimoto, J. M. and Grossmann, M. V. E. (2003). Effects of extrusion conditions on quality of cassava bran/cassava starch extrudates. *International Journal of Food Science & Technology,* 38: 511–517.

38. Hashimoto, J. M., Elizabeth H. N., Helio, S. C., A´lvaro, R. G., Fernando, M. B., and Yoon, K. L. (2002). Effect of processing conditions on some functional characteristics of extrusion-cooked cassava starch/wheat gluten blends. *Journal of the Science of Food and Agriculture*. 82: 924-930.

39. Hirth, M., Leiter, A., Beck, M. S., and Heike, P. S. (2014). Effect of extrusion cooking process parameters on the retention of bilberry anthocyanins in starch based foods. Journal of Food Engineering 125: 139-146.

40. Ilo, S., Liu, Y., and Berghofer, E. (1999). Extrusion cooking of rice flour with amaranth blends. LWT, 32, 79.

41. Jacobsen, S. E., Mujica, A., and Ortiz, R. (2003). The Global Potential for Quinoa and Other Andean Crops. *Food Reviews International*.19: 139-148.

42. Jyothi, A. N., Sasikiran, K., Sajeev, M. S., Revamma, R., and Moorthy, S. N. (2005). Gelatinisation properties of cassava starch in the presence of salts, acids and oxidising agents. *Starch-Stärke.* 57(11), 547-555.

43. Karwe, M. V. (2003). Food extrusion, in Encyclopedia of Life Support Systems (EOLSS), Developed under the Auspices of the UNESCO, EOLSS Publishers, Oxford, UK.

44. Karwe, M. V. (2014). Lecture Notes from Food Engineering Fundamental course (16:400:507). Personal Communication.

45. Kirby, A. R., Ollett, A. L., Parker, R., and Smith, A.C. (1988). An experimental study of screw configuration effects in the twin-screw extrusion-cooking of maize grits. *Journal of Food Engineering*. 8: 247–272.

46. Kokini, J. L., Cocero, A. M., Madeka, H., and Graaf, E. (1994). The development of state diagrams for cereal proeins. *Trends in Food Science & Technology.* 5: 281-288.

47. Koziol, M. J. (1992). Chemical composition and nutritional evaluation of Quinoa (Chenopodium quinoa Willd.). *Journal of food composition and analysis*. 5: 35-68.

48. Lai, L. S. and Kokini, J. (1991). Physicochemical changes and rheological properties of starch during extrusion. *Biotechnology Progress*. 7 (3): 251–266.

49. Launay, B. and Lisch, J. M. (1983). Twin-screw extrusion cooking of starches: Flow behavior of starch pastes, expansion and mechanical properties of extrudates. *Journal of Food Engineering*. 2: 259–280.

50. Laus, N. M., Anna, G., Mario, S., Zina, F., and Donato, P. (2012). Antioxidant activity of free and bound compounds in quinoa (chenopodium quinoa willd.) seeds in comparison with durum wheat and emmer. *Journal of Food Science.* 77: 1150-1155.

51. Leonel, M., Taila S. F., and Martha, M. M. (2009). Physical characteristics of extruded cassava starch. *Scientia Agricola (Piracicaba, Braz.)*. 66(4): 486-493.

52. Linko, P., Kervinen, R., Karppinen R., Rautalinna, E. K., and Vainionpaa, J. (1985). Extrusion cooking for cereal-based intermediate-moisture products. properties of water in foods. ISBN 978-94-010-8756-8.465-479.

53. Maga, J. A. and Kim, C. H. (1989). Co-extrusion of rice flour with dried fruits and fruit concentrates. Food Science and Technology. *Lebensmittel--Wissenschaft und ¹Technologie*. 22: 182-187.

54. Mantius, H. L. and Peterson, P. R. (1995). Fruit extraction and infusion, Patent no: 5,419,251.

55. Mariotti, M., Alamprese, C., Pagani, M.A., and Lucisano, M. (2006). Effect of puffing on ultrastructure and physical characteristics of cereal grains and flours. *Journal of cereal science*. 43:47-56

56. McKay, D. L., and Jeffrey, B. B. (2007). Cranberries (Vaccinium macrocarpon) and Cardiovascular Disease Risk Factors. *Nutrition Reviews.* 65(11): 490-502.

57. Mejía-Agüero, L., Galeno F., Hernández-Hernández, O., Matehus, J., and Tovar, J. (2012). Starch determination, amylose content and susceptibility to in vitro amylolysis in flours from the roots of 25 cassava varieties. *Journal of the Science of Food and Agriculture*. 92: 673-678.

58. Montagnac, A. J., Christopher, R. D., and Sherry, A. T. (2009). Nutritional Value of Cassava for Use as a Staple Food and Recent Advances for Improvement. *Comprehensive Reviews in Food Science and Food Safety*. 8: 181-194.

59. Moreau, R., Whitaker, B., and Hick, K. (2002). Phytosterols, phytostanols, and their conjugates in foods: Structural diversity, quantitative analysis, and health-promoting uses. *Progress in Lipid Research*. 41(6): 457–500.

60. Mundigler, N. (1998). Isolation and determination of starch from amaranth (Amaranthus cruentus) and quinoa (Chenopodium quinoa). *Starch*. 50(2-3): 67–69.

61. Nabeshima, E. H. and Grossmann, M. V. E. (2001). Functional properties of pregelatinized and cross-linked cassava starch obtained by extrusion with sodium trimetaphosphate. *Carbohydrate Polymers*, *45*(4), 347-353.

62. NASS (National Agriculture Statistics Service). 2010. Cranberry forecast [Internet]. Available from:

http://www.nass.usda.gov/Statistics_by_State/New_England_includes/Publications/cran0808.pdf. Accessed on Oct 1, 2014.

63. Nesaretnam, K. (2008). Multitargeted therapy of cancer by tocotrienols. *Cancer Letters*. 269(2): 388–395.

64. Nunzia, C., Maria T. L., Margherita, P., Mariassunta, V., Vincenzo, L. (2009). A reproducible, rapid and inexpensive Folin–Ciocalteu micro-method in determining phenolics of plant methanol extracts. *Microchemical Journal*. 91: 107–110.

65. Oshodi, A., Ogungbenle, H., and Oladimeji, M. (1999). Chemical composition, nutritionally valuable minerals and functional properties of benniseed, pearl millet and quinoa flours. *International Journal of Food Science and Nutrition*. 50: 325–331.

66. Pokorny, J. and Schmidt, S. (2006). Natural antioxidant functionality during food processing. In J. Pokorny, N. Yanishlieva, & M. Gordon (Eds.). Antioxidants in food. Washington, DC: CRC Press. 380: 331-351.

67. Potter, R., Valentina, S., and Andrew, P. (2013). The use of fruit powders in extruded snacks suitable for Children's diets. *LWT - Food Science and Technology.* 51: 537-544.

68. Prego, I., Maldonado, S., and Otegui, M. (1998). Seed structure and localization of reserves in *Chenopodium quinoa*. *Annals of Botany*. 82: 481-488.

69. Prior, L., Ronald, L., Ellen, F., Hongping, J., Amy, H., Christian, N., Mark, J. P., and Jess Reed. (2009). Multi-laboratory validation of a standard method for quantifying proanthocyanidins in cranberry powders. *Journal of the Science of Food and Agriculture*. 90: 1473–1478.

70. Przybylski, R., Chauhan, G., and Eskin, N. (1994). Characterization of quinoa (Chenopodium quinoa) lipid. *Food Chemistry*. 51(2): 187–192.

71. Qian, J. and Kuhn, M. (1999). Characterization of Amaranthus cruentus and Chenopodium quinoa starch. *Starch*. 51(4), 116–120.

72. Rampersad, R., Badrie, N., and Comissiong, E. (2003). Physico-chemical and Sensory Characteristics of Flavored Snacks from Extruded Cassava/Pigeonpea Flour. *Journal of food science*. *68*(1): 363-367.

73. Ranhotra, G., Gelroth, J., Glaser, B., Lorenz, K., and Johnson, D. (1993). Composition and protein nutritional quality of quinoa. *Cereal Chemistry*. 70(3), 303–305.

74. Rekhy, R. and McConchie, R. (2014). Promoting consumption of fruit and vegetables for better health. Have campaigns delivered on the goals. *Appetite*. 79: 113-123.

75. Riaz, M. N. (2000). Extruders in food applications. 1st ed., Lancaster, PA, Technomic Publishing Company, Inc.

76. Rocha, T. S., Ana, P. A. C., and Celia, M. L. F. (2010). Effect of enzymatic hydrolysis on some physicochemical properties of root and tuber granular starches. *Ciênc. Tecnologia Aliment.,Campinas*. 30(2): 544-551.

77. Ruales, J. and Nair, B. M. (1993). Content of fat, vitamins and minerals in quinoa (Chenopodium quinoa Willd.) seeds. *Food Chemistry*. 48: 131–136.

78. Ryan, E., Galvin, K., O'Connor, T., Maguire, A., and O'Brien, N. (2007). Phytosterol, squalene, tocopherol content and fatty acid profile of selected seeds, grains, and legumes. *Plant Foods for Human Nutrition*. 62: 85–91.

79. Sarkar, P., Nikhil, S., and Gour S. C., (2011). Extrusion Processing of Cactus Pear. *Advanced Journal of Food Science and Technology*. 3(2): 102-110.

80. Schlick, G. and Bubenheim, D. (1993). 'Quinoa: An Emerging "New" Crop with Potential for CELSS', Technical Paper 3422. NASA, California, USA.

81. Seth, D. and Gopirajah, R. (2012). Development of extruded snacks using soy, sorghum, millet and rice blend – A response surface methodology approach. *International Journal of Food Science and Technology*. 47: 1526–153.

82. Sharma, P., Gujral, H. S., and Singh, B. (2012). Antioxidant activity of barley as affected by extrusion cooking. *Food Chemistry*. 131: 1406–1413.

83. Singh, N. and Smith, A. C. (1997). A comparison of wheat starch, whole wheat meal and oat flour in the extrusion cooking process. *Journal of Food Engineering*. 34: 15–32.

84. Singh, S., Shirani, G., and Lara, W. (2007). Nutritional aspect of food extrusion: a review. *International Journal of Food Science and Technology*. 42: 916-929.

85. Singleton, V. L. and Rossi, J. A. (1965). Colorimetry of total phenolics with phosphomolybdicphosphotungstic acid reagents. *American Journal of Enology and Viticulture. 16*: 144-158.

86. Sriburi, P. and Hill, S. E. (2000). Extrusion of cassava starch with either variations in ascorbic acid concentration or pH. *International Journal of Food Science & Technology*. *35*(2): 141-154.

87. Stintzing, F. C. and Carle, R. (2004). Functional properties of anthocyanins and betalains in plants, food, and in human nutrition. *Trends in Food Science and Technology*. 15: 19-38.

88. Stojceska, V. P. A., Andrew, P., Esra I., and Senol, I. (2008). Cauliflower by-products as a new source of dietary fibre, antioxidants and proteins in cereal based ready-to-eat expanded snacks. *Journal of Food Engineering.* 87: 554–563.

89. Swamy, G. J., Sangamithra, A., and Chandrasekar, V. (2014). Response surface modeling and process optimization of aqueous extraction of natural pigments from Beta vulgaris using Box-Behnken design of experiments. *Dyes and Pigments*. 111: 64-74.

90. Tacer-Caba, Z., Dilar, N., Hikmet, B. M., and Perry, K. W., and Ng, P. K. (2014). Evaluating the effects of amylose and Concord grape extract powder substitution on pysicochemical properties of wheat flour extrudates produced at different temperatures. *Food Chemistry.* 157: 476–484.

91. Taverna, L. G., Leonel, M., and Mischan, M. M. (2012). Changes in physical properties of extruded sour cassava starch and quinoa flour blend snacks. *Ciência e Tecnologia de Alimentos, Campinas*. 32, 4: 826-834.

92. Thomas, G. R., Pamela, R. P., Jaspreet, K. C., and Ahujaa, E. S. (2013) Recent trends in ready-to-eat breakfast cereals in the U.S. *Procedia Food Science.* 2: 20 – 26.

93. Tivana L. D., Petr D., and Björn B. (2010). Characterization of the agglomeration of roasted shredded cassava (Manihot esculenta crantz) roots. *Starch.* 62:637-646.

94. UK AID. Oversees development institute. Food Prices March 2012 update & Annual Review April 2011 to March 2012.

95. Uwieczkowska, A., Kawecki, Z., and Stanys, V. (2004). Growth and yielding of the large cranberry Vaccinum macrocarpon Ait. fertilized with nitrogen and potassium. 2. The quality of berries. *Horticulture and Vegetable Growing*. 23: 36–40.

96. Varriano-Marston, E. and DeFrancisco, A. (1984). Ultrastructure of quinoa fruit. *Food Microstructure.* 3: 165–173.

97. Vega-Gálvez, A., Miranda, M., Vergara, J., Uribe, E., Puente, L., Martínez, E. A. (2010). Nutrition facts and functional potential of quinoa (Chenopodium quinoa willd.), an ancient Andean grain: a review. *Journal of the Science of Food and Agriculture*. 90(15): 2541-2547.

98. Velilla, S. (1998). A note on the behavior of residual plots in regression. *Statistics & Probability Letters*. 37: 269-278.

99. Viskelis, P., Rubinskiene, M., Jasutiene, I., Sarkinas, A., Daubaras, R., and Cesoniene L. (2009). Anthocyanins, Antioxidative, And Antimicrobial Properties of American Cranberry (*Vaccinium Macrocarpon* Ait.) and yheir Press Cakes. *Journal of Food Science*. 74: 157-161.

100. Waramboi, G. J., Gidley, J. M., and Sopade, A. P. (2014). Influence of extrusion on expansion, functional and digestibility properties of whole sweet potato flour. *LWT - Food Science and Technology.* 59: 1136-1145.

101. Wheately, C. C. and Chuzel, G. (1993). Cassava:the nature of tuber and use as raw material.In Macrare, R. Robinson, R.K. and Sadler, M.J (eds) Encyclopedia of Food Science. Food Technology and Nutrition. Academic Press, San Diego, California, 732-743.

102. White, B. L., Howard, L. R., and Prior, R. L. (2010). Polyphenolic composition and antioxidant capacity of extruded cranberry pomace. *Journal of Agriculture and Food Chemistry.* 58, 4037–4042.

103. White, B. L., Howard, L. R., and Prior, R. L. (2011). Impact of different stages of juice processing on the anthocyanin, flavonol, and procyanidin contents of cranberries. *Journal of Agriculture and Food Chemistry*. 59: 4692–4698.

104. Wildflower center. http://www.wildflower.org/plants/result.php?id_plant=VAMA, Accesed on August 15, 2014.

105. Wrolstad, R. E., Acree, T. E., Decker, E. A., Penner, M. H., Reid, D. S., Schwartz, S. J., Shoemaker C. F., Smith, D., and Sporns, P. (2005). Handbook of food analytical chemistry vol. 2: Pigments, colorants, flavors, texture, and bioactive food components. 1st ed., Hoboken, NJ, John Wiley & Sons, Inc.

106. Youdim, K., Martin, A., and Joseph, J. (2000). Essential fatty acids and the brain: Possible health implications. *International Journal Developmental. Neuroscience*. 18(4–5): 383–399.

107. Zhang, J., Sokhansanj, S., Wu, S., Fang, R., Yang, W., and Winter, P. (1998). A transformation technique from RGB signals to the Munsell system for color analysis of tobacco leaves. *Computers and Electronics in Agriculture*. 19: 155–166.

108. Zhang, Y., Zuqiang H., Cong, Y., Aimin, H., Huayu, H., Zhanqiang, G., Guosong, S., and Kelin, H. (2013). Material properties of partially pregelatinized cassava starch prepared by mechanical activation. *Starch*. 65: 461–468.

109. Zielinski, H., Kozlowska, H., and Lewczuk, B. (2001). Bioactive compounds in the cereal grains before and after hydrothermal processing. *Innovative Food Science and Emerging Technologies*. 2(111): 159–169.

110. Zielinski, H., Michalska, A., Piskula, M. K., and Kozlowska, H. (2006). Antioxidants in thermally treated buckwheat groats. *Molecular Nutrition & Food Research.* 50: 824–832.

APPENDIX

Typical datasheet generated by SAS v9.2 for statistical analysis

ADX Report

Today's date: 14SEP2014
Experiment creation date: 11AUG2014

DESIGN POINTS (Coded)

RUN	BARTEMP	FDMOIS	CRANSOL	REI	BD	BRSTRNG	TOTPHEN	ANTHLOSS
1	-1	-1	0	1.78	0.684	1.02	81.13	64.18
2	-1	1	0	1.78	0.670	0.68	68.00	79.01
3	1	-1	0	1.67	0.281	0.46	84.96	64.49
4	1	1	0	1.28	0.413	1.17	79.54	54.69
5	0	-1	-1	1.73	0.523	0.82	77.45	66.67
6	0	-1	1	1.67	0.518	0.91	80.16	62.16
7	0	1	-1	1.53	0.634	1.37	67.43	71.72
8	0	1	1	1.45	0.721	1.26	79.09	75.39
9	-1	0	-1	1.66	0.693	1.07	70.40	64.29
10	1	0	-1	1.55	0.339	0.61	82.29	63.74
11	-1	0	1	1.61	0.718	1.44	80.87	73.98
12	1	0	1	1.42	0.425	0.85	83.48	69.05
13	0	0	0	1.54	0.665	1.21	72.90	64.40
14	0	0	0	1.56	0.640	1.22	72.28	66.83
15	0	0	0	1.58	0.584	1.23	72.32	68.06

DESIGN POINTS (Uncoded)

RUN	BARTEMP	FDMOIS	CRANSOL	REI	BD	BRSTRNG	TOTPHEN	ANTHLOSS
1	120	16	4	1.78	0.684	1.02	81.13	64.18
2	120	20	4	1.78	0.670	0.68	68.00	79.01
3	160	16	4	1.67	0.281	0.46	84.96	64.49
4	160	20	4	1.28	0.413	1.17	79.54	54.69
5	140	16	3	1.73	0.523	0.82	77.45	66.67
6	140	16	5	1.67	0.518	0.91	80.16	62.16

7	140	20	3	1.53	0.634	1.37	67.43	71.72
8	140	20	5	1.45	0.721	1.26	79.09	75.39
9	120	18	3	1.66	0.693	1.07	70.40	64.29
10	160	18	3	1.55	0.339	0.61	82.29	63.74
11	120	18	5	1.61	0.718	1.44	80.87	73.98
12	160	18	5	1.42	0.425	0.85	83.48	69.05
13	140	18	4	1.54	0.665	1.21	72.90	64.40
14	140	18	4	1.56	0.640	1.22	72.28	66.83
15	140	18	4	1.58	0.584	1.23	72.32	68.06

FIT DETAILS FOR TOTAL PHENENOLICS:

TOTAL PHENENOLICS Check Assumptions Analysis

Response Transformation
- Optimal power from Box-Cox plot: 1/TOTPHEN**2
- Power recommended by ADX: TOTPHEN
- Power applied for response transformation: TOTPHEN
- Response Scaling Shift: 0

Outlier Observations
- Run numbers deleted from analysis: None

Influential Observations
- Run numbers deleted from analysis: None

ANOVA for TOTAL PHENENOLICS

	Master Model					Predictive Model				
Source	DF	SS	MS	F	Pr > F	DF	SS	MS	F	Pr > F
BARTEMP	1	111.5271	111.5271	67.92254	0.0004	1	111.5271	111.5271	45.09248	0.0005
FDMOIS	1	109.8162	109.8162	66.88056	0.0004	1	109.8162	109.8162	44.40073	0.0006
CRANSOL	1	84.69511	84.69511	51.58124	0.0008	1	84.69511	84.69511	34.24381	0.0011
BARTEMP*BARTEMP	1	77.02913	77.02913	46.91249	0.0010	1	74.0297	74.0297	29.93158	0.0016
BARTEMP*FDMOIS	1	14.86103	14.86103	9.050701	0.0298	1	14.86103	14.86103	6.008589	0.0497
BARTEMP*CRANSOL	1	21.5296	21.5296	13.11201	0.0152	1	21.5296	21.5296	8.704817	0.0256
FDMOIS*FDMOIS	1	6.629908	6.629908	4.037764	0.1007					

FDMOIS*CRANSOL	1	20.02563	20.02563	12.19606	0.0174	1	20.02563	20.02563	8.096732	0.0294
CRANSOL*CRANSOL	1	17.74913	17.74913	10.80962	0.0218	1	16.21542	16.21542	6.556194	0.0429
Model	9	454.8175	50.53528	30.77713	0.0007	8	448.1876	56.02345	22.65132	0.0006
(Linear)	3	306.0384	102.0128	62.12811	0.0002					
(Quadratic)	3	92.36285	30.78762	18.75036	0.0038					
(Cross Product)	3	56.41625	18.80542	11.45293	0.0112					
Error	5	8.209875	1.641975			6	14.83978	2.473297		
(Lack of fit)	3	7.969075	2.656358	22.06278	0.0437	4	14.59898	3.649746	30.3135	0.0322
(Pure Error)	2	0.2408	0.1204			2	0.2408	0.1204		
Total	14	463.0274				14	463.0274			

Fit Statistics for TOTAL PHENENOLICS

	Master Model	Predictive Model
Mean	76.82	76.82
R-square	98.23%	96.80%
Adj. R-square	95.04%	92.52%
RMSE	1.281396	1.572672
CV	1.66805	2.047217

Canonical Analysis: Stationary point for TOTAL PHENENOLICS

Stationary point:	Critical value is a Minimum
Predicted response at stationary point:	-20.4068
Standard error of predicted value:	579.0788

Canonical Analysis: Critical value for TOTAL PHENENOLICS

Factor Name	Coded	Uncoded
BARTEMP	-10.0992	-61.9834
FDMOIS	23.9142	65.8284
CRANSOL	-18.2878	-14.2878

Canonical Analysis: Eigenvectors for TOTAL PHENENOLICS

Eigenvalues	BARTEMP	FDMOIS	CRANSOL
5.10940	0.93723	0.14558	-0.31688
2.89867	0.15595	0.63780	0.75425
0.09193	0.31191	-0.75632	0.57506

Ridge Analysis for TOTAL PHENENOLICS

Radius	Predicted Response	Standard Error	Dependent variable	Type of ridge	BARTEMP	FDMOIS	CRANSOL
0.0	72.5000	0.73981	TOTPHEN	MINIMUM	0.00000	0.00000	0.00000
0.1	71.8870	0.73752	TOTPHEN	MINIMUM	-0.05688	0.06199	-0.05406
0.2	71.2829	0.73085	TOTPHEN	MINIMUM	-0.10814	0.12720	-0.11012
0.3	70.6855	0.72045	TOTPHEN	MINIMUM	-0.15532	0.19463	-0.16732
0.4	70.0934	0.70751	TOTPHEN	MINIMUM	-0.19952	0.26363	-0.22514
0.5	69.5058	0.69379	TOTPHEN	MINIMUM	-0.24148	0.33380	-0.28332
0.6	68.9219	0.68177	TOTPHEN	MINIMUM	-0.28172	0.40483	-0.34168
0.7	68.3414	0.67470	TOTPHEN	MINIMUM	-0.32062	0.47654	-0.40014
0.8	67.7640	0.67643	TOTPHEN	MINIMUM	-0.35846	0.54879	-0.45863
0.9	67.1893	0.69113	TOTPHEN	MINIMUM	-0.39544	0.62146	-0.51712
1.0	66.6173	0.72257	TOTPHEN	MINIMUM	-0.43172	0.69449	-0.57560
0.0	72.5000	0.73981	TOTPHEN	MAXIMUM	0.00000	0.00000	0.00000
0.1	73.1255	0.73752	TOTPHEN	MAXIMUM	0.06469	-0.05716	0.05048
0.2	73.7692	0.73085	TOTPHEN	MAXIMUM	0.13987	-0.10708	0.09471
0.3	74.4406	0.72054	TOTPHEN	MAXIMUM	0.22771	-0.14670	0.12894
0.4	75.1528	0.70808	TOTPHEN	MAXIMUM	0.32776	-0.17369	0.14969
0.5	75.9214	0.69611	TOTPHEN	MAXIMUM	0.43601	-0.18832	0.15631
0.6	76.7604	0.68851	TOTPHEN	MAXIMUM	0.54746	-0.19335	0.15135
0.7	77.6802	0.69008	TOTPHEN	MAXIMUM	0.65880	-0.19196	0.13831
0.8	78.6877	0.70598	TOTPHEN	MAXIMUM	0.76865	-0.18649	0.11999
0.9	79.7874	0.74081	TOTPHEN	MAXIMUM	0.87665	-0.17845	0.09820
1.0	80.9820	0.79776	TOTPHEN	MAXIMUM	0.98287	-0.16872	0.07410

Alias Structure for TOTAL PHENENOLICS

Master Model	Predictive Model
No effects aliased.	No effects aliased.

Predictive Model for TOTAL PHENENOLICS

Coded Levels(-1,1):

TOTAL PHENENOLICS = 73.32462 + 3.73375*BARTEMP - 3.705*FDMOIS + 3.25375*CRANSOL
+ 4.464423*BARTEMP*BARTEMP + 1.9275*BARTEMP*FDMOIS
- 2.32*BARTEMP*CRANSOL + 2.2375*FDMOIS*CRANSOL
+ 2.089423*CRANSOL*CRANSOL

Uncoded Levels:

TOTAL PHENENOLICS = 456.7284 - 3.341784*BARTEMP - 13.07375*FDMOIS - 17.35913*CRANSOL
+ 0.011161*BARTEMP*BARTEMP + 0.048188*BARTEMP*FDMOIS
- 0.116*BARTEMP*CRANSOL + 1.11875*FDMOIS*CRANSOL
+ 2.089423*CRANSOL*CRANSOL

Effect Estimates for TOTAL PHENENOLICS

	Master Model				Predictive Model			
Term	Estimate	Std Err	t	Pr > |t|	Estimate	Std Err	t	Pr > |t|
BARTEMP	3.73375	0.453042	8.241513	0.0004	3.73375	0.556024	6.715094	0.0005
FDMOIS	-3.705	0.453042	-8.17805	0.0004	-3.705	0.556024	-6.66339	0.0006
CRANSOL	3.25375	0.453042	7.182008	0.0008	3.25375	0.556024	5.851821	0.0011
BARTEMP*BARTEMP	4.5675	0.666859	6.849269	0.0010	4.4644231	0.816019	5.470977	0.0016
BARTEMP*FDMOIS	1.9275	0.640698	3.008438	0.0298	1.9275	0.786336	2.451242	0.0497
BARTEMP*CRANSOL	-2.32	0.640698	-3.62105	0.0152	-2.32	0.786336	-2.95039	0.0256
FDMOIS*FDMOIS	1.34	0.666859	2.009419	0.1007				
FDMOIS*CRANSOL	2.2375	0.640698	3.492286	0.0174	2.2375	0.786336	2.845476	0.0294
CRANSOL*CRANSOL	2.1925	0.666859	3.287799	0.0218	2.0894231	0.816019	2.560507	0.0429

ANOVA for all responses

ANOVA for REI

	Master Model					Predictive Model				
Source	DF	SS	MS	F	Pr > F	DF	SS	MS	F	Pr > F
BARTEMP	1	0.103513	0.103513	39.43333	0.0015	1	0.103513	0.103513	28.79468	0.0002
FDMOIS	1	0.082012	0.082012	31.24286	0.0025	1	0.082012	0.082012	22.8139	0.0006
CRANSOL	1	0.0128	0.0128	4.87619	0.0783					
BARTEMP*BARTEMP	1	0.000975	0.000975	0.371429	0.5689					
BARTEMP*FDMOIS	1	0.038025	0.038025	14.48571	0.0126	1	0.038025	0.038025	10.57764	0.0077
BARTEMP*CRANSOL	1	0.0016	0.0016	0.609524	0.4703					
FDMOIS*FDMOIS	1	0.009698	0.009698	3.694505	0.1126					
FDMOIS*CRANSOL	1	0.0001	0.0001	0.038095	0.8529					
CRANSOL*CRANSOL	1	0.000975	0.000975	0.371429	0.5689					
Model	9	0.249968	0.027774	10.58067	0.0091	3	0.22355	0.074517	20.72874	<.0001
(Linear)	3	0.198325	0.066108	25.18413	0.0019					
(Quadratic)	3	0.011918	0.003973	1.513439	0.3192					
(Cross Product)	3	0.039725	0.013242	5.044444	0.0568					
Error	5	0.013125	0.002625			11	0.039543	0.003595		
(Lack of fit)	3	0.012325	0.004108	10.27083	0.0900	5	0.024043	0.004809	1.861419	0.2355
(Pure Error)	2	0.0008	0.0004			6	0.0155	0.002583		
Total	14	0.263093				14	0.263093			

ANOVA for Bulk Density

	Master Model				Predictive Model				
Source	DF	SS	MS	F	Pr > F	DF	SS	MS	F	Pr > F
BARTEMP	1	0.213531	0.213531	127.5739	<.0001	1	0.213531	0.213531	93.84631	<.0001
FDMOIS	1	0.023328	0.023328	13.93729	0.0135	1	0.023328	0.023328	10.25259	0.0084
CRANSOL	1	0.004656	0.004656	2.781797	0.1562					
BARTEMP*BARTEMP	1	0.0276	0.0276	16.48969	0.0097	1	0.026511	0.026511	11.65136	0.0058
BARTEMP*FDMOIS	1	0.005329	0.005329	3.183805	0.1344					
BARTEMP*CRANSOL	1	0.00093	0.00093	0.555777	0.4895					
FDMOIS*FDMOIS	1	0.003596	0.003596	2.148522	0.2026					
FDMOIS*CRANSOL	1	0.002116	0.002116	1.264202	0.3119					
CRANSOL*CRANSOL	1	1.083E-6	1.083E-6	0.000647	0.9807					
Model	9	0.280029	0.031114	18.58926	0.0025	3	0.26337	0.08779	38.58342	<.0001
(Linear)	3	0.241515	0.080505	48.09767	0.0004					
(Quadratic)	3	0.030139	0.010046	6.002167	0.0412					
(Cross Product)	3	0.008375	0.002792	1.667928	0.2876					
Error	5	0.008369	0.001674			11	0.025029	0.002275		
(Lack of fit)	3	0.004928	0.001643	0.954902	0.5481	5	0.01378	0.002756	1.470153	0.3236
(Pure Error)	2	0.003441	0.00172			6	0.011248	0.001875		
Total	14	0.288398				14	0.288398			

ANOVA for Breaking Strength

	Master Model					Predictive Model				
Source	DF	SS	MS	F	Pr > F	DF	SS	MS	F	Pr > F
BARTEMP	1	0.1568	0.1568	3.824857	0.1079	1	0.1568	0.1568	3.159346	0.1031
FDMOIS	1	0.201613	0.201613	4.917978	0.0774	1	0.201613	0.201613	4.062268	0.0689
CRANSOL	1	0.043512	0.043512	1.06141	0.3501					
BARTEMP*BARTEMP	1	0.217131	0.217131	5.296518	0.0696					
BARTEMP*FDMOIS	1	0.275625	0.275625	6.723381	0.0487	1	0.275625	0.275625	5.553537	0.0380
BARTEMP*CRANSOL	1	0.004225	0.004225	0.103061	0.7612					
FDMOIS*FDMOIS	1	0.077631	0.077631	1.893664	0.2272					
FDMOIS*CRANSOL	1	0.01	0.01	0.243932	0.6423					
CRANSOL*CRANSOL	1	0.000831	0.000831	0.020265	0.8924					
Model	9	0.974998	0.108333	2.642594	0.1485	3	0.634038	0.211346	4.258384	0.0317
(Linear)	3	0.401925	0.133975	3.268081	0.1175					
(Quadratic)	3	0.283223	0.094408	2.30291	0.1943					
(Cross Product)	3	0.28985	0.096617	2.356791	0.1884					
Error	5	0.204975	0.040995			11	0.545936	0.049631		
(Lack of fit)	3	0.204775	0.068258	682.5833	0.0015	5	0.438386	0.087677	4.891334	0.0395
(Pure Error)	2	0.0002	0.0001			6	0.10755	0.017925		
Total	14	1.179973				14	1.179973			

ANOVA for WAI

	Master Model					Predictive Model				
Source	DF	SS	MS	F	Pr > F	DF	SS	MS	F	Pr > F
BARTEMP	1	3.20045	3.20045	20.09029	0.0065	1	3.20045	3.20045	17.50025	0.0011
FDMOIST	1	0.18	0.18	1.12992	0.3364					
CRANSOLI	1	0.0018	0.0018	0.011299	0.9195					
BARTEMP*BARTEMP	1	0.725703	0.725703	4.555476	0.0859					
BARTEMP*FDMOIST	1	0.0196	0.0196	0.123036	0.7401					
BARTEMP*CRANSOLI	1	0.2209	0.2209	1.386663	0.2920					
FDMOIST*FDMOIST	1	0.102564	0.102564	0.643829	0.4588					
FDMOIST*CRANSOLI	1	0.2704	0.2704	1.697391	0.2494					
CRANSOLI*CRANSOLI	1	0.022656	0.022656	0.142222	0.7216					
Model	9	4.781377	0.531264	3.334921	0.0990	1	3.20045	3.20045	17.50025	0.0011
(Linear)	3	3.38225	1.127417	7.077169	0.0300					
(Quadratic)	3	0.888227	0.296076	1.858565	0.2541					
(Cross Product)	3	0.5109	0.1703	1.06903	0.4408					
Error	5	0.796517	0.159303			13	2.377443	0.18288		
(Lack of fit)	3	0.61325	0.204417	2.230811	0.3244	1	0.7548	0.7548	5.582008	0.0359
(Pure Error)	2	0.183267	0.091633			12	1.622643	0.13522		
Total	14	5.577893				14	5.577893			

ANOVA for WSI

	Master Model					Predictive Model				
Source	DF	SS	MS	F	Pr > F	DF	SS	MS	F	Pr > F
BARTEMP	1	284.0536	284.0536	74.96325	0.0003	1	284.0536	284.0536	61.15976	<.0001
FDMOIST	1	18.39211	18.39211	4.853776	0.0788					
CRANSOLI	1	0.14045	0.14045	0.037065	0.8549					
BARTEMP*BARTEMP	1	3.187756	3.187756	0.841266	0.4011					
BARTEMP*FDMOIST	1	1.5376	1.5376	0.405781	0.5521					
BARTEMP*CRANSOLI	1	0.216225	0.216225	0.057063	0.8207					
FDMOIST*FDMOIST	1	0.516926	0.516926	0.136419	0.7270					
FDMOIST*CRANSOLI	1	17.43063	17.43063	4.600034	0.0848					
CRANSOLI*CRANSOLI	1	0.370256	0.370256	0.097713	0.7672					
Model	9	325.4853	36.16503	9.544143	0.0115	1	284.0536	284.0536	61.15976	<.0001
(Linear)	3	302.5862	100.8621	26.61803	0.0017					
(Quadratic)	3	3.714677	1.238226	0.326774	0.8069					
(Cross Product)	3	19.18445	6.394817	1.687626	0.2838					
Error	5	18.94619	3.789238			13	60.37788	4.644452		
(Lack of fit)	3	16.72992	5.576642	5.032465	0.1702	1	2.88992	2.88992	0.60324	0.4524
(Pure Error)	2	2.216267	1.108133			12	57.48796	4.790663		
Total	14	344.4315				14	344.4315			

ANOVA for HUE

	Master Model					Predictive Model				
Source	DF	SS	MS	F	Pr > F	DF	SS	MS	F	Pr > F
BARTEMP	1	377.8501	377.8501	222.3003	<.0001	1	377.8501	377.8501	194.8698	<.0001
FEDMOIS	1	0.332112	0.332112	0.195392	0.6769					
CRANSOL	1	609.5286	609.5286	358.6035	<.0001	1	609.5286	609.5286	314.3541	<.0001
BARTEMP*BARTEMP	1	38.35271	38.35271	22.56402	0.0051	1	35.34201	35.34201	18.22705	0.0013
BARTEMP*FEDMOIS	1	1	1	0.588329	0.4777					
BARTEMP*CRANSOL	1	0.4356	0.4356	0.256276	0.6342					
FEDMOIS*FEDMOIS	1	7.875016	7.875016	4.633103	0.0840					
FEDMOIS*CRANSOL	1	2.356225	2.356225	1.386236	0.2920					
CRANSOL*CRANSOL	1	1.265401	1.265401	0.744472	0.4277					
Model	9	1035.551	115.0612	67.69388	0.0001	3	1022.721	340.9069	175.817	<.0001
(Linear)	3	987.7108	329.2369	193.6997	<.0001					
(Quadratic)	3	44.04829	14.68276	8.6383	0.0202					
(Cross Product)	3	3.791825	1.263942	0.743614	0.5704					
Error	5	8.498642	1.699728			11	21.32886	1.938987		
(Lack of fit)	3	6.533575	2.177858	2.216575	0.3259	5	13.39634	2.679268	2.026546	0.2075
(Pure Error)	2	1.965067	0.982533			6	7.932517	1.322086		
Total	14	1044.05				14	1044.05			

ANOVA for CHROMA

	Master Model					Predictive Model				
Source	DF	SS	MS	F	Pr > F	DF	SS	MS	F	Pr > F
BARTEMP	1	7.050013	7.050013	19.56064	0.0069	1	7.050013	7.050013	20.58744	0.0007
FEDMOIS	1	0.3872	0.3872	1.074307	0.3475					
CRANSOL	1	9.180612	9.180612	25.4721	0.0039	1	9.180612	9.180612	26.80922	0.0002
BARTEMP*BARTEMP	1	0.023385	0.023385	0.064884	0.8091					
BARTEMP*FEDMOIS	1	0.16	0.16	0.443929	0.5347					
BARTEMP*CRANSOL	1	1.243225	1.243225	3.449394	0.1224					
FEDMOIS*FEDMOIS	1	0.265031	0.265031	0.735344	0.4303					
FEDMOIS*CRANSOL	1	0.0529	0.0529	0.146774	0.7174					
CRANSOL*CRANSOL	1	0.139801	0.139801	0.387884	0.5607					
Model	9	18.53784	2.05976	5.714915	0.0347	2	16.23062	8.115312	23.69833	<.0001
(Linear)	3	16.61782	5.539275	15.36902	0.0059					
(Quadratic)	3	0.463892	0.154631	0.429031	0.7413					
(Cross Product)	3	1.456125	0.485375	1.346699	0.3588					
Error	5	1.802092	0.360418			12	4.109308	0.342442		
(Lack of fit)	3	1.106825	0.368942	1.061295	0.5187	6	2.554742	0.42579	1.643379	0.2807
(Pure Error)	2	0.695267	0.347633			6	1.554567	0.259094		
Total	14	20.33993				14	20.33993			

ANOVA for TPC

	Master Model					Predictive Model				
Source	DF	SS	MS	F	Pr > F	DF	SS	MS	F	Pr > F
BARTEMP	1	111.5271	111.5271	67.92254	0.0004	1	111.5271	111.5271	45.09248	0.0005
FDMOIS	1	109.8162	109.8162	66.88056	0.0004	1	109.8162	109.8162	44.40073	0.0006
CRANSOL	1	84.69511	84.69511	51.58124	0.0008	1	84.69511	84.69511	34.24381	0.0011
BARTEMP*BARTEMP	1	77.02913	77.02913	46.91249	0.0010	1	74.0297	74.0297	29.93158	0.0016
BARTEMP*FDMOIS	1	14.86103	14.86103	9.050701	0.0298	1	14.86103	14.86103	6.008589	0.0497
BARTEMP*CRANSOL	1	21.5296	21.5296	13.11201	0.0152	1	21.5296	21.5296	8.704817	0.0256
FDMOIS*FDMOIS	1	6.629908	6.629908	4.037764	0.1007					
FDMOIS*CRANSOL	1	20.02563	20.02563	12.19606	0.0174	1	20.02563	20.02563	8.096732	0.0294
CRANSOL*CRANSOL	1	17.74913	17.74913	10.80962	0.0218	1	16.21542	16.21542	6.556194	0.0429
Model	9	454.8175	50.53528	30.77713	0.0007	8	448.1876	56.02345	22.65132	0.0006
(Linear)	3	306.0384	102.0128	62.12811	0.0002					
(Quadratic)	3	92.36285	30.78762	18.75036	0.0038					
(Cross Product)	3	56.41625	18.80542	11.45293	0.0112					
Error	5	8.209875	1.641975			6	14.83978	2.473297		
(Lack of fit)	3	7.969075	2.656358	22.06278	0.0437	4	14.59898	3.649746	30.3135	0.0322
(Pure Error)	2	0.2408	0.1204			2	0.2408	0.1204		
Total	14	463.0274				14	463.0274			

ANOVA for Anthocyanins

	Master Model					Predictive Model				
Source	DF	SS	MS	F	Pr > F	DF	SS	MS	F	Pr > F
BARTEMP	1	4.851613	4.851613	5.785337	0.0612	1	4.851613	4.851613	6.429332	0.0296
FDMOIST	1	3.30245	3.30245	3.938028	0.1040	1	3.30245	3.30245	4.37639	0.0629
CRANSOLI	1	12.47501	12.47501	14.87591	0.0119	1	12.47501	12.47501	16.53182	0.0023
BARTEMP*BARTEMP	1	0.042669	0.042669	0.050881	0.8305					
BARTEMP*FDMOIST	1	6.275025	6.275025	7.482694	0.0410	1	6.275025	6.275025	8.315631	0.0163
BARTEMP*CRANSOLI	1	0.3481	0.3481	0.415094	0.5478					
FDMOIST*FDMOIST	1	0.013292	0.013292	0.01585	0.9047					
FDMOIST*CRANSOLI	1	1.677025	1.677025	1.999779	0.2165					
CRANSOLI*CRANSOLI	1	1.210177	1.210177	1.443083	0.2834					
Model	9	30.25714	3.361904	4.008924	0.0703	4	26.9041	6.726025	8.913294	0.0025
(Linear)	3	20.62907	6.876358	8.199758	0.0224					
(Quadratic)	3	1.32791	0.442637	0.527825	0.6823					
(Cross Product)	3	8.30015	2.766717	3.299189	0.1158					
Error	5	4.193025	0.838605			10	7.54606	0.754606		
(Lack of fit)	3	3.909625	1.303208	9.196954	0.0996	8	7.26266	0.907833	6.406722	0.1420
(Pure Error)	2	0.2834	0.1417			2	0.2834	0.1417		
Total	14	34.45016				14	34.45016			

Fit statistics for all responses

Fit Statistics for REI

	Master Model	Predictive Model
Mean	1.587333	1.587333
R-square	95.01%	84.97%
Adj. R-square	86.03%	80.87%
RMSE	0.051235	0.059957
CV	3.227725	3.777219

Fit Statistics for Bulk Density

	Master Model	Predictive Model
Mean	0.5672	0.5672
R-square	97.10%	91.32%
Adj. R-square	91.87%	88.95%
RMSE	0.040912	0.0477
CV	7.212958	8.409802

Fit Statistics for Breaking Strength

	Master Model	Predictive Model
Mean	1.021333	1.021333
R-square	82.63%	53.73%
Adj. R-square	51.36%	41.11%
RMSE	0.202472	0.222779
CV	19.8243	21.81258

Fit Statistics for WAI

	Master Model	Predictive Model
Mean	6.562667	6.562667
R-square	85.72%	57.38%
Adj. R-square	60.02%	54.10%
RMSE	0.399128	0.427645
CV	6.081799	6.51633

Fit Statistics for WSI

	Master Model	Predictive Model
Mean	13.47067	13.47067
R-square	94.50%	82.47%
Adj. R-square	84.60%	81.12%
RMSE	1.946597	2.155099
CV	14.45063	15.99846

Fit Statistics for HUE

	Master Model	Predictive Model
Mean	48.65667	48.65667
R-square	99.19%	97.96%
Adj. R-square	97.72%	97.40%
RMSE	1.303736	1.392475
CV	2.679461	2.861838

Fit Statistics for CHROMA

	Master Model	Predictive Model
Mean	19.71667	19.71667
R-square	91.14%	79.80%
Adj. R-square	75.19%	76.43%
RMSE	0.600349	0.585186
CV	3.044878	2.967975

Fit Statistics for TPC

	Master Model	Predictive Model
Mean	76.82	76.82
R-square	98.23%	96.80%
Adj. R-square	95.04%	92.52%
RMSE	1.281396	1.572672
CV	1.66805	2.047217

Fit Statistics for Anthocyanins

	Master Model	Predictive Model
Mean	6.614	6.614
R-square	87.83%	78.10%
Adj. R-square	65.92%	69.33%
RMSE	0.915754	0.868681
CV	13.84569	13.13397

Texture Analyzer data

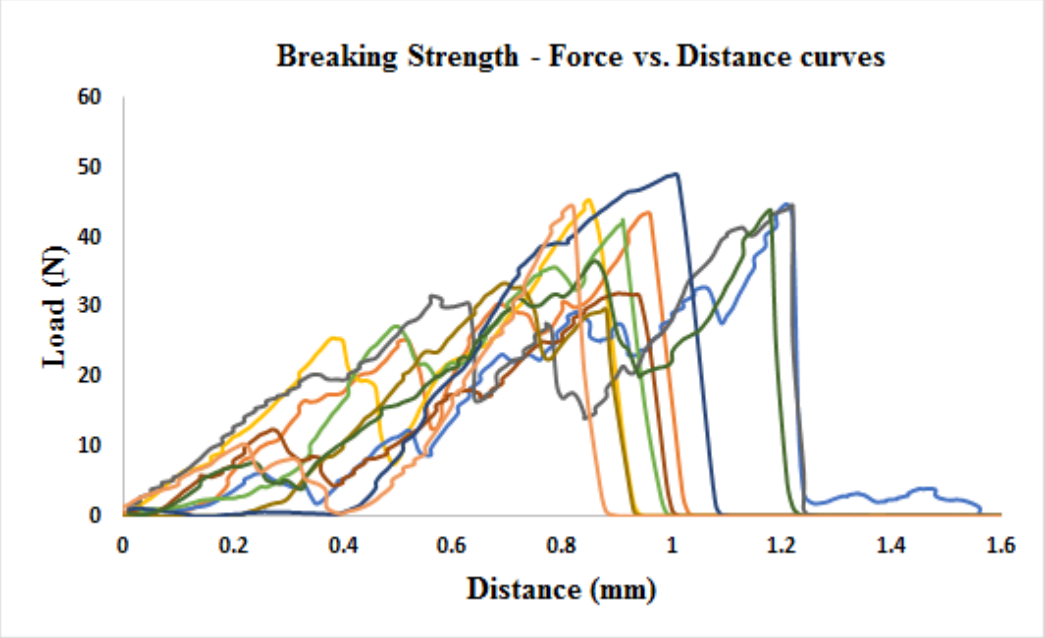

The graph shows curves obtained from ten different extrudates sample processed under 140 °C barrel temperature, 18 % feed moisture and 4 % cranberry solids.

Typical chromatogram of anthocyanins – HPLC analysis

Data File C:\CHEM32\...OCY2014\ANTHOCY140430A RUTGERS 2014-04-30 17-35-57\ANTHOCY1401549.D
Sample Name: AS-140424-014 A Rutgers Filtered

```
Acq. Operator   : SYSTEM                          Seq. Line :  17
Acq. Instrument : HPLC3                           Location : Vial 16
Injection Date  : 5/1/2014 12:03:46 AM                 Inj :  1
                                                  Inj Volume : 5.000 µl
Acq. Method     : M:\LABDATA\AGILENT_HPLC3\DAD 3\DATA\ANTHOCY2014\ANTHOCY140430A RUTGERS
                  2014-04-30 17-35-57\ANTHOCYANIN METHOD4.M
Last changed    : 4/30/2014 5:35:57 PM by SYSTEM
Analysis Method : C:\CHEM32\1\METHODS\ANTHOCYANIN METHOD4.M
Last changed    : 9/5/2014 11:52:45 AM by SYSTEM
                  (modified after loading)
Method Info     : New Anthocyanin method with Phenomenx Kinetex 2.6 u C18 50 x 4.6 mm

Additional Info : Peak(s) manually integrated
```

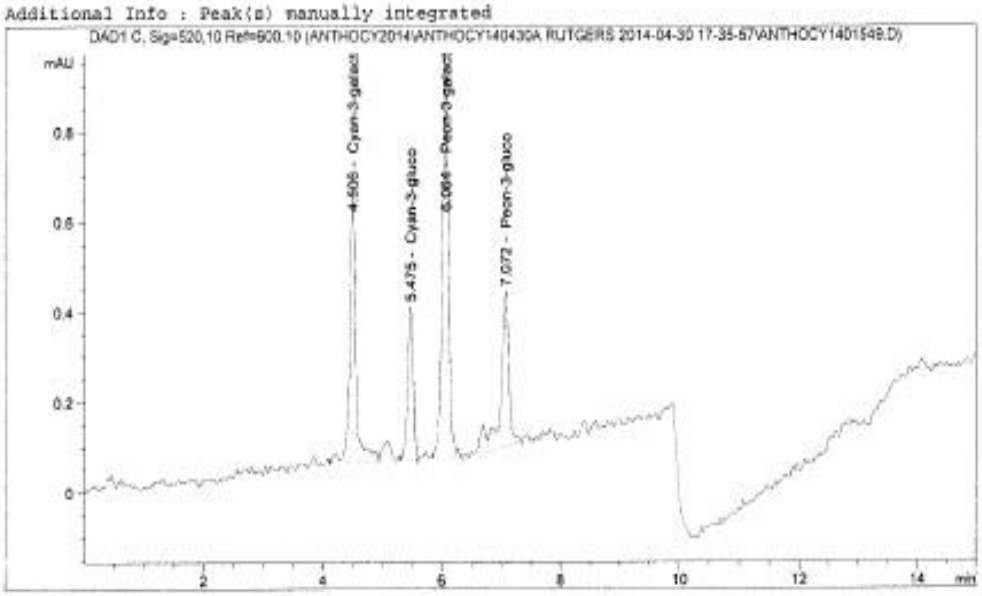


```
                        External Standard Report

Sorted By             :      Signal
Calib. Data Modified  :      9/5/2014 11:55:35 AM
Multiplier            :      1.0000
Dilution              :      4.6500
Use Multiplier & Dilution Factor with ISTDs

Signal 1: DAD1 C, Sig=520,10 Ref=600,10
Uncalibrated Peaks    :      using compound Cyan-3-galact
```

RetTime [min]	Type	Area [mAU*s]	Amt/Area	Amount [ppm]	Grp	Name
4.506	BV	4.49274	8.51432e-2	1.77875	1	Cyan-3-galact
4.940		-	-	-	1	Cyan-3-arabino
5.475	VB	2.13756	1.00609e-1	1.00002	1	Cyan-3-gluco